The Use of n-Dodecane as a Solvent in the Extraction of Light Alcohols from Water

Rinay Bhownath

Department of Chemical Engineering
University of Kwa-Zulu Natal
Durban, South Africa

June 2008

A thesis submitted to the University of Kwa-Zulu Natal in fulfillment of the requirements for the degree of Master of Science in Engineering

"I have spread my dreams under your feet;
Tread softly because you tread on my dreams."

-William Butler Yeats

STATEMENT OF ORIGINALITY

I, Rinay Bhownath, declare that this thesis does not incorporate without acknowledgement any material previously submitted for a degree or diploma in any university; and that to the best of my knowledge it does not contain any material previously published or written by another individual where due reference is made in the text.

Rinay Bhownath

Supervisor: Dr. P. Naidoo

Supervisor: Prof. D. Ramjugernath

ABSTRACT

Phase equilibrium data is essential in the operation, design and development of industrial separation processes. n-Dodecane is used by the industrial oil company, Sasol Ltd., as a solvent in the extraction of light alcohols from water. Sasol Ltd. required phase equilibrium data to optimise existing processes and this study was focused on phase equilibrium data measurement of selected binary vapour-liquid-equilibrium and ternary liquid-liquid-equilibrium systems containing n-dodecane, water, ethanol and 2-propanol. The choice of combination of chemical mixtures and operating conditions were based on industrial importance at the commencement of this study.

Two binary VLE systems n-dodecane + 2-propanol and n-dodecane + ethanol were selected for measurement, both having a high relative volatility. A modified recirculating VLE still as described in Ndlovu [2005] was used to acquire the binary VLE data. An innovative mixing system was incorporated into VLE still of Ndlovu [2005]. The isothermal binary VLE data measurements were undertaken for n-dodecane + ethanol at 333.15 K and 343.15 K, and n-dodecane + 2-propanol at 333.15 K, 343.15 K and 353.15 K.

The measured binary VLE data were regressed using the gamma-phi approach. Second virial coefficients (Pitzer and Curl [1957] and Tsonopoulos [1974]) were employed to compute the vapour phase non-ideality. The liquid phase non-ideality was evaluated using Gibbs excess energy models namely the Wilson, NRTL and UNIQUAC models.

Ternary LLE data measurements were acquired using the LLE still of Ndlovu [2005]. All LLE data measurements were undertaken at atmospheric pressure. Ternary LLE data measurements were carried out for n-dodecane + water + ethanol at 323.15 K and 333.15 K, and n-dodecane, + water + 2-propanol at 328.15 K and 333.1 5K.

The measured ternary LLE data was regressed independently using two methods: tie line correlation and binodial curve correlation. The tie line data was correlated using the NRTL model of Renon and Prausnitz [1968] and also the modified UNIQUAC model of Anderson and Prausnitz [1978]. The binodial curves were modelled using the log γ equation [Letcher et al., 1989]) and the β-density function [Letcher et al, 1986].

ACKNOWLEDGEMENTS

- First and foremost I would like to thank my parents for all the help, guidance and love. I would not be where I am today without them.

- All my thanks to God for everything that He has provided for me.

- To my supervisors, Prof Ramjugernath and Dr. Naidoo for all the knowledge and help they provided for me.

- To my colleagues Prashant, Minal, Jason, Kugs, Arayan, Suds, Rakesh, Shaniel, Devlin, Sam, Mesham, Reshen, Reagan, Shalin, Suren, Wayne, Shalen, Prebantha, Carl, David, Shaneel, Shudir, Shameer, Etienne, Ayanda, Tyrone and Scott. For all the helpful ideas and friendships.

- To the workshop staff Les, Ken, Danny and Kelly. For the help in bridging theory with practicality.

- To Mr P. Siegling for the considerable amount of glass work preformed on my apparatus.

CONTENTS

LIST OF FIGURES

Chapter 2

Chapter 3

Chapter 4

Chapter 5

Chapter 6

Chapter 7

LIST OF TABLES

Chapter 5

Chapter 6

Chapter 7

NOMENCLATURE

English Letters

A	Constant in the Antoine vapour pressure equation
a'	Parameter in the Tsonopoulos [1974] correlation
B	Constant in the Antoine vapour pressure equation
B^o	Parameter in the Pitzer-Curl [1957] correlation
Bii	Second virial coefficient of pure component I [cm^3/mol]
Bij	Second virial coefficient for the species i – species j interaction [cm^3/mol]
C	Constant in the Antoine vapour pressure equation
C_1, C_2, C_3	Parameters in the correlation of Letcher et al. (1986)
c	Numerical Constant
D	Constant in the Wagner vapour pressure equation
f	Fugacity [Kpa]
$\hat{f}$	Fugacity in solution [Kpa]
G	Molar Gibbs Energy [J/mol]
$G12$	Parameter in the NRTL equation
$G21$	Parameter in the NRTL equation
$\check{G}$	Partial molar Gibbs energy [J/mol]
$gij - gii$	Parameter representing energy interactions between species in the NRTL equation
H	Enthalpy [J/mol]
k	mixing rule parameter
K	Equilibrium constant
li	Parameter in the UNIQUAC model
M	A general thermodynamic property
n	Number of moles
P	Pressure (Kpa)
P'	Parachor
Q	Quadratic sum of second Virial coefficients
R	Universal Gas constant [J/mol]
Rd	Mean radius of gyration [A]

i	Pure- component parameter in the UNIQUAC model
S	Entropy [cm^3/mol]
T	Temperature [^{o}C or K]
V	Molar or specific volume [cm^3/mol]
x	liquid phase mole fraction
y	vapour phase mole fraction
Z	Compressibility factor
z	Co-ordination number

Greek Letters

α *12*	Parameter in the NRTL model representing the solution non-randomness
α,β	Denotes a thermodynamic phase
δ	Denotes a residual (e.g. δ P)
δ *ij*	Term relating the second virial coefficients
ε	Tolerance in iterations also Constant temperature term and Constant Pressure term in the Van Ness Direct Test
Φ	Ratio of fugacity coefficients with the Poynting correction factor (Equation 3-48)
Φ_1	Segment fraction in the UNIQUAC model
ϕ	Fugacity coefficient
$\hat{\phi}$	Fugacity coefficient in solution
γ	Activity coefficient
η	Solvation parameter
Λ_{ij}	Parameter in Wilson equation
$\lambda_{ij} - \lambda_{ii}$	Parameter representing molar interactions between species in the Wilson and UNIQUAC model
μ	Dipole moment [Debye] and Chemical potential
θ	Area fraction in the UNIQUAC model
τ*ij*	Parameter in the NRTL model
ω	Acentric factor

Subscripts

1	Denotes component 1
2	Denotes component 2
ad	Denotes absolute deviation
n	Denotes critical property
Ant	Denotes Antione equation

Superscripts

E	Denotes excess property
Exp	Denotes experimental value
Cal	Denotes calculated value
id	Denotes ideal solution
ig	Denotes ideal gas
l	Denotes liquid phase
Sat	Denotes a saturated value
∞	Denotes the infinite pressure value

CHAPTER 1
INTRODUCTION

Phase equilibrium data (PED) plays an important role in Chemical Engineering. The use of which extends onto industrial separations process such as absorption, distillation, extractive distillation, azeotropic distillation and vapour-liquid separation. There exist three primary methods to acquire PED namely, predictive models, experimental methods and molecular simulations. Computer simulations and predictive models are slowly overshadowing experimental methods. This may be attributed to experimental methods being costly and time consuming. However, experimental methods currently remain both an accurate means of data acquisition and validation of predictive methods.

A petrochemical company, Sasol Ltd., uses extractive distillation to remove light alcohols from water using n-dodecane as a solvent. n-Dodecane is largely immiscible in water and a large relative volatility exists between n-dodecane and light alcohols. After using n-dodecane as solvent the light alcohol can be easily separated from the heavier hydrocarbon using classical distillation methods. Sasol Ltd. separates light alcohols from water using this method and consequently requires accurate VLE and LLE data for the design and optimization of existing industrial process equipment. The choice of chemical mixtures and operating conditions in this study depended upon the industrial need at that present time and it resulted with two light alcohols, ethanol and 2-propanol being chosen for this study.

This study was aimed to measure and model binary VLE data of n-dodecane with 2-propanol and ethanol and ternary LLE data of n-dodecane + water + 2-propanol and n-dodecane + water + ethanol at predefined system conditions. The operating conditions of each data system were influence based on the limitations of the equipment used, and/or the characteristics of the systems. However, after modelling the measured data systems, the parameters obtained from data regression may be used to predict PED at the conditions of interest to industry were applicable.

CHAPTER 2

REVIEW OF EXPERIMENTAL METHODS FOR PHASE EQUILIBRIUM DATA MEASUREMENT: CIRCULATION METHODS

Vapour-liquid equilibrium (VLE) data and liquid-liquid equilibrium (LLE) data are needed for the design of industrial processes such as liquid-liquid extraction, classical distillation, solvent extraction and azeotropic distillation. Both VLE and LLE data measurements can be difficult and tedious to undertake, depending on the miscibility of the components and of the state of the system. However, to date experimental methods remain an accurate means of acquiring low pressure phase equilibrium data (PED). Consequently, this chapter is aimed at presenting a concise review of apparatus pertinent to experimental methods employed in this study for measurement of low pressure VLE data and atmospheric pressure LLE data.

2.1. VLE equipment

Experimental methods for low pressure VLE (LPVLE) measurement are extensive and well documented. For simplicity, this section presents a succinct review of selected LPVLE stills applicable to apparatus used in this study . A diagrammatic overview of this section is shown in Figure 2.1. Hala et al. [1967] classifies VLE experimental methods into the following groups: dew and bubble point methods, distillation methods, circulation methods, and static methods. Only the LPVLE stills using the circulation method will be discussed in detail in this chapter.

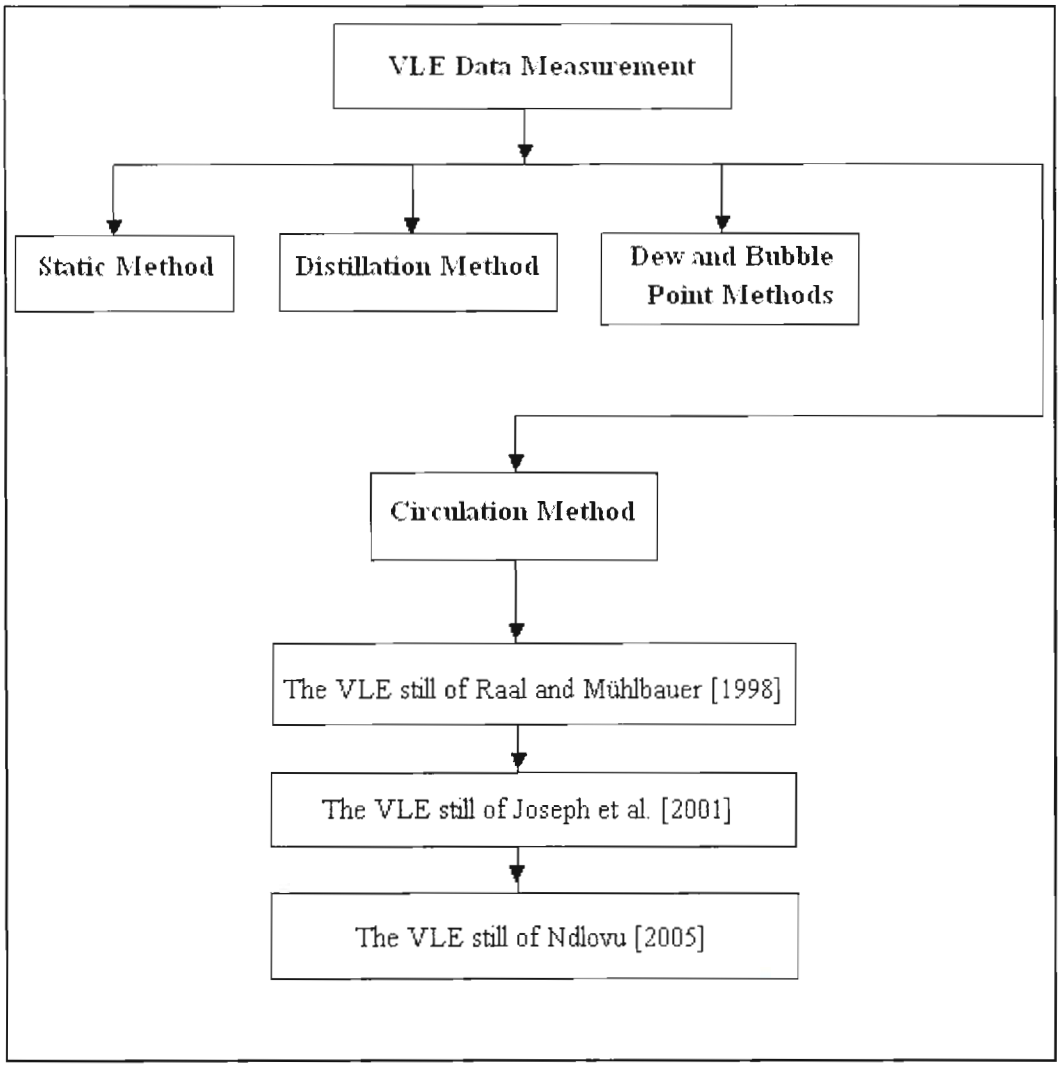

Figure 2.1 Overview of VLE data measurement

2.1.1 Distillation method

Distillation is one of the earliest methods used to acquire VLE data. It involved the boiling off of vapour from a large liquid charge. One of the first documented VLE stills that employed this technique was the VLE still of Carveth [1899]. This method was plagued by large errors caused by vapour condensation on the cold sides of the flask during the heating process. The still of Carveth [1899] was later improved by Rosnoff et al. [1914] and was verified to give good results by Young [1922]. However, the disadvantage of the condensate on the cold side of flask still remained. "This method has the advantage of simplicity but is seldom used today", [Hala et al., 1967]. A comprehensive study of classical distillation methods are detailed in Hala et al. [1967].

2.1.2 Static Methods

The static method involved charging a static cell with a liquid mixture. This liquid mixture was then agitated mechanically until it achieved equilibrium with its vapour at a fixed temperature. Static cells are normally immersed in water baths kept at constant temperature which produces isothermal data. "The largest disadvantage in the static method is the necessity for complete degassing of the system", [Raal and Mühlbauer, 1998]. "Even small amounts of remaining gas are capable of yielding useless results", [Abbot, 1986]. Comprehensive studies of static methods are detailed by Raal and Mühlbauer [1998].

2.1.3 Dew and Bubble point methods

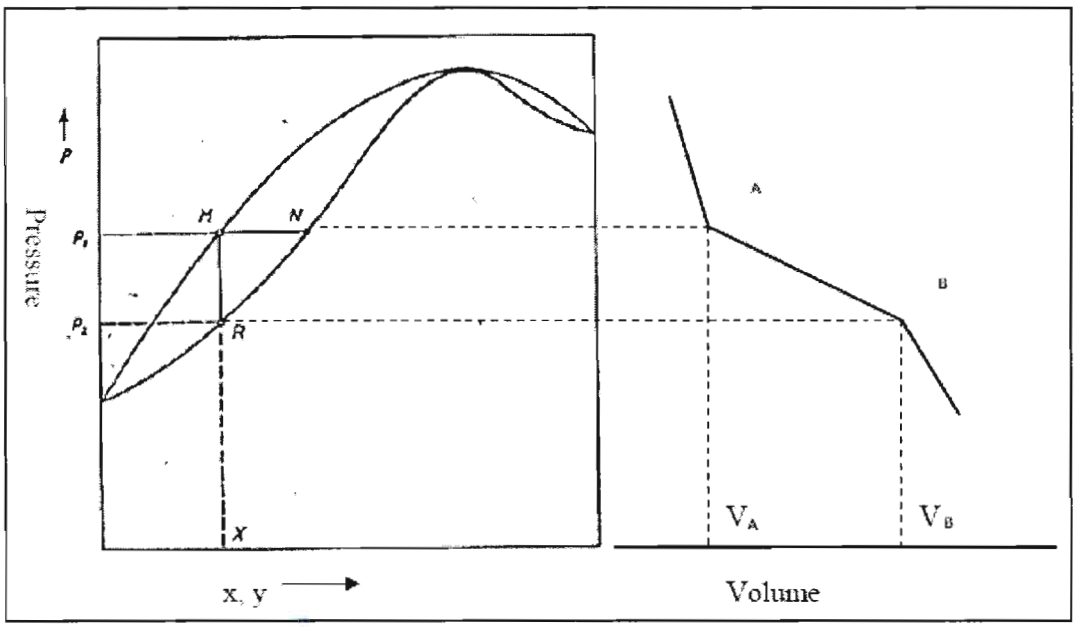

Figure 2.2 Dew and bubble point diagram, Smith et al. [1996]

Dew and bubble point methods are commonly used when the mixture is either entirely liquid or vapour. This method may be preformed in three different variants, namely by varying temperature, pressure or composition. "The more favoured has been the variation of pressure of a mixture of known composition by variation of the volume", [Raal and Mühlbauer, 1998]. The dew and bubble point pressures are determined from breaks in the P-V curve shown in Figure 2.2 as points A and B. Dew and bubble point methods have lost favour as a result of developments of faster, more reliable stills. Comprehensive studies of dew and bubble methods are detailed by Raal and Mühlbauer [1998].

2.1.4 Circulation method

The circulation method, also known as the dynamic method, allows VLE data of high accuracy to be measured. It has the advantages of being simple, reliable and requiring smaller amounts of chemical to operate than experimental methods discussed in this chapter. "All circulation methods have in common the principle of the continuous separation of vapour phase evolved from a liquid phase under steady-state conditions and recirculation of vapour phase", [Malanowski, 1982]. These VLE stills may operate either isobarically or isothermally under steady-state conditions whereby thermodynamic properties such as temperature, pressure, liquid and vapour composition may be recorded. Circulation methods may be classified into two separate categories depending on which phase is circulated, specifically the circulation of the vapour phase only, and circulation of both the liquid and vapour phases. The LPVLE stills pertinent to the re-design of the LPVLE apparatus used in this study are discussed in subsequent sections. A comprehensive study of classical circulation methods are detailed by Raal and Mühlbauer [1998].

2.1.4.1 Still of Raal and Mühlbauer [1998]

The still of Raal and Mühlbauer [1998] was based on the designs of Heertjies [1960] and Yerazunis [1964]. Most notable features are:

a) A packed equilibrium chamber where the liquid and vapour phases are forced downward co-currently to achieve rapid and dynamic equilibrium.
b) The packed equilibrium chamber is vacuum jacketed preventing condensation of vapours.
c) Simple to operate.
d) An equilibrium chamber is used to increase the contact time and contact area for equilibrium to be reached.
e) Efficient magnetic stirring in both the condensate receiver and the boiling chamber eliminates temperature gradients and prevents flashing in the boiling chamber.
f) Liquid is heated by both and internal and external heaters attached to the boiling chamber.

The still of Raal and Mühlbauer [1998] accurately measured binary LPVLE data for ideal systems. However, this still had the inability to measure binary LPVLE systems of high relative volatility.

2.1.4.2The still of Joseph et al. [2001]

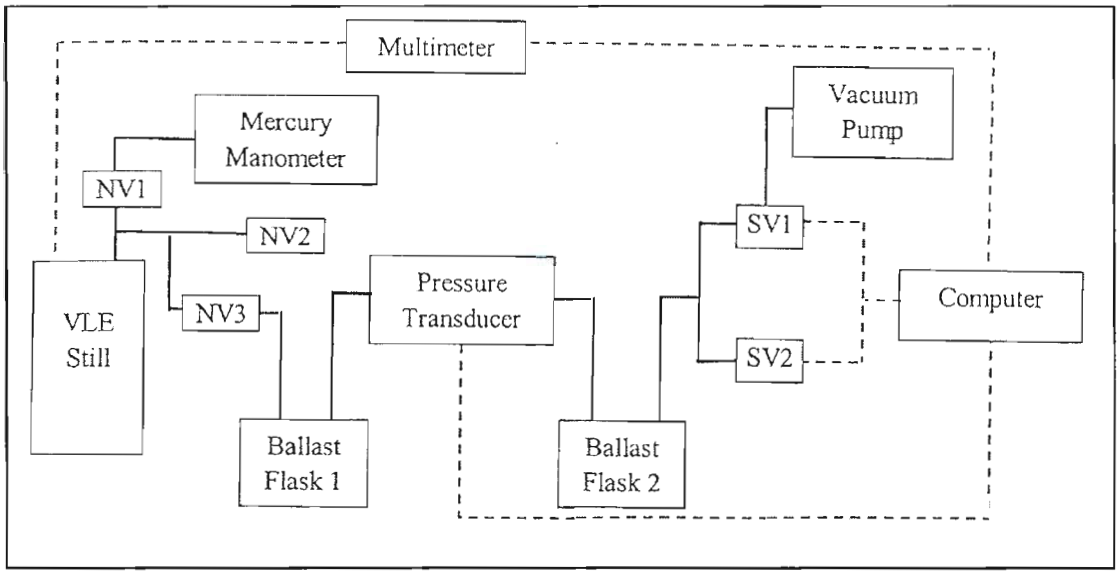

Figure 2.3 Block diagram of the apparatus of Joseph et al. [2001]

Joseph et al. [2001] improved the isothermal operation of the still of Raal and Mühlbauer [1998]. The still of Raal and Mühlbauer [1998] operated isobarically using a pressure controller. However, isothermal operation was accomplished by manually changing the setting of the pressure controller to achieve the desired temperature. This mode of operation proved problematic and could yield inaccurate binary LPVLE data. Joseph et al. [2001] improved on this control strategy by implementing a design based on pulse-width modulation of two solenoid valves with the aid of computer control. A block diagram of the VLE apparatus used by Joesph et al. [2001] is shown in Figure 2.3. The new control scheme improved the attainment of isothermal data but was unable to acquire binary VLE data for systems with high relative volatility.

2.1.4.3 The still of Ndlovu [2005]

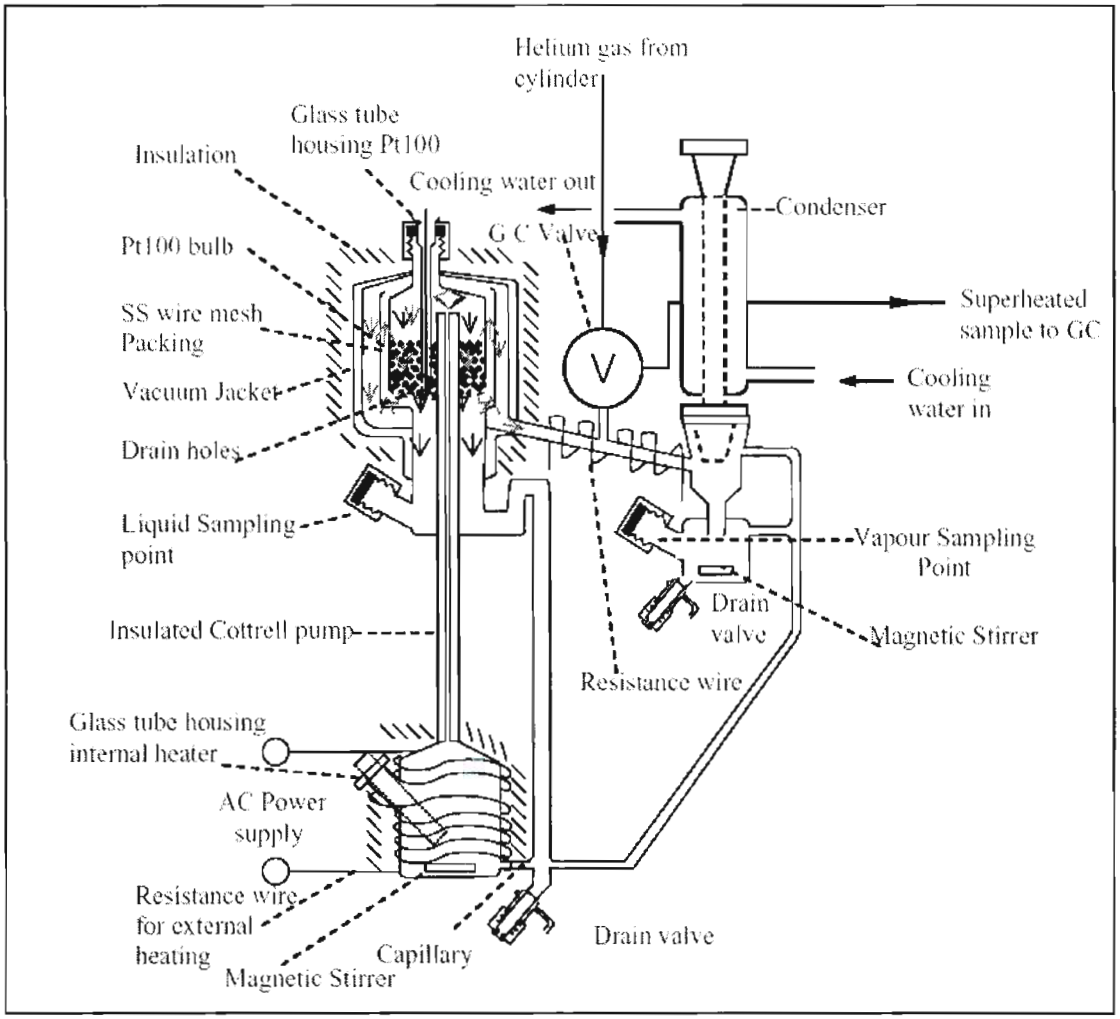

Figure 2.4 The VLE still of Ndlovu [2005]

Ndlovu [2005] implemented an innovative design modification to the still of Joseph et al. [2001], enabling the still of Ndlovu [2005] to attain binary LPVLE data for partially miscible systems. The still of Joseph et al. [2001] generated partial vapour condensation due to contact with the outside walls throughout the downward pass of vapour in the equilibrium chamber. Unlike homogenous systems where the partial condensation of the vapour in the line does not effect the vapour composition; in systems of partial immiscibility any minute condensation of the vapour before sampling must be avoided. Ndlovu [2005] improved the vapour sampling whereby a vapour sample would be sent directly to the gas chromatograph as shown in Figure 2.4. Partial condensation was circumvented by slightly superheating the vapour exiting the equilibrium chamber and withdrawing a vapour sample via a six-port GC (gas chromatography) valve thus eliminating sampling inaccuracies inherent to the VLE apparatus of Joseph et al. [2001].

2.2 LLE measurement methods

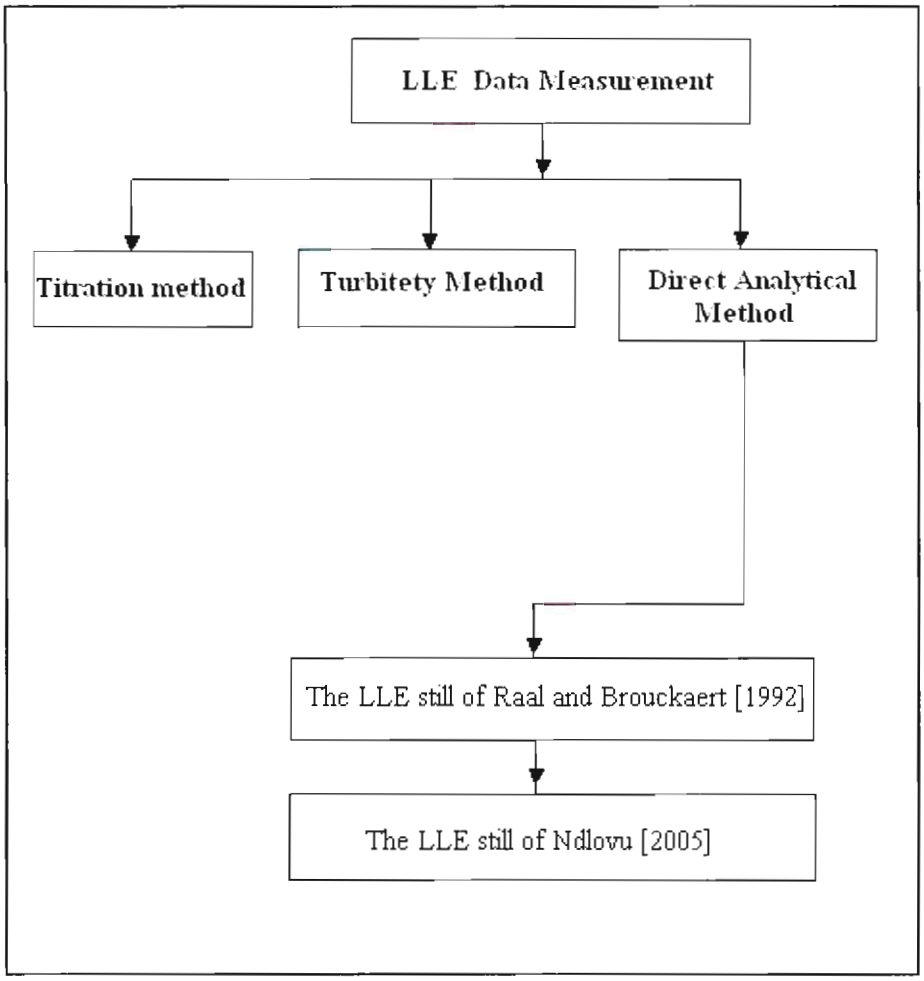

Figure 2.5 Overview of LLE section

Historically, LLE data measurement was much easier than VLE data measurement. This may be attributed to liquids being less affected by small pressure fluctuations. Common methods to acquire LLE data are the direct method, titration and turbidimetry techniques. An overview of this section is shown in Figure 2.5.

2.2.1 Titration method

For the titration method, one component is continuously added to a known amount of the other component or mixture of components with unlimited miscibility in an agitated vessel until turbity appears or disappears. Using this information the binodial curve and tie lines can be constructed. The Karl-Fischer titration method can also be used to obtain tie line data provided one of the components is water. The major disadvantage of this method was the onset of turbity in titration which is subjective. A more detailed description of titration methods are presented by Brigg and Cummings [1943].

2.2.2 Turbidity method

The turbidity method entails charging a mixture of known overall composition into an equilibrium cell (either homogenous or heterogeneous). The equilibrium cell temperature is varied until the appearance or disappearance of a second phase noted. An advantage of the turbidity method is that no phase analysis at equilibrium is necessary while this method suffered from the same disadvantage outlined for the titration method. However, this disadvantage can be minimized with suitable instruments. Reviews of the experimental LLE stills employing the turbidity method are discussed in Raal and Mühlbauer [1998].

2.2.3 Direct Analytical Method

The direct method simply involves charging a liquid mixture into a well stirred equilibrium cell kept at constant temperature. This was commonly accomplished by jacketing the vessel or immersing the cell in a temperature controlled water bath. Efficient stirring was necessary to reach equilibrium but not to emulsify the mixture. The liquid mixture is left to equilibrate and sampling of phases then occurs. This was the method chosen to measure isobaric binary and ternary LLE data. The LLE still of Ndlovu [2005] is discussed in detail in Chapter 4. Ndlovu [2005] modified the LLE still of Raal and Brouckaert [1992] (discussed in section 2.2.3.1). A comprehensive review of LLE stills employing the direct analytical method are discussed further in Raal and Mühlbauer [1998].

2.2.3.1 The LLE still of Raal and Brouckaert [1992]

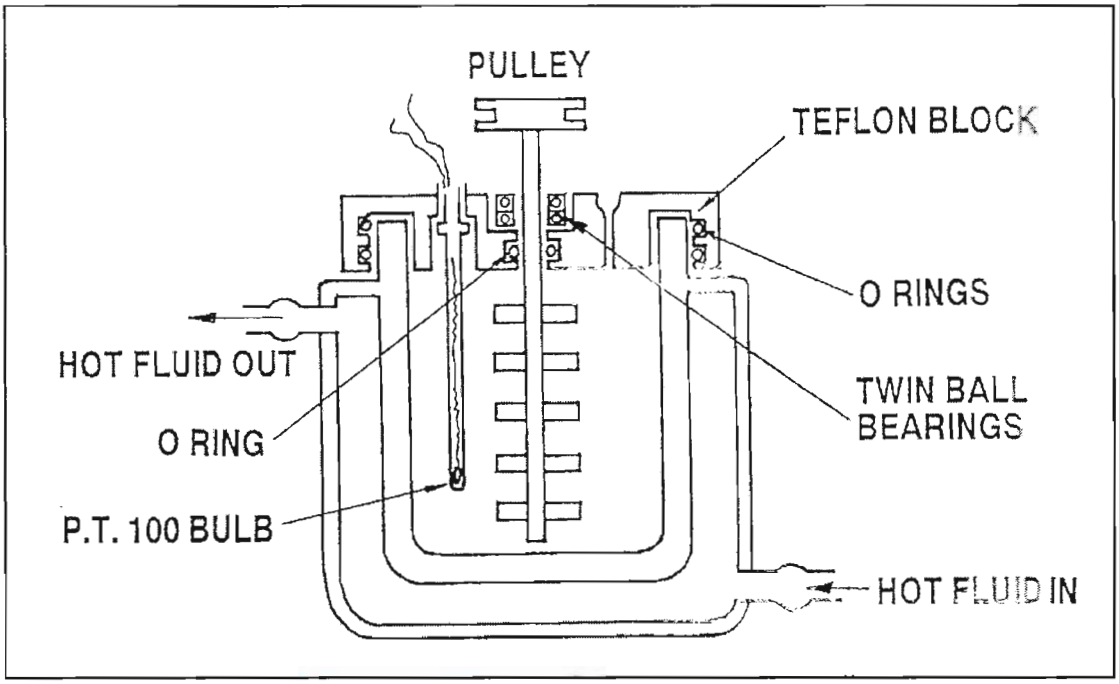

Figure 2.6 The LLE still of Raal and Brouckaert [1992]

A diagrammatic representation of the LLE still of Raal and Brouckaert [1992] is shown in Figure 2.6. A jacketed glass cell was fitted on top of a Teflon header with o-rings as shown in Figure 2.6. A thin walled stainless steel tube housed the temperature probe. The mechanical stirrer was driven by a DC power supply and temperature was controlled to within 0.02 K by circulating water heated in a water bath. The major disadvantage was the sample syringe had to be injected through the top phase to sample the bottom phase thereby disturbing the liquid interface. The LLE still of Ndlovu [2005] eliminated this design flaw (discussed in chapter 4).

2.3 Conclusion

Traditionally, LLE data is easier to measure than VLE data. The LLE still of Raal and Brouckaert [1992] has proved to yield accurate binary LLE data but it has inherent sampling errors (discussed in Section 2.2.3.1) for the denser liquid. The still of Ndlovu [2005] eliminates this problem (discussed in chapter 4) and was shown by Narasigadu [2006] and Ndlovu [2005] to produce reliable ternary LLE data. Therefore, the LLE still of Ndlovu [2005] was employed in this study to acquire binary and ternary LLE data.

VLE data measurement can be conducted by various methods (detailed in Raal and Mulhbauer

[1998]). The circulation method is a fast and proven method used to obtain reliable LPVLE data. The most recent LPVLE re-circulating still was that of Ndlovu [2005] which can measure data for binary systems of partial miscibility but was incapable of accurately measuring binary LPVLE data for systems with high relative volatility. The VLE still of Ndlovu [2005] incorporated tested and novel features proved by Raal and Mühlbauer [1998] and Joseph et al. [2001] to yield accurate binary LPVLE data (discussed in Section 2.1.4.1 and 2.1.4.2). Hence, it was concluded to redesign the VLE still of Ndlovu [2005] to handle VLE systems of high relative volatility.

CHAPTER 3
THEORETICAL ASPECTS OF VAPOUR-LIQUID AND LIQUID-LIQUID EQUILIBRUIM

Theoretical aspects of VLE and LLE are essential for separation process design and optimization. This chapter presents a brief overview of important thermodynamic principles such as chemical potential, calculation of fugacity and activity coefficients, as well as methods to evaluate thermodynamic consistency of phase equilibrium data (PED). An overview of solution thermodynamics as applied to PED is shown in Figure 3.1. A rigorous theoretical treatment of phase equilibrium thermodynamics for VLE and LLE can be found in Smith et al. [1996].

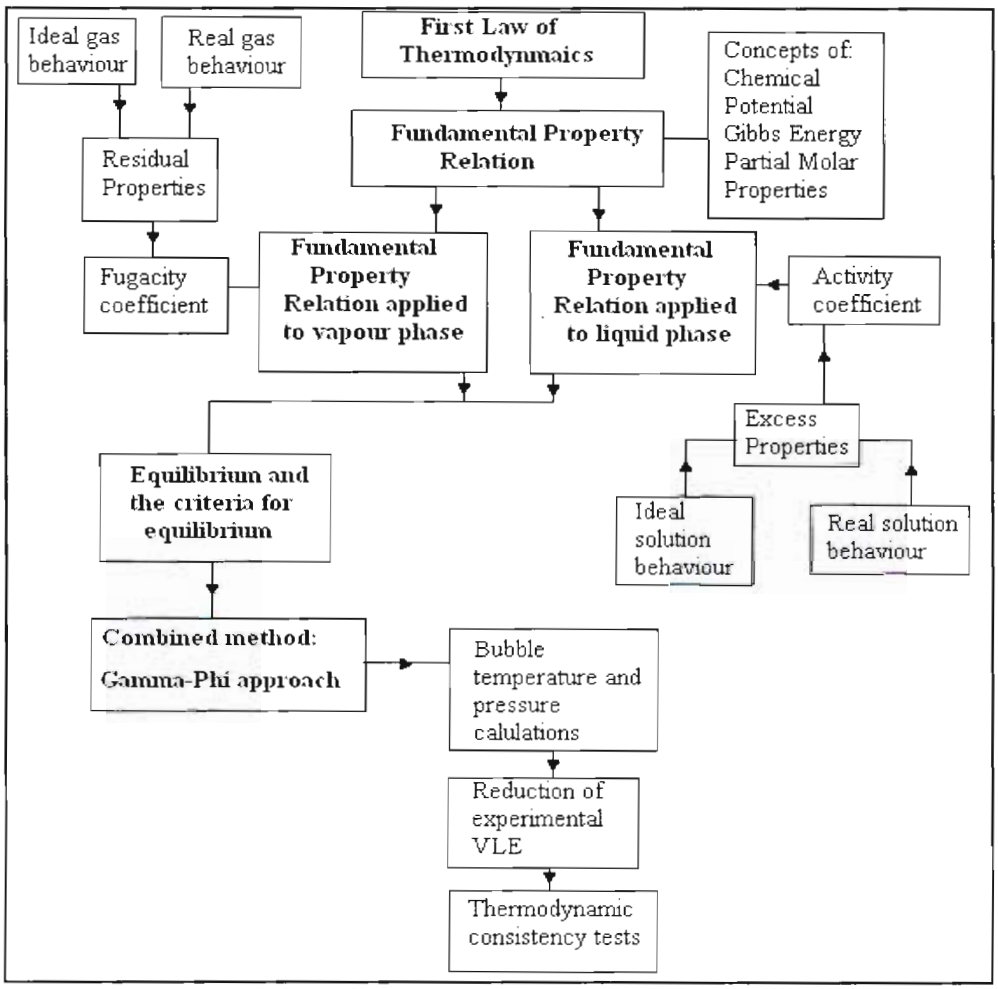

Figure 3.1 Overview of thermodynamics for phase equilibria

3.1 Fugacity and fugacity coefficient

"Equilibrium is a static condition devoid of change", [Smith et al. [1996]. Multiple phases are in equilibrium when the temperature of each phase is equal and the chemical potential, μ_i of each phase are equal. Thus, at equilibrium for a closed system consisting of N chemical species and π phases (Full derivation is given in Smith et al. [1996]):

$$\mu_i^{\beta} = \mu_i^{\alpha} = \mu_i^{\pi} \qquad (i = 1,2,3,...N) \qquad (3\text{-}1)$$

Chemical potential, while a theoretically sound concept is an awkward mathematical quantity not related to measurable quantities. This can be overcome by defining a new quantity known as fugacity which can be related to measurable properties, e.g. P, V, T data:

$$d\mu_i = RTd\ln\hat{f}_i + \theta(T) \qquad (3\text{-}2)$$

At constant temperature $\theta(T) = 0$, it therefore follows:

$$\hat{f}_i^{\beta} = \hat{f}_i^{\alpha} \qquad (3\text{-}3)$$

Equation (3-3) can now be related to measurable quantities by using dimensionless auxiliary functions, $\hat{\phi}_i$, which is the fugacity coefficient in solution of component i that accounts for the non-ideal vapour phase and γ_i, the activity coefficient of component i which accounts for the non-ideal liquid phase.

3.2 Vapour Liquid Equilibrium (VLE)

The criterion for phase equilibrium requires that for multiple phases at equilibrium the fugacity in solution of each component must be the same in, for this study, the vapour and liquid phases:

$$\hat{f}_i^{V} = \hat{f}_i^{L} \qquad (3\text{-}4)$$

Now it is a matter of relating the respective fugacities to measurable quantities such as temperature, pressure and phase composition. This can be achieved by introducing two new functions γ_i for the liquid phase and $\hat{\phi}_i$ for the vapour phase. Substituting for the respective fugacities the following equations are derived (detailed derivation given in Smith et al. [1996]):

$$\hat{\phi}_i = \frac{\hat{f}_i^V}{y_i P} \tag{3-5}$$

For the liquid phase:

$$\hat{f}_i^L = x_i \gamma_i \hat{\phi}_i^{sat} P_i^{sat} \exp[\frac{-V_i(P - P_i^{sat})}{RT}] \tag{3-6}$$

Combining the equation (3-5) and equation (3-6):

$$y_i \hat{\phi}_i P = x_i \gamma_i \hat{\phi}_i^{sat} P_i^{sat} \exp[\frac{-V_i(P - P_i^{sat})}{RT}] \tag{3-7}$$

The definition of Raoult's law:

$$y_i \Phi_i P = x_i \gamma_i P_i^{sat} \tag{3-8}$$

Whereby Φ is defined as:

$$\Phi = \frac{\hat{\phi}_i^{sat}}{\hat{\phi}_i^t} \exp[-\frac{V_i(P - P_i^{sat})}{RT}] \tag{3-9}$$

This holds assuming the liquid is incompressible between the system pressure P and saturated pressure P_i^{sat}. Typical VLE curves are shown in Figure 3.2 and are explained fully in Raal and Mühlbauer [1998].

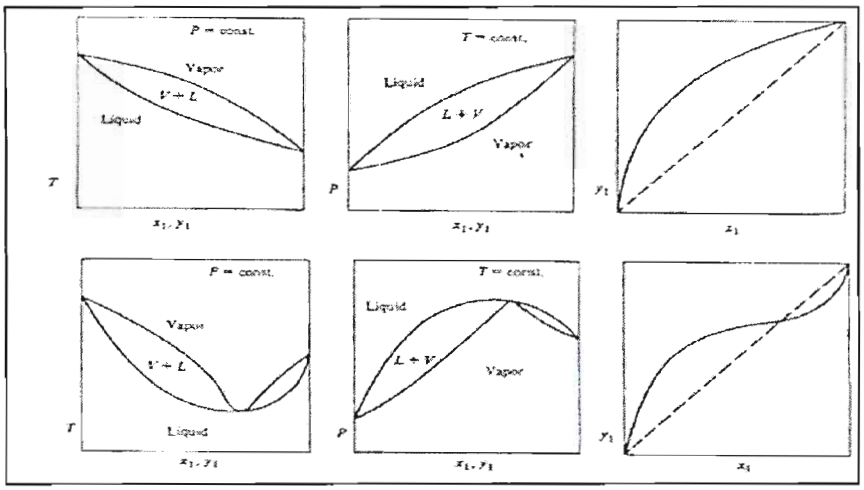

Figure 3.2 VLE diagrams, Smith et al [1996]

3.2.1 Vapour phase non-ideality: Fugacity Coefficient

The fugacity is related to fugacity coefficient by the following relationship:

$$\phi = \frac{f}{P} \tag{3-10}$$

and for a component *i* in solution (detailed derivation given in Smith et al. [1996]):

$$\hat{\phi}_i = \frac{\hat{f}_i}{y_i P} \tag{3-11}$$

3.2.2 Determining Fugacities

To calculate the fugacity of a pure liquid at a pressure above its saturated pressure is a two-step procedure. Using a suitable equation of state and starting the first step at saturation (detailed derivation given in Smith et al. [1996]):

$$\hat{f}_i^{L.} = \hat{f}_i^{sat} = \phi_i^{sat} P_i^{sat} \tag{3-12}$$

The second step accounts for a change in the liquid phase fugacity for an increase in pressure at constant temperature. Fugacity is related to pressure at constant temperature by the following equation:

$$dG_i = V_i dP - S_i dT = RTd \ln \hat{f}_i \tag{3-13}$$

Rearranging the above equations and integrating from P_i^{sat} to P and using equation (3-12) to eliminate f^{sat}:

$$\hat{f}_i^L = \hat{\phi}_i^{sat} P_i^{sat} \; exp[\frac{V_i^L (P - P_i^{sat})}{RT}] \tag{3-14}$$

Liquid molar volumes can be evaluated from the Rackett [1970] equation.

3.2.3 Calculating the fugacity from the Virial equation of state

The virial equation of state has sound theoretical basis in statistical mechanics. "For a system at low pressure the virial equation adequately describes the vapour phase and it is sufficient to consider the two term viral equation of state", [Perry and Green, 1998] defined as (detailed derivation given in Smith et al. [1996]):

$$Z = 1 + \frac{BP}{RT} \tag{3-15}$$

B is the second virial coefficient and is a function of temperature only for pure components. In a mixture B is a function of composition and is calculated from the equation based on statistical mechanics:

$$B_{mix} = \sum_i \sum_j y_i y_j B_{ij} \tag{3-16}$$

Note $B_{ij} = B_{ji}$ and y_i is the vapour mole fraction. For two components the fugacity coefficient is obtained when Equation (3-12) is substituted into Equation (3-13):

$$\Phi_i = \exp\left[\frac{(B_i - V_i^l)(P - P_i^{sat}) + P y_j^2 (2B_{ij} - B_{ii} - B_{jj})}{RT}\right] \quad (3\text{-}17)$$

The next two sections discuss methods to calculate the second viral coefficients.

3.2.3.1 The Pitzer-type correlation

This correlation is derived using Equation (3-15) combined with the correction for the compressibility factor $Z = Z^o + \omega Z^l$, where Z^o and Z^l are functions of residual temperature and pressure, one obtains (Detailed derivation given by Pitzer and Curl, [1957]):

$$B_{ij} = \frac{RT_{cij}}{P_{cij}}(B^{(O)} + \omega_{ij} B^{(1)}) \quad (3\text{-}18)$$

where $B^{(O)}$ and $B^{(1)}$ can be calculated from Pitzer and Curl [1957]:

$$B^{(O)} = 0.1445 - \frac{0.330}{T_r} - \frac{0.1385}{T_r^2} - \frac{0.0121}{T_r^3} \quad (3\text{-}19)$$

$$B^{(1)} = 0.073 + \frac{0.46}{T_r} - \frac{0.5}{T_r^2} - \frac{0.097}{T_r^3} - \frac{0.0073}{T_r^4} \quad (3\text{-}20)$$

The methods to estimate the cross coefficient are detailed in Prausnitz *et al.* [1986].

3.2.3.2 The Tsonopoulos correlation

Tsonopoulos [1974] modified the correlation of Pitzer and Curl [1957] for calculating virial coefficients. Tsonopoulos [1974] presents different expressions for polar and non-polar compounds (Detailed derivation given in Tsonopoulos [1974]).

For non-polar compounds Tsonopoulos [1974] presents a slight modification to Equations (3-19) and (3-20):

$$B^{(0)} = B^{(0)} - \frac{0.000607}{T_r^8} \tag{3-21}$$

$$B^{(1)} = 0.0637 + \frac{0.331}{T^2{}_r} - \frac{0.432}{T_r^3} - \frac{0.008}{T_r^8} \tag{3-22}$$

Note, the viral equation is given by Equation (3-18)

For polar compounds, with a non-zero dipole moment, an additional parameter is included into Equation (3-18):

$$B_{ij} = \frac{RT_{cij}}{P_{cij}}(B^{(0)} + \omega_{ij}B^{(1)} + B^{(2)}) \tag{3-23}$$

where

$$B^{(2)} = \frac{a_T}{T_r^6} \tag{3-24}$$

a_T is a function of the reduced dipole moment. However, for compounds containing hydrogen bonding the following term is used:

$$B^{(2)} = \frac{a_T}{T_r^6} - \frac{b_T}{T_r^8} \tag{3-25}$$

The parameters a and b are dependent on the dipole moments of each compound and are found through regression of available experimental data of B. Tsonopoulos [1974] tabulated a number of these parameters for different alcohols.

3.2.4 Liquid phase non-ideality: Activity coefficients

The concept of activity coefficients were introduced to account for deviation from ideality for the liquid phase whereby the activity coefficient is defined as:

$$\gamma_i = \frac{\hat{f}_i}{x_i f_i} \tag{3-26}$$

The fundamental excess property below can be derived using Equation (3-13) in combination with the partial Gibbs energy, $\bar{G}_i^E = RT \ln \gamma_i$, for n components (derivation can be found in Smith et al. [1996]):

$$\ln \gamma_i = \left(\frac{\partial (nG^E{}_i / RT)}{\partial n_i} \right) \tag{3-27}$$

3.2.5 Evaluating activity coefficients: Excess Gibbs energy models

3.2.5.1 Wilson Equation

The Wilson equation is based on the assumption that interactions between molecules can be described by "local compositions" realizing that molecules do have a tendency to arrange "themselves based on the interactions between the molecules.

Wilson's equation for a system of *m* components:

$$\frac{G^E}{RT} = \sum_{i=1}^{m} x_i \ln \left(\sum_{j=1}^{m} x_j \Lambda_{ij} \right) \tag{3.28}$$

where

$$\Lambda_{ij} = \frac{V_j}{V_i} \exp \left(-\frac{\lambda_{ij} - \lambda_{ii}}{RT} \right) \tag{3.29}$$

$$\Lambda_{ji} = \frac{V_i}{V_j} \exp \left(-\frac{\lambda_{ji} - \lambda_{jj}}{RT} \right) \tag{3.30}$$

Consequently, the adjustable parameters are ($\lambda_{12} - \lambda_{11}$) and ($\lambda_{21} - \lambda_{22}$) for a binary mixture.

Applying the partial molar property operator the activity coefficients yields:

$$\ln \gamma_k = -\ln\left(\sum_{j=1}^{m} \Lambda_{kj} x_j\right) + 1 - \sum_{i=1}^{m} \frac{x_i \Lambda_{ik}}{\sum_{j=1}^{m} \Lambda_{ij}} \tag{3.31}$$

The Wilson equation is able to treat highly non-ideal systems. One of the main downfalls is "the failure of the expression to treat systems that exhibit limited miscibility and cannot represent extrema in the activity coefficients", [Walas, 1985].

3.2.5.2 The Non-Random Two-Liquid (NRTL) Equation

The NRTL equation was proposed by Renon and Prausnitz [1986] as an improvement to the Wilson equation. "The NRTL model is based on the "local composition" concept of Wilson [1964] and the two-liquid theory of Scott", [Hildebrand and Scott, 1964]. The NRTL equation is as follows:

$$\frac{G^E}{RT} = \sum_{i=1}^{m} x_i \frac{\sum_{j=1}^{m} \tau_{ji} G_{ji} x_j}{\sum_{l=1}^{m} G_{li} x_l} \tag{3.32}$$

where

$$\tau_{ij} = \frac{\left(g_{ji} - g_{ii}\right)}{RT} \tag{3.33}$$

$$G_{ji} = \exp\left(-\alpha_{ij} \tau_{ji}\right) \tag{3.34}$$

The activity coefficient expressions for the NRTL equation can be represented as follows:

$$\ln \gamma_i = \frac{\sum_{j=1}^{m} \tau_{ji} G_{ji} x_j}{\sum_{l=1}^{m} G_{li} x_l} + \sum_{j=1}^{m} \frac{x_j G_{ij}}{\sum_{l=1}^{m} G_{lj} x_l} \left(\tau_{ij} - \frac{\sum_{r=1}^{m} x_r \tau_{rj} G_{rj}}{\sum_{l=1}^{m} G_{lj} x_l} \right) \tag{3.25}$$

The NRTL equation for a binary mixture is able to represent highly non-ideal systems well and consists of three adjustable parameters ($g_{ij} - g_{ii}$), ($g_{12} - g_{22}$) and α_{12} . As with the Wilson

equation, the NRTL equation can be extended to multi-component systems with only the use of binary interaction parameters. The interaction energy parameters are in the form of ($g_{21} - g_{11}$), ($g_{12} - g_{22}$). These parameters can be regarded as independent of temperature for small ranges. The parameter α_{12} is a constant that is the characteristic of the randomness of the system. Walas [1985] recommends a value of 0.3 for non-aqueous mixture and 0.4 for aqueous organic mixtures. However, Raal and Mühlbauer [1998] recommend a suitable value for α_{12} be calculated through the regression of experimental VLE data.

3.2.5.3 The Universal Quasi-Chemical (UNIQUAC) Equation

UNIQUAC is the combination of the concepts put forward from the Wilson and NRTL excess model. It applies the local composition concept and the two-fluid theory to produce a two-parameter expression. This model breaks down to the Wilson and NRTL equations by applying certain simplifications. "The equation is actually an approximation of the excess molar Helmholtz energy with that of the excess molar Gibbs energy", [Abrams and Prausnitz, 1975].

The UNIQUAC equation for *m* components:

$$\frac{G^E}{RT} = \frac{G^E_{combinational}}{RT} + \frac{G^E_{residual}}{RT} \tag{3.26}$$

$$\frac{G^E_{combinational}}{RT} = \sum_{i=1}^{m} x_i \ln \frac{\Phi_i^*}{x_i} + \frac{z}{2} \sum_{i=1}^{m} q_i x_i \ln \frac{\theta_i}{\Phi_i^*} \tag{3.27}$$

$$\frac{G^E_{residual}}{RT} = -\sum_{i=1}^{m} q_i' x_i \ln\left(\sum_{j=1}^{m} \theta_j' \tau_{ji} \right) \tag{3.28}$$

where:

$$\Phi_i^* = \frac{x_i r_i}{\sum_{j=1}^{m} r_j x_j} \tag{3.29}$$

$$\theta_i = \frac{x_i q_i}{\sum_{j=1}^{m} q_j x_j} \tag{3.30}$$

$$\theta_i' = \frac{x_i q_i'}{\sum_{j=1}^{m} q_j' x_j} \tag{3.31}$$

$$\tau_{ji} = \left[-\frac{(u_{ji} - u_{ii})}{RT} \right] \tag{3.32}$$

The activity coefficient expressions are a combination of the combinational and residual contributions:

$$\ln \gamma_i = \ln \gamma_i^C + \ln_i^R \tag{3.33}$$

$$\ln \gamma_1^C = \ln \frac{\Phi_1}{x_1} + \frac{z}{2} q_1 \ln \frac{\theta_1}{\Phi_1} l_i - \frac{\Phi_i}{x_i} \sum_{j=1}^{m} x_j l_j \tag{3.34}$$

$$\ln \gamma_1^R = -q_1 \ln \left(\sum_{j=1}^{m} \theta_j' \tau_{ji} \right) + q_i' - q_i' \sum_{j=1}^{m} \frac{\theta_j' \tau_{ji}}{\sum_{k=1}^{m} \theta_k' \tau_{kj}} \tag{3.35}$$

where

$$l_i = \frac{z}{2}(r_i - q_i) - (r_i - 1) \tag{3.36}$$

As was the case with the preceding models based on the "local composition concept", the UNIQUAC equation like the NRTL and Wilson is readily extendable to handle multi-component mixtures. The UNIQUAC model has limited explicit temperature dependence", [Prausnitz et al., 1980].

3.2.6 Low pressure VLE (LPVLE) data regression

LPVLE data regression involved determining which relevant model (Gibbs excess models, discussed in this chapter) provides the best representation of LPVLE data. The number of experimental VLE data points exceeds the number of adjustable parameters such that an exact solution of Equation (3.8) is not possible. "An exact fit for the data within the empirical or semi-theoretical framework of the model is not achievable due to random and systematic errors and shortcomings of the model", [Prausnitz *et al.*, 1980]. Thus optimum parameters and a "best fit" model must be obtained to best represent the Equation (3.8). The method chosen for LPVLE data regression is the gamma-phi method discussed below. This method uses an equation of state to calculate the fugacity coefficients and Gibbs excess models to evaluated activity coefficients. Other methods to regress LPVLE are detailed in Smith et al. [1996].

3.2.6.1. Gamma-phi method

"The goal with the gamma-phi method is to obtain the fitting constraints in a feasible model equation for activity coefficients", [Raal and Mühlbauer, 1998]. The calculation of the composition of one phase from the specification of the other at a desired temperature and pressure range may be accomplished using this method. The gamma-phi method to regress T-xi (Bubble point pressure calculation) and P-xi (Bubble point temperature calculation) is illustrated by the Figure 3.3 and Figure 3.4:

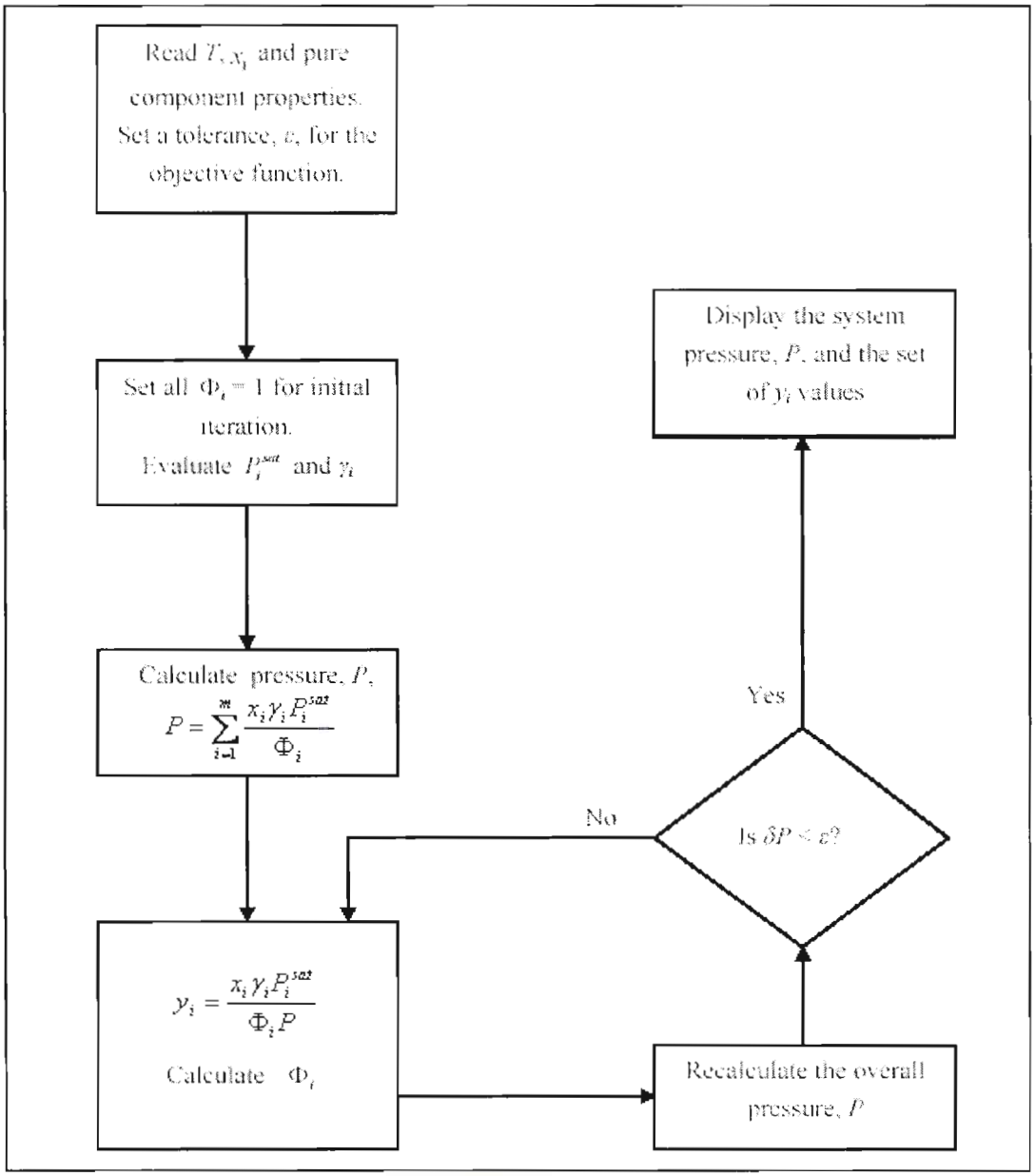

Figure 3.3 Block diagram of Bubble Pressure calculation, Smith et al [1996]

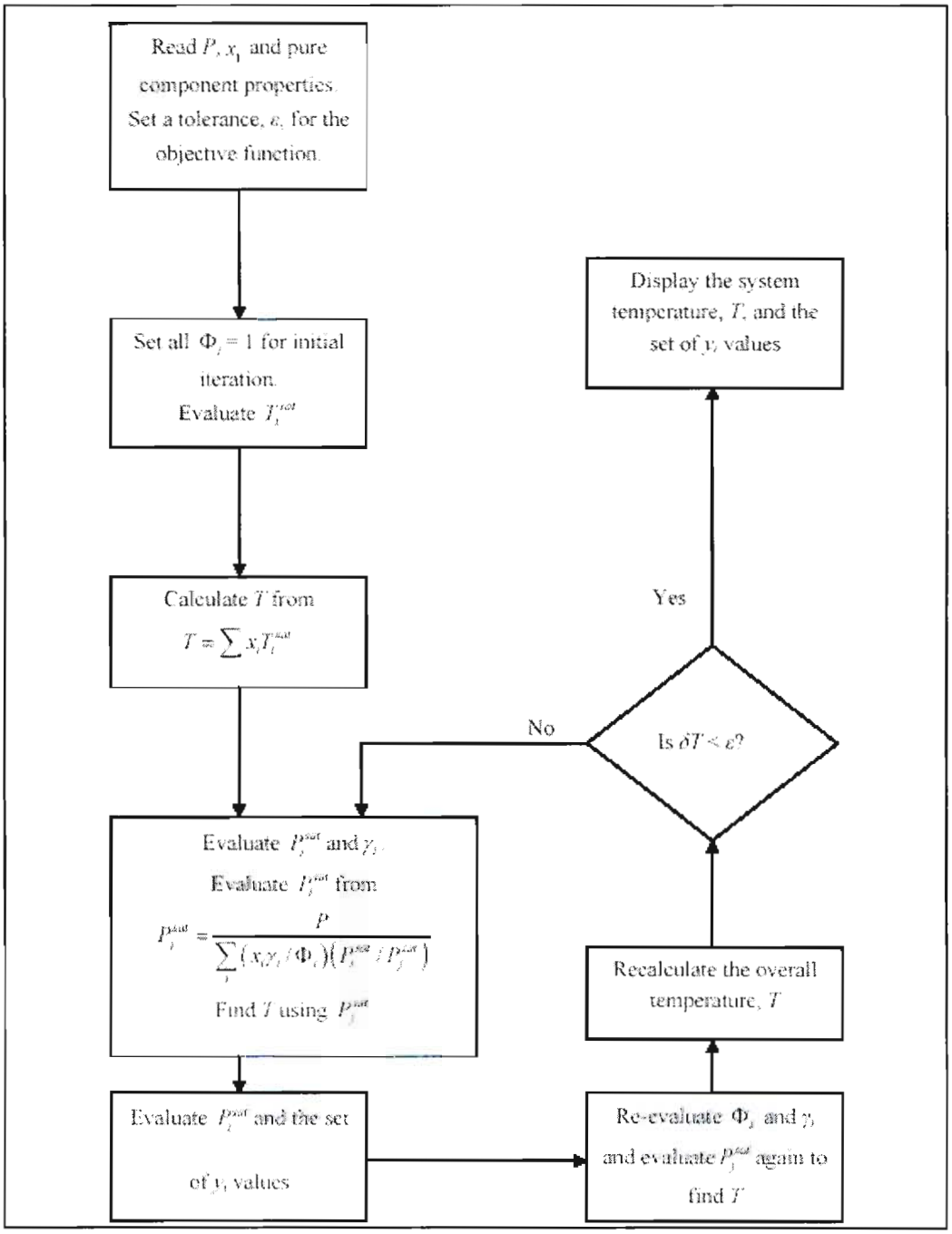

Figure 3.4 Block diagram of Bubble Temperature calculation, Smith et al [1996]

$$S = \sum \left(\partial P\right)^2 \tag{3-37}$$

The difference between the model and experimental values is termed the residual and symbolised by using δ. Other objective functions may also be used such as $\delta y1$, $\delta \gamma 1$, $\delta \gamma 2$ and δ (G^E/RT) but Van Ness et al. [1978] states that Equation (3-37) is the simplest and most direct objective function. Van Ness and Abbott [1982] recommend replacing the pressure with temperature in Equation (3-36), provides an objective function for regressing isobaric data which was used to determine model parameters. The sum of the squares of the difference between the calculated and the measured pressures was used as the object function, Equation (3-37)

3.3 Liquid-liquid equilibrium (LLE)

Two immiscible liquid components that are mixed together at constant temperature and pressure will split forming two or more separate liquid phases of different compositions at a particular overall composition. If the phases reach equilibrium then this is called LLE. LLE has many applications in industry e.g. solvent extraction. Figure 3.5 shows three different variations of binary LLE described in detail in Smith et al. [1996].

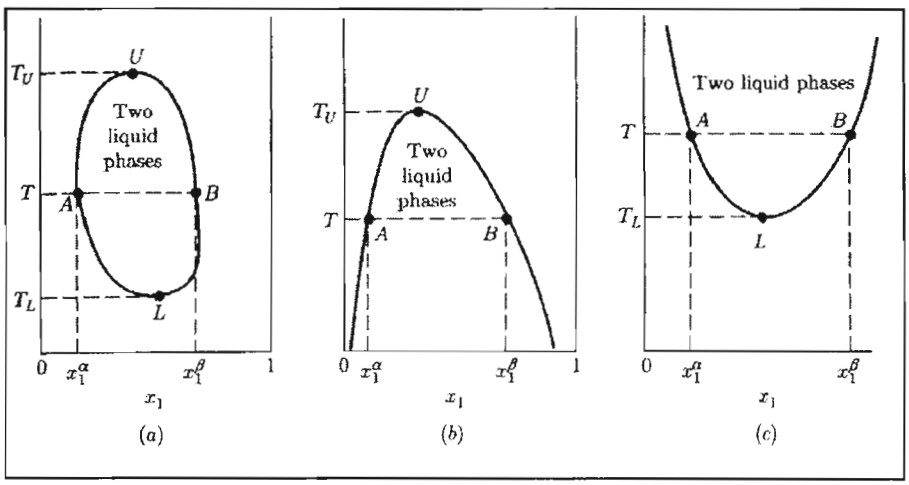

Figure 3.5: Three types of constant pressure binary liquid-liquid Equilibrium, Smith et al. [1996]

3.3.1 Ternary LLE

Ternary LLE data is measured at constant temperature and pressure. For ternary systems there exist two common types (described in detail in Treybel [1976]). Type I systems have only one binary pair partially miscible. Type II systems have two binary pairs partially miscible and the third binary completely immiscible, shown in Figure 3.5. "Ternary LLE can be predicted if the binary solubility LLE data and VLE data is available", [Prausnitz *et al*, 1986].

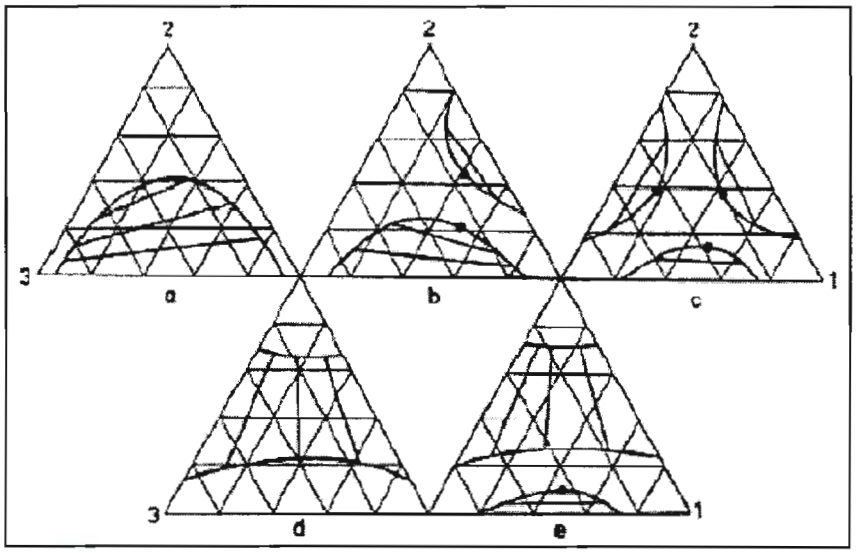

Figure 3.5 Ternary LLE diagrams, Walas [1982]

3.3.2Theoretical aspects of LLE

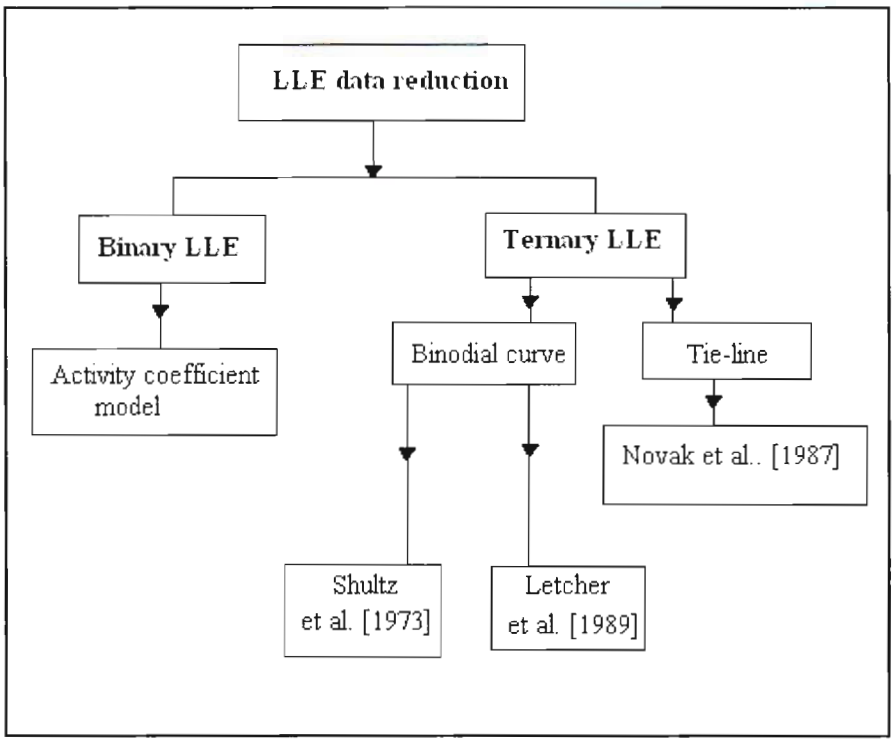

Figure 3.6 An overview of LLE data regression

LLE data regression requires activity coefficients to model each phase. At equilibrium using the fugacities and denoting the two phases by α and β, Equation (3-14) gives (Full derivation given by Walas, [1982]):

$$\hat{f}_i^{\beta} = \hat{f}_i^{\alpha} \qquad (i = 1, 2 \ldots\ldots N) \qquad (3\text{-}38)$$

After introducing activity coefficients:

$$x_i^{\alpha} \gamma_i^{\alpha} = x_i^{b} \gamma_i^{b} \qquad (3\text{-}39)$$

If fugacity, f, for each pure species can exist as liquid at the temperature of the system then they are equal.

3.3.3 LLE Modelling

In the following sub-sections, a discussion on the modelling of mutual solubility data for binary systems, the regression of tie-line data for ternary systems and the correlation of binodial curves for ternary systems is presented. Ternary LLE is correlated independently as the binodial curve and the tie-lie. This section presents the activity coefficient models, binodial curve models and object functions used in this study. A more detailed description of models outlined in this section can be found in Walas [1985].

3.3.4 Binary LLE: Activity Coefficient Model

The following two models were chosen based on their algebraic simplicity and extensive use in binary LLE representation (detailed derivation in Raal and Mühlbauer [1998]). The Margules three suffix:

$$\frac{G^E}{RT} = x_1 x_2 \left[A_{12} x_2 + A_{21} x_1\right] \tag{3-40}$$

The activity coefficients can then be derived as for γ_1 and γ_2:

$$\ln \gamma_1 = \left[A_{12} + 2(A_{21} - A_{12}) x_1\right] x_2^2 \tag{3-41}$$

$$\ln \gamma_1 = \left[A_{12} + 2(A_{21} - A_{12}) x_1\right] x_2^2 \tag{3-42}$$

Applying the above two equations to the equilibrium criterion for binary LLE allows the parameters A_{12} and A_{21} to be found:

$$\frac{A_{12}}{A_{21}} = \frac{2\psi_2 \ln\left(\frac{x_2^\beta}{x_2^\alpha}\right) + \zeta_1 \ln\left(\frac{x_1^\beta}{x_1^\alpha}\right)}{2\psi_1 \ln\left(\frac{x_1^\beta}{x_1^\alpha}\right) + \zeta_2 \ln\left(\frac{x_2^\beta}{x_2^\alpha}\right)} \tag{3-43}$$

$$A_{21} = \frac{\ln\left(\frac{1-x_1^{\beta}}{1-x_1^{\alpha}}\right)}{\left(x_1^{\alpha}\right)^2\left[1+2x_2^{\alpha}\left(\frac{A_{12}}{A_{21}}-1\right)\right]-\left(x_1^{\beta}\right)^2\left[1+2x_2^{\beta}\left(\frac{A_{12}}{A_{21}}-1\right)\right]} \tag{3-44}$$

where

$$\psi_i = \left(x_i^{\alpha}\right)^2 - \left(x_i^{\beta}\right)^2 - \left(x_i^{\alpha}\right)^3 + \left(x_i^{\beta}\right)^3$$
$$\zeta = \left(x_i^{\alpha}\right)^2 - \left(x_i^{\beta}\right)^2 - 2\left(x_i^{\alpha}\right)^3 + 2\left(x_i^{\beta}\right)^3 \tag{3-45}$$

For the Van Laar [1910] the Excess Gibbs energy is defined as:

$$\frac{G^E}{RT} = \frac{A_{12}A_{21}x_1x_2}{x_1A_{12}+x_2A_{21}} \tag{3-46}$$

The activity coefficients can be derived:

$$\ln\gamma_1 = A_{12}\left[\frac{A_{21}x_2}{x_1A_{12}+x_2A_{21}}\right]^2 \tag{3-47}$$

$$\ln\gamma_2 = A_{21}\left[\frac{A_{12}x_1}{x_1A_{12}+x_2A_{21}}\right]^2 \tag{3-48}$$

Similarly, by applying equation (3-45):

$$\frac{A_{12}}{A_{21}} = \frac{\left(\frac{x_1^{\alpha}}{x_2^{\alpha}}+\frac{x_1^{\beta}}{x_2^{\beta}}\right)\left[\frac{\ln\left(x_1^{\beta}/x_1^{\alpha}\right)}{\ln\left(x_2^{\beta}/x_2^{\alpha}\right)}\right]-2}{\frac{x_1^{\alpha}}{x_2^{\alpha}}+\frac{x_1^{\beta}}{x_2^{\beta}}-2\frac{x_1^{\alpha}x_1^{\beta}\ln\left(x_1^{\beta}/x_1^{\alpha}\right)}{x_2^{\alpha}x_2^{\beta}\ln\left(x_2^{\beta}/x_2^{\alpha}\right)}} \tag{3-49}$$

$$A_{12} = \frac{\ln\left(\frac{x_1^{\beta}}{x_1^{\alpha}}\right)}{\left[1+\left(\frac{A_{12}}{A_{21}}\right)\left(\frac{x_1^{\alpha}}{x_2^{\alpha}}\right)\right]^{-2} - \left[1+\left(\frac{A_{12}}{A_{21}}\right)\left(\frac{x_1^{\beta}}{x_2^{\beta}}\right)\right]^{-2}} \tag{3-50}$$

3.3.5 Ternary LLE Binodial curve

The models given below have no thermodynamic basis but are rather mathematically based. Detailed derivations may be found in Shultz et al. [1973] and Letcher et al. [1989].

The β function (Shultz et al. [1973]):

$$x_2 = B_1(1-x_A)^{B_2} x_A^{B_3} \tag{3-51}$$

The log-γ function (Letcher et al. [1989]):

$$x_2 = C_1(-\ln x_A)^{C_2} x_A^{C_3} \tag{3-52}$$

The constants in the above equation would have to be mathematically fitted using experimental data. The above two functions were minimized using the following standard deviation:

$$\sigma = \left[\left(\sum_{i=1}^{n} x_2 calc - x_2 \exp\right)^2 / (n-3)\right]^{0.5} \tag{3-53}$$

3.3.6 Tie line

The tie line data was regressed using the multi-component form of the NRTL and UNIQUAC. Both equations mentioned before can handle highly non-ideal systems. Solving both of these equations require non-linear objective functions. Novak et al. [1987] suggested the use of the least square objective function optimization. The method employed is given in Novak et al. [1987]:

$$F(P) = \sum_{i=1}^{n} \left\langle x_{1i}^{\alpha}(\exp) - x_{1i}^{\alpha}(calc)(P,T) \right\rangle_i^2 + \left\langle x_{2i}^{\alpha}(\exp) - x_{2i}^{\alpha}(calc)(P,T) \right\rangle_i^2 + \left\langle x_{1i}^{\alpha}(\exp) - x_{1i}^{\alpha}(calc)(P,T) \right\rangle_i^2 + \left\langle x_{2i}^{\alpha}(\exp) - x_{2i}^{\alpha}(calc)(P,T) \right\rangle_i^2 \quad (3\text{-}54)$$

The root mean square deviation (RMSD) was used as an indication of the precision of the correlation:

$$RMSD = \left[\frac{\sum_a \sum_b \sum_c x_{abc}(\exp)^2 - x_{abc}(calc)^2}{6k} \right] \quad (3\text{-}55)$$

3.7 Thermodynamic Consistency

Experimental data normally contains temperature, pressure and both vapour and liquid compositions which represents an over-specification of VLE. These directly measured variables are subject to systematic errors. Thermodynamic consistency tests validate experimental data and check the conformity to the Gibbs-Duhem equation. "The main purpose for measuring the vapour composition is for thermodynamic consistency testing", [Van Ness et al., 1978]. Other thermodynamic consistency tests are detailed in Raal and Mühlbauer [1998].

3.7.1 The Point Test

When all four variables are measured for a binary VLE data set, an over-specification of the system is obtained. According to the phase rule of Gibbs, three experimentally determined variables can be used to obtain the fourth variable. Vapour compositions introduce the most error and are thus used to test for thermodynamic consistency.

This test compares the measured vapour compositions (y_{exp}) to the calculated values (y_{calc}) (residual value). "The magnitude of the residual value provides and indication of the consistency of the VLE data", [Raal and Mühlbauer, 1998] and y_{ad}, should be less than 0.01 for the data to be thermodynamically consistent:

$$\Delta y_{ad} = \frac{1}{n}\left(\left| y_{\exp} - y_{calc} \right|\right) \quad (3.56)$$

CHAPTER 4

DESCRIPTION OF EXPERIMENTAL EQUIPMENT

This chapter aims to describe in detail the experimental apparatus used to acquire phase equilibrium data (PED). The modified VLE re-circulating still used by Ndlovu [2005] and the peripheral pieces of equipment used in the VLE apparatus will be discussed along with modifications made for binary VLE systems with a high relative volatility. The LLE data measurements were conducted using the LLE still of Ndlovu [2005]. This chapter aims to cover the following aspects:

1. Modified VLE still of Ndlovu [2005]
2. Modifications to the VLE still
3. Temperature measurement and control, pressure measurement and control, and composition measurement of the equilibrium phases.
4. LLE still of Ndlovu [205]
5. Temperature measurement and control, pressure and composition measurement for the LLE still

4.1 VLE apparatus

The VLE apparatus used in this study was based on that used by Ndlovu [2005]. The structural modifications made to enhance the operation of the still are discussed in Section 4.2. This section details the peripheral equipment used to aid the modified VLE still of Ndlovu [2005]. A schematic representation of the VLE apparatus is shown in Figure 4.1.

The newly measured binary VLE systems of interest in this study have a very high relative volatility and proved difficult to measure using dynamic re-circulating VLE apparatus, [Gillespie, 1976]. The re-circulating VLE still of Ndlovu [2005] based on the design of the VLE still of Raal and Mühlbauer [1998] was a robust VLE still capable of acquiring low pressure VLE data from systems of partial miscibility but could not measure systems of high relative volatility. This can be largely attributed to poor equipment design and experimental procedure. This study is aimed to eliminate these two limitations using a modified dynamic re-circulation VLE apparatus.

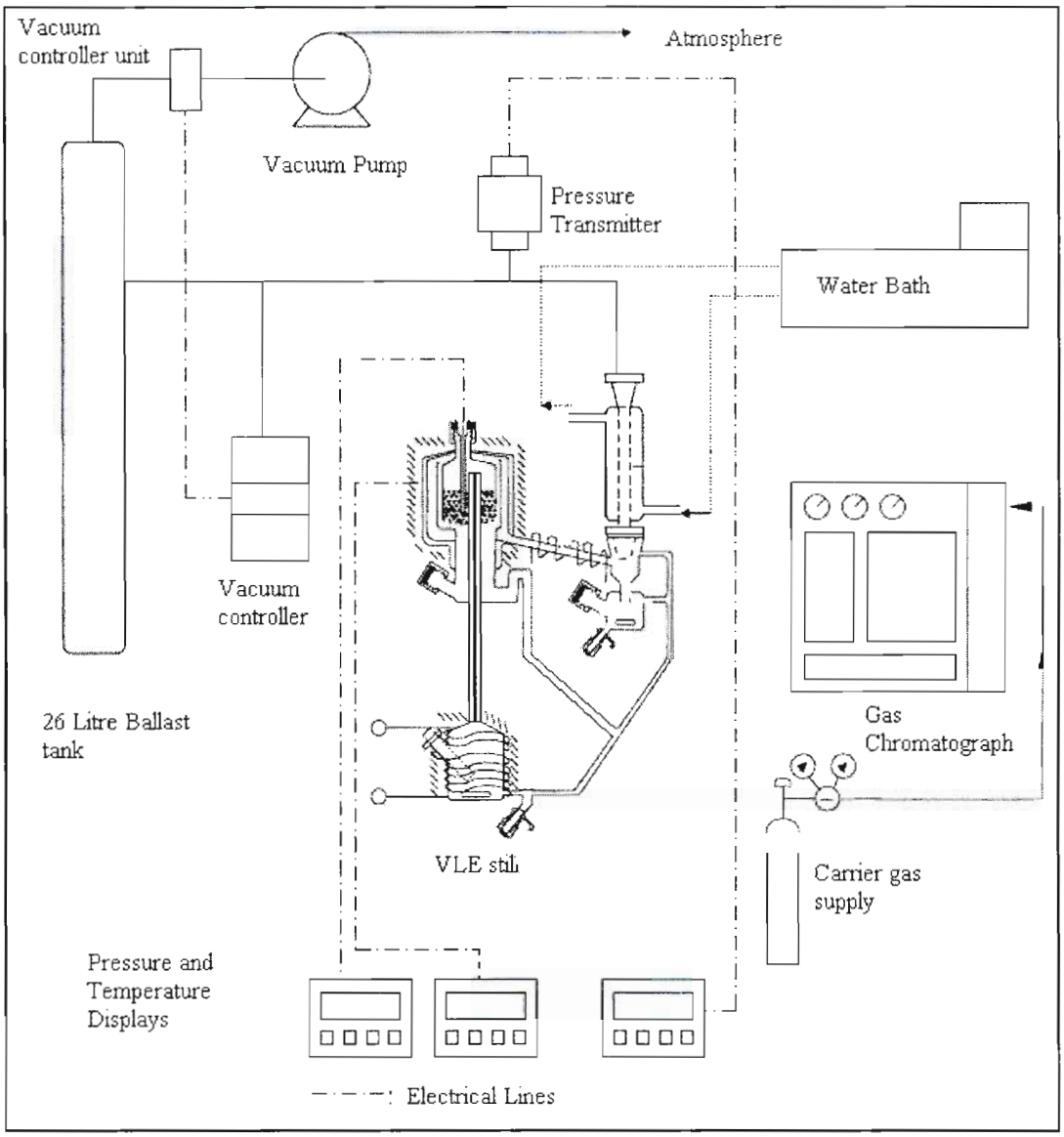

Figure 4.1 Schematic representation of the VLE apparatus

The VLE apparatus consisted of the following:

- The VLE dynamic still (discussed in more detail in Section 4.1.1).
- A 25 L ballast tank.
- A Labotech cooling coil unit.
- A WIKA model P10 pressure transmitter.
- A Hewlett Packard multi-meter (model 3440) 6 ½ digit pressure display.
- Four Pt-100 temperature sensors.
- A Labotech water bath complete with ethylene glycol solution as the cooling medium and a water pump.

- Two power pack motors
- DC power supply
- A KNF vacuum pump-controller unit
- The Hewlett Packard Model 5890 Series II gas chromatograph.

The KNF vacuum pump controller unit operates by evacuating incondensable gasses from the VLE still until the measured pressure reaches the controller set-point pressure. Once the set-point pressure has been reached the vacuum controller shuts off the vacuum pump. As it is nearly impossible to create a perfectly air tight apparatus, any increase in pressure exceeding the set tolerance will cause the vacuum pump to start up again until the pressure set-point is reached.

4.1.1 Modified VLE still of Ndlovu [2005]

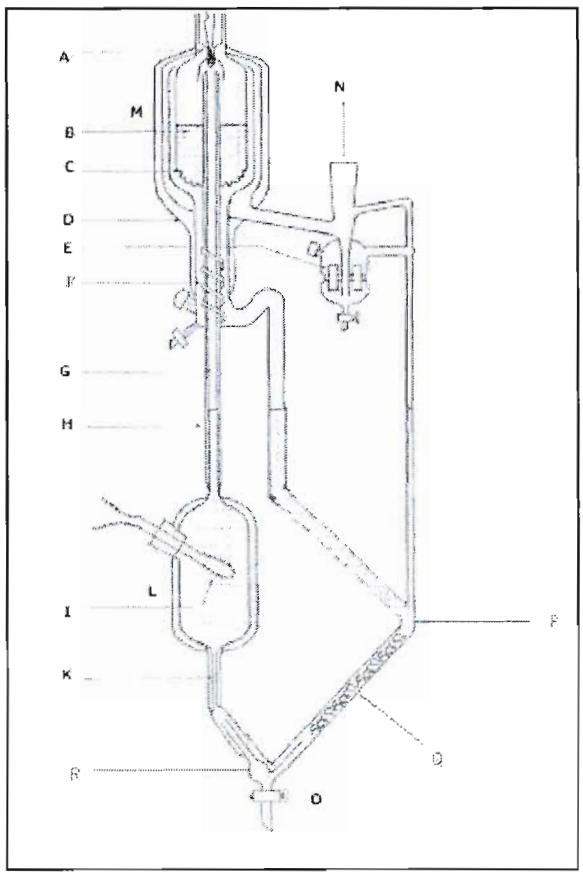

Figure 4.2 VLE still of Ndlovu [2005]

A-Temperature sensor, B-s/s wire mesh packing, C-Equilibrium chamber, D-Vacuum jacket, E-magnetic stirrer, F- s/s spiral, G-Cottrell tube, H-Vacuum jacket, I-Glass tube, K-Capillary, L-Reboiler, M-Equilibrium chamber, N-Inlet to condenser , O-Drain Valve, P-Mixing tee, Q-Glass spiral, R-mixing chamber

The VLE still is shown in Figure 4.2. Initially, a binary liquid solution is charged into the boiling chamber (L). Heat is added to the boiling chamber (L) via an internal and external heater which boils the solution. The external heater compromises of resistance wire wrapped around the boiling chamber (L). The external heater accounts for heat lost to the surroundings. A heating cartridge was placed in a glass tube (I) into the boiling chamber (L) to initiate the boiling process. The glass tube (I) was roughened to promote nucleation. The vapour-liquid mixture generated in the boiling chamber (L) moves up through the vacuum insulated Cottrell tube (G) (thermal lift pump). The mixture flows downward through the vacuum jacketed equilibrium chamber (M) packed with 3mm wire mesh. This created larger interfacial surface area and increased contact times between the phases as stated by Yerazunis [1964]. A themo-well (A) housing a Pt-100 temperature sensor measured equilibrium temperature at the base of the packing where the phases disengage ensuring maximum contact time. The vapour flows upwards and around the equilibrium chamber (M) creating adiabatic conditions around the equilibrium chamber (M). The vapour moves to the condenser (N) and is collected in the sampling point (E) where is magnetically stirred. The liquid flows out of holes in the base of the equilibrium chamber and into the liquid sampling trap (F). Both liquid and vapour condensate are combined and returned to the boiling chamber via the mixing tee (P). Other features of the still include:

1. The equilibrium chamber is angular symmetric about the Cottrell tube (G). This ensures no preferential radial flow of the vapour-liquid mixture.
2. Magnetic stirring in the vapour condensate trap (E) and inside the boiling chamber.
3. Contains a siphon break tube (K) to eliminate backflow into sample traps.
4. Sampling traps contain septa whereby a sample may be withdrawn without effecting the operation of the VLE still.
5. Very low pressure drop across the packing in equilibrium chamber.

4.2 Modifications to VLE still

4.2.1 Return Tee

The VLE still of Ndlovu [2005] combined the return lines of the liquid and vapour condensate at point O, Figure 4.2, before flowing into the boiling chamber. This design creates little mixing and contact times for the liquid in the return lines. The boiling chamber is magnetically stirred and this design is applicable to chemical mixtures displaying close to ideal liquid behaviour as shown by Joseph et al. [2001].

However, systems that display high relative volatility exhibit large differences in concentration between the vapour condensate and liquid in the return lines. These differences in concentration generate significant difference in densities between the return liquids and require greater agitation to create a homogeneous mixture. Failure to correctly mix this mixture could lead to flashing of the more volatile component in the boiling chamber due to short contact times and inadequate mixing. (P), Figure 4.2, illustrates the design modification implemented to correct this problem.

The vapour condensate and liquid return lines were combined into a tee formation. The tee was constructed from clear glass and a clear glass mixing spiral was added as shown in Figure 4.2, (Q). This modification increased the contact time and mixing times of the liquid mixture by combining the return lines. The glass spiral alters the conventional flow and reduces the effect of channelling of the more volatile component into the boiling chamber. It conceptually, would shorten equilibrium time for chemical mixtures displaying close to ideal liquid behaviour. The tee design does not interfere with the hold-up of the liquid. The spiral was constructed out of glass to eliminate corrosion since the spiral could not be removed without breaking the still. The drain valve was altered to incorporate the mixing chamber (discussed in section 4.2.2).

4.2.2 Mixing chamber

A circular mixing chamber was added for further agitation of the liquid mixture shown in Figure 4.1, (R). The liquid mixture from the return tee enters the mixing chamber tangentially creating a vortex similar in principal to liquid feed entering a hydro-cyclone. The swirling solution creates a small vortex in this chamber vigorously agitating the liquid before entering the siphon break tube. This modification was constructed by Mr. P. Siegling (glassblower).

4.2.3 Heat loads

Resistance wire was wrapped around the return tee design (P) and mixing chamber (R). This served two purposes:

1. Pre-heating the solution before entering the boiling chamber thus reducing flashing of the more volatile component and reducing the heat load of the boiling chamber.
2. Reduce heat losses to the environment.

This resistance wire around the tee and mixing chamber operated independently of the resistance wire around the boiling chamber and was adjusted depending on conditions.

4.3 Temperature Measurement and Control

Equilibrium temperature was measured by Pt-100 temperature sensor housed in a glass tube shown in Figure 4.1(A) extending to the base of the equilibrium chamber. The Pt-100 was connected to a Hewlett-Packard (model 3440) 6 ½ digit multi-meter displaying resistance. Accuracy of temperature measurement was estimated to be ± 0.02 K.

Temperature was controlled at fixed values by manually adjusting the pressure set-point in the KNF pressure controller. Lowering the pressure decreased the temperature and raising the temperature increased the temperature. The accuracy of this temperature control was estimated to vary between 0.01 K and 0.05 K. Temperature calibrations are detailed in Chapter 5.

4.3.1 Pressure Measurement and Control

Pressure was measured using a WIKA model P10 pressure transmitter and calibrated using Vaisala electronic pressure transmitter (model PTB100A). Pressure control was facilitated by a KNF vacuum pump-controller unit. The vacuum pump was connected to a 25 liter ballast tank to reduce fluctuations in pressure. The pressure accuracy was estimated to be ±0.04 kPa. Pressure calibrations are detailed in Chapter 5.

4.3.2 Sampling and Composition measurement

Equilibrium samples were withdrawn from the sample traps using a 1 µl gas-tight liquid GC syringe through a chemically resistant septum. Sampling with the gas-tight syringe did not interfere with the operation of the VLE still. The gas-tight liquid syringe used for sampling had a needle diameter of 0.1 mm and when injected through the chemical resistant septum did not effect either the measured equilibrium pressure or the temperature in the VLE still. Such findings were also reported by Ndlovu [2005].

A Hewlett Packard 5890 Series II Gas Chromatograph was used to accurately analyse compositions of the equilibrium liquid and vapour samples. The GC was operated with a thermal conductivity detector (TCD) and a 2.5m long stainless steel column (2.2 mm in diameter) packed with 80/100 mesh Chromosorb P. The composition measurements were estimated to be accurate to within ± 0.001 of a mole fraction. Calibrations and operating procedure are discussed in Chapter 5.

4.4 LLE apparatus

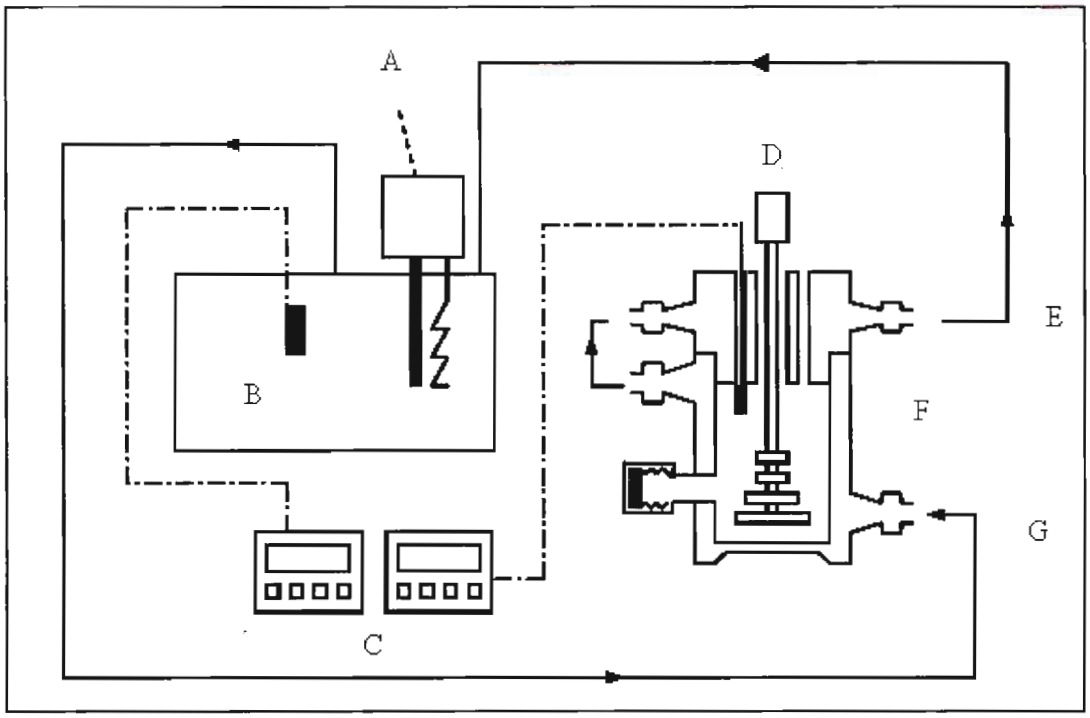

Figure 4.3 LLE apparatus

A-temperature controller, B-water-bath, C-temperature display, D- stirrer, E- cold liquid out, F-LLE still, G-hot liquid in

Figure 4.3 presents a schematic the layout of the LLE apparatus. It comprises of a double walled glass cell, Labcon water bath, 2x Pt-100 temperature sensors and respective temperature displays and a motor stirrer with DC power supply.

4.4.1 The LLE Still

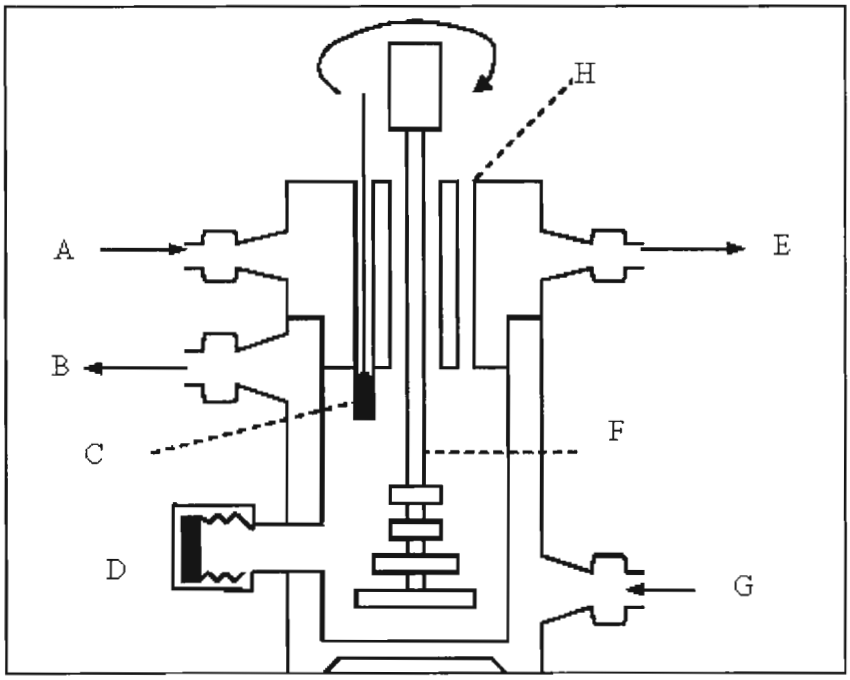

Figure 4.4 LLE still of Ndlovu [2005]

A-hot fluid in, B-hot fluid out, C-Pt-100 thermo-well, D and H-sample points, E-hot liquid out, F-stirrer, G-hot liquid in

The LLE still was used in LLE apparatus of Ndlovu [2005]. The double walled cell is operated isothermally by a temperature controller (G) circulating a hot fluid through the lid which has a thermo-well in which a Pt-100 temperature sensor (H) is housed. The heterogeneous liquid mixture was mixed by a stirrer (D) driven by a miniature variable speed DC motor. Two different sampling points are provided (I, J) for the two phases shown in Figure 4.4. A Teflon bush (K) held the stirrer in the upright position and decreased vibrations.

4.2.2 Temperature measurement and control

The temperature was recorded using the temperature sensors measuring the water bath temperature and equilibrium temperature. Two Pt-100 temperature sensors were used to measure these temperatures. The Pt-100 sensor for the bath temperature was fitted into a thin walled stainless steel tube and fully immersed into the bath while that for the equilibrium temperature

was housed inside a thermo-well (C) on the cell shown in Figure 4.4. The temperature control was estimated to be ±0.02 K. Temperature calibration is detailed in Chapter 5.

4.2.3 Sampling and composition analysis

One micolitre gas-tight liquid GC syringes were used to sample the two liquid phases in equilibrium. The samples were analysed using the Hewlett Packard 5890 Series II gas chromatograph as described for the VLE apparatus. Calibration of the GC is treated is detailed in Chapter 5.

CHAPTER 5
EXPERIMENTAL PROCEDURE

This chapter details the experimental procedure and methods followed when operating the VLE and LLE apparatus discussed in Chapter 4. The following sections will be covered:

1. Preparation of the experimental equipment
2. Operation of the VLE and LLE apparatus
3. Calibration of equipment used in the apparatus

5.1 VLE still

5.1.1 Preparation of VLE apparatus

5.1.1.1 Leak detection

Chemicals used in the VLE still have to be of the highest purity. Any small impurity or foreign substance would affect the quality of data. Thus, it was imperative to eliminate any leaks in the still as VLE measurements were conducted at sub-atmospheric pressures.

The leaks were detected by setting the pressure control to a set-point below atmospheric pressure. The VLE still was then isolated by shutting of the necessary valves and any increase of pressure recorded. Joint leaks were detected by adding liquid acetone on the outside of joints. If a small spike in pressure was detected then a leak was identified. The spike in pressure is caused by liquid acetone flashing in the still due to the low pressure in the VLE still. Leaks were eliminated by adding vacuum grease onto glass joints and vacuum seal to steel joints.

5.1.1.2 Cleaning of still

Cleaning of the still was undertaken before calibrations or before a new binary VLE system was measured. This was achieved by operating the still isobarically with pure acetone at a pre-determined pressure for an hour. Thereafter, the still was drained and the process repeated until only the acetone peak was detected after a GC analysis. The resulting acetone was drained and still placed at a very low pressure to allow excess acetone to vaporize.

5.1.2. Pressure Calibration

Equilibrium pressure inside the system was measured by a WIKA P-10 pressure transmitter. This device was calibrated by attaching a NIST certified electronic pressure transmitter (VAISALA Model PTB100A) together with the WIKA P-10 pressure transmitter to the VLE still. The pressure controller was allowed to control pressure at set-points in the range of 5kPa to 100kPa and the both pressure readings from the electronic pressure transmitter and the WIKA P-10 transmitter were recorded. Consequently using this data, a linear plot of actual pressure vs. displayed pressure was recorded shown in Figure 5.1.

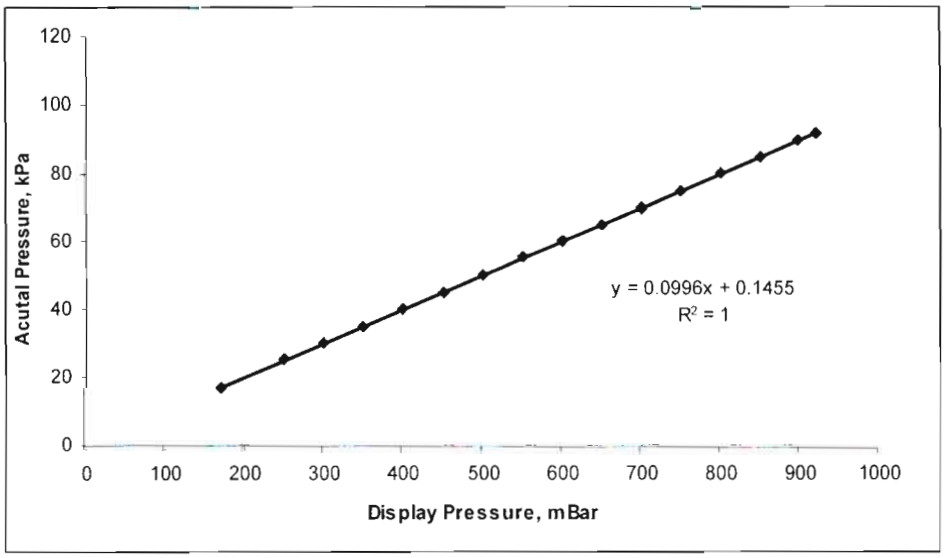

Figure 5.1 Pressure transmitter calibration

5.1.3 Temperature Calibration

Equilibrium temperature was measured inside the equilibrium chamber by a Pt-100 temperature sensor. The Pt-100 temperature sensor was connected to a HP 34401 multi-meter and the resistance was recorded. The temperature calibration was carried out using chemicals of the highest available purity (> 99.5%). A low boiler (ethyl acetate) and a high boiler (octane) were used to calibrate the sensor across a wide temperature range, known as the "in-situ" temperature calibration.

The VLE still was operated isobarically and the resistance recorded using the HP multi-meter along with the pressure. The true temperature of the system was calculated using the Antoine equation obtained from Reid et al. [1988]. Thus a graph of the resistance vs. the actual temperature was generated shown in Appendix C.

5.1.4 Gas Chromatograph (GC) Calibration

GC analysis is a critical aspect of VLE data measurement. A Hewlett Packard 5890 series II GC with a TCD (thermal conductivity detector) was used to analyse compositions. A packed column was used to analyse each VLE system presented. The operating conditions for the GC are tabulated in Table 5.1. The detector was calibrated by the area ratio method detailed in Raal and Mühlbauer [1998].

For a binary mixture, liquid samples were prepared by gravimetrically weighing samples with mole fraction ratios (x_1/x_2) evenly across the entire composition range. Zero point five micro-litre samples were injected into the GC and the ratio of the response factors (F_1/F_2) calculated. The response factors were generated by plotting the area ratios against the composition ratios, A_1/A_2 vs. x_1/x_2 and A_2/A_1 vs. x_2/x_1. If the plot is linear then the inverse of the gradient of the first response factor must equal the gradient of the second response factor. This is a test for the calibration procedure as stated by Raal and Mühlbauer [1998]. GC calibration plots are shown in Appendix B.

Normally the number of moles (n) passing through a detector is proportional to the peak area (A) generated by the integrator.

$$n_i = F_i A_i \tag{5.1}$$

where F_i is the response factor. By applying the area ratio method to a binary mixture the following is derived:

$$\frac{n_i}{n_2} = \left(\frac{F_1}{F_2}\right)\left(\frac{A_1}{A_2}\right) = \frac{x_1}{x_2} \tag{5.2}$$

Extending this to a mixture containing l components [Detailed derivation given in Raal and Mühlbauer, 1998]:

$$x_1 = \frac{1}{1 + \sum_{l=2}^{n} \frac{x_l}{x_1}} \tag{5.3}$$

Ternary LLE calibrations were carried out using binary pairs as detailed in Raal and Mühlbauer [1998]. The GC operating conditions for the light alkanols + water are tabulated in Table 5.1.

Table 5.1 HP GC operating conditions

System	Cyclohexane + Ethanol	n-Dodecane + Ethanol	n-Dodecane + 2-Propanol	Water + alkanol
Gas flow rate, ml/min	28	28	28	28
Oven init temp, K	423	378	393	378
Init time, min	-	7	7	-
Rate rise, K/min	-	47	47	-
Final Temp, K	-	533	533	-
Hold Time, min	-	4	4	-
Detector Temp, K	473	518	518	518
Attenuation	1	1	1	1
Range	-	-	-	-
Injector Temp, K	473	493	493	493

5.2 Operational Procedure for the VLE apparatus

5.2.1 Isobaric measurement

The following procedure was undertaken for isobaric measurement:

1. The HP multi-meter, stirrer motors, pressure transmitter, pressure display and vacuum pump are switched on.
2. The cold finger (Labotech) was switched on and the temperature of the cooling fluid (ethylene glycol) in the water bath was allowed to cool to 0°C.

3. One of the pure components is charged into the clean VLE still to a level approximately 4cm above the boiling chamber. Cooling liquid is re-circulated through the condenser and the pressure set-point is entered.
4. The external heater is switched on and the voltage varied until the liquid starts to boil. This heater is used to prevent heat losses to the surroundings. The internal heater is switched on and varied until such time that a fast pumping action in the Cottrell pump is achieved. The voltage is further increased until the temperature of the mixture remains constant (plateau region), regardless of a small increase or decrease in voltage at stated by Kneisl et al. [1989].
5. Equilibration time depends on Cottrell pump re-circulation rate and on the system properties. Equilibrium is normally achieved in approximately 30-45minutes. Good circulation rates and large drop rates should be apparent at equilibrium. At equilibrium, temperature remains constant ±0.02 K and when no large fluctuations are noticed in the vapour and liquid return line levels.
6. When equilibrium is established the temperature is recorded and vapour (condensate) and liquid sample are withdrawn using a 1µl gas tight GC syringe. Theses samples are immediately injected into the GC. Three samples are taken for each phase or until such time that compositions remain constant.
7. After the vapour and liquid samples are analyzed, the VLE still is allowed to cool and a small amount of liquid is withdrawn and a predetermined amount of the second liquid is injected into the still. Thereafter, steps 2-5 are repeated until half of the phase diagram is complete.
8. The still is then cleaned and dried (described in 5.1.1) and steps 1-6 repeated starting with the second pure component.

5.2.2 Isothermal operation

Isobaric operation of the VLE still precedes the isothermal operation. Hence, the correct operation of the still isobarically is critical. The VLE still is first operated isobarically, as discussed in section 5.2.1. Once the liquid in the still is circulating properly the isobaric operation is halted and the temperature manually adjusted to the desired value. This is

accomplished by manually increasing or decreasing the pressure set-point in the vacuum controller until the desired temperature is reached and the plateau region found again. Sampling was the same for isobaric operation.

5.3 LLE still

5.3.1 Preparation

5.3.1.1 Cleaning of the LLE cell

The LLE still was much easier to clean than the VLE still. The still was easily dismantled and was cleaned with acetone and allowed to dry for 30 minutes in a fume cupboard and repeated once more. This was done before each new system.

5.3.2 Calibration

5.3.2.1 Cell temperature calibration

A standard temperature probe TE 4023 (WIKA) was used to calibrate the LLE still temperature sensor (see Section4.2.2). Distilled water was allowed to re-circulate inside the LLE still. Hot water was then re-circulated inside the LLE still jacket via a temperature controller mounted in a water bath. The standard probe was placed in the LLE still to give the water temperature. The still was left to reach thermal equilibrium after which the two temperatures, one given by the standard probe and the other by the temperature sensor in the thermo well inside the LLE still, were recorded. The water circulating in the jacket was then increased and the above process repeated for a range of temperatures. From which the LLE still and standard temperatures were used to plot actual temperature vs. the measured temperature. Temperature calibration plots are shown in Appendix B.

The water bath temperature sensor was calibrated following the same procedure outlined for the cell temperature sensor using a standard probe.

5.3.3 LLE Still Operational Procedure

All LLE data measurements were conducted at atmospheric pressure.

5.3.3.1 Binary LLE operation

The LLE still was cleaned as described in 5.3.1.1 and the following operating procedure was used:

1. Two pure components were added in the appropriate amounts such that the interface between the two phases was above the sampling point of the denser liquid.
2. The temperature controller in the water bath was set and the motor stirrers were switched on.
3. The contents of the still were stirred for 30 minutes and then the motor was turned off and the contents allowed to equilibrate for 30 to 60 minutes depending on system.
4. Liquid samples for each phase were withdrawn with a 1µl gas tight liquid syringe and injected into the GC. Equilibrium was determined when the composition of each sample for each phase remained constant and the temperature recorded.
5. The temperature was then increased and steps 2-4 repeated.

After the measuring the LLE data, the still was allowed to cooled and was dismantled and cleaned.

5.3.3.2 Ternary LLE operation

This mode of operation is detailed by, Alders [1959]. The still is initially operated as for a binary LLE mixture (as detailed in Section 5.3.3.1). The equilibrium compositions for this binary mixture were analysed as stated in Section 5.3.3.1 for the desired temperature.

Afterwards, a small volume of the third component is then added to the LLE cell. The stirrer was then switched on for approximately 45 minutes and the heterogeneous mixture was allowed to equilibrate for an hour (depending on the system). The compositions of each phase were then analysed as described for a binary LLE operation. The cell was then drained, cleaned and the above procedure repeated for a larger increment of the third component.

CHAPTER 6
EXPERIMENTAL RESULTS

This chapter presents binary VLE/LLE data as well as ternary LLE data measured in this study. Binary VLE data was measured using the modified VLE still of Ndlovu [2005] and all LLE data measurements were acquired using the LLE still of Ndlovu [2005].

Measured vapour pressure data for ethanol and 2-propanol are presented and compared against literature data, as with isobaric and isothermal binary VLE data for cyclohexane + ethanol at 313.15 K and 40 kPa respectively. The aim of measuring these data sets was to demonstrate the accuracy of the experimental procedures and operation of the VLE apparatus (outlined in Chapter 5). Previously unmeasured binary VLE data for n-dodecane + ethanol at 333.15 K and 343.15 K and binary VLE data for n-dodecane + 2-propanol at 333.15 K, 343.15 K and 353.15 K are presented.

As with the VLE data analysis, binary LLE data was measured for n-heptane + methanol system and presented against literature data to verify the experimental procedures and operation of the LLE apparatus (detailed in Chapter 5). Previously unmeasured ternary LLE data for n-dodecane + ethanol + water at 333.15 K ant 343.15 K and n-dodecane + 2-propanol + water and 328.15 K and 333.15 K are presented. All LLE data was acquired at atmospheric pressure.

6.1 Vapour Pressure curves

Vapour pressure measurements for ethanol and 2-propanol at sub-atmospheric pressures are presented against literature data shown in Figure 6.1 and Figure 6.2. The literature data for each vapour pressure curve was taken from Reid et al. [1988]. Vapour pressure measurements are tabulated in Table 6.1 and Table 6.2. The measured vapour pressure data compares well with literature data as is evident from Figure 6.1 and 6.2.

Table 6.1 Experimental Vapour pressure measurements

P (kPa)	T (K)
Ethanol	
6.60	292.97
12.32	305.82
16.39	311.73
23.28	319.03
34.32	327.17
51.52	335.74
60.42	339.12
74.29	343.50
84.53	346.76
2-Propanol	
4.04	291.23
9.46	305.85
18.83	318.74
31.62	329.15
49.94	338.87
53.54	340.44
83.10	350.47
92.57	353.02

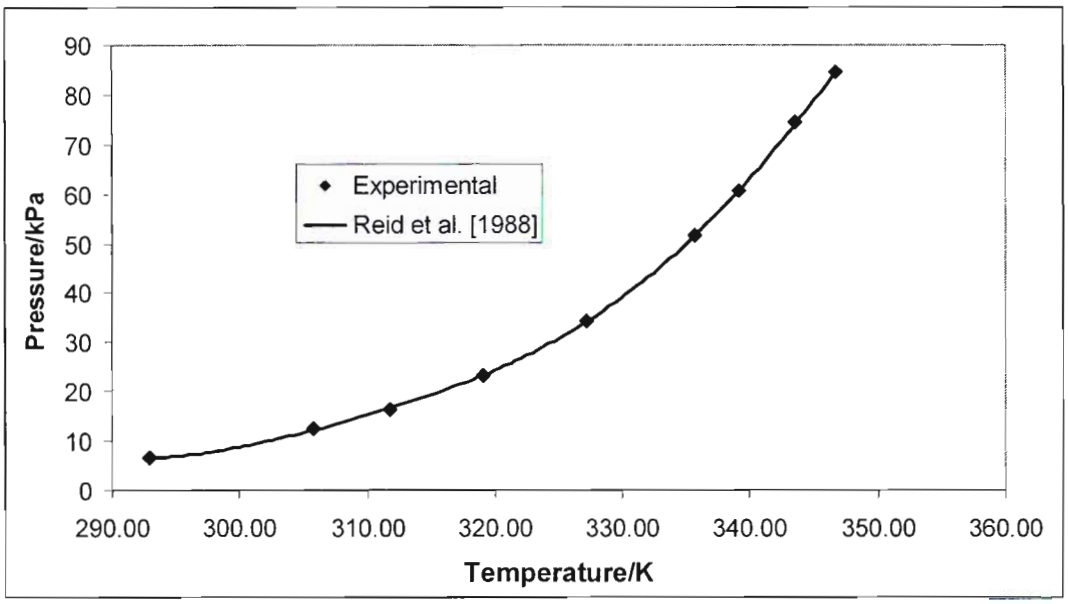

Figure 6.1 Vapour pressure of ethanol

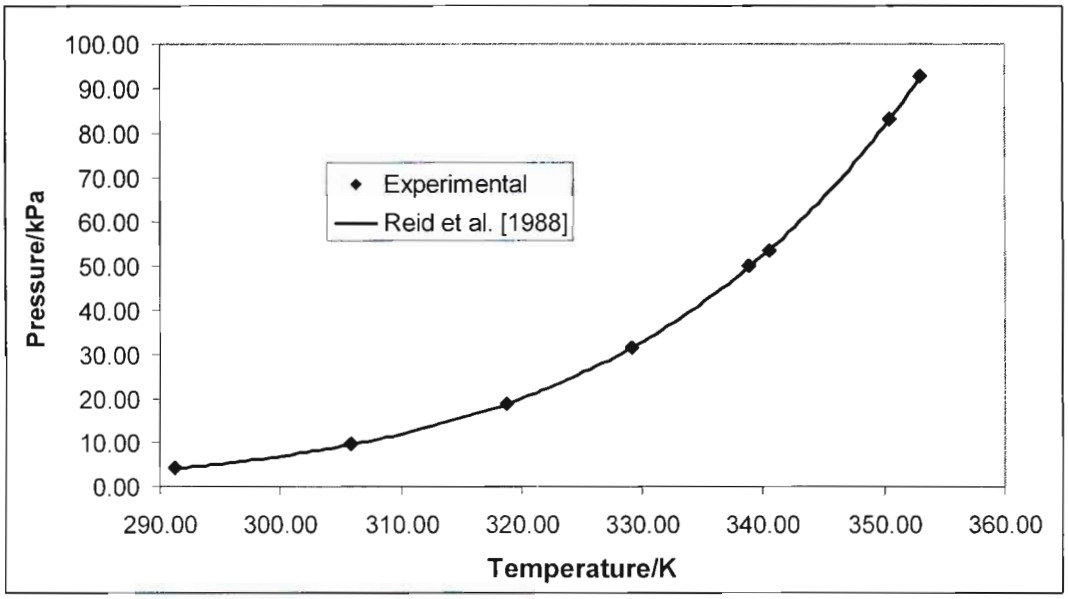

Figure 6.2 Vapour pressure of 2-propanol

6.2 Binary VLE measurements

6.2.1 Cyclohexane (1) + ethanol (2) system

Isothermal and isobaric data were measured for the cyclohexane + ethanol system at 313.15 K and 40 kPa respectively. The measured VLE data is listed in Table 6.2 and is shown in Figures 6.3 to 6.6 against literature data. The cyclohexane + ethanol system is highly non-ideal and has reliable literature data available. The experimental VLE data is presented against the data of Joseph et al. [2001]. The data presented given in Joseph et al. [2001] was acquired using a similar VLE apparatus. The measured VLE data is in good agreement with literature data.

Table 6.2 VLE measurements for ethanol (1) and cyclohexane (2) system at 313.15 K and 40 kPa

313.15 K			40 kPa		
P (kPa)	x_1	y_1	T (K)	x_1	y_1
17.89	0.000	0.000	329.67	0.000	0.000
26.59	0.053	0.344	328.29	0.069	0.007
31.64	0.113	0.473	324.35	0.228	0.031
34.81	0.191	0.539	319.08	0.430	0.102
37.18	0.353	0.596	314.92	0.594	0.408
37.61	0.493	0.609	314.82	0.604	0.455
37.69	0.596	0.62	314.74	0.626	0.637
37.65	0.721	0.63	314.76	0.641	0.760
37.46	0.802	0.639	315.16	0.654	0.892
36.33	0.918	0.673	315.48	0.668	0.920
24.64	1.000	1.000	315.82	0.679	0.941
			318.00	0.743	0.969
			325.69	1.000	1.000

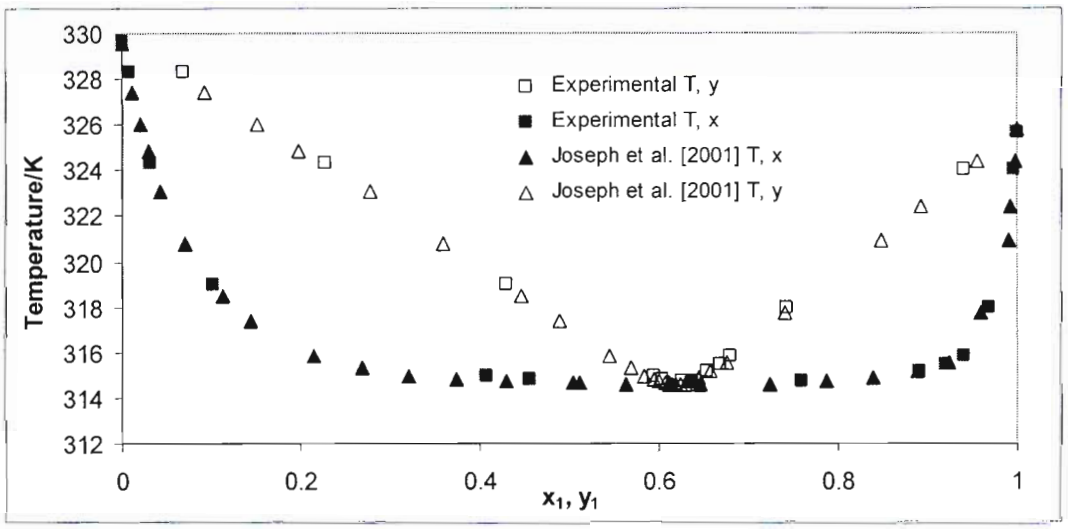

Figure 6.3 T-x-y plot for cyclohexane (1) + ethanol (2) system at 40 kPa

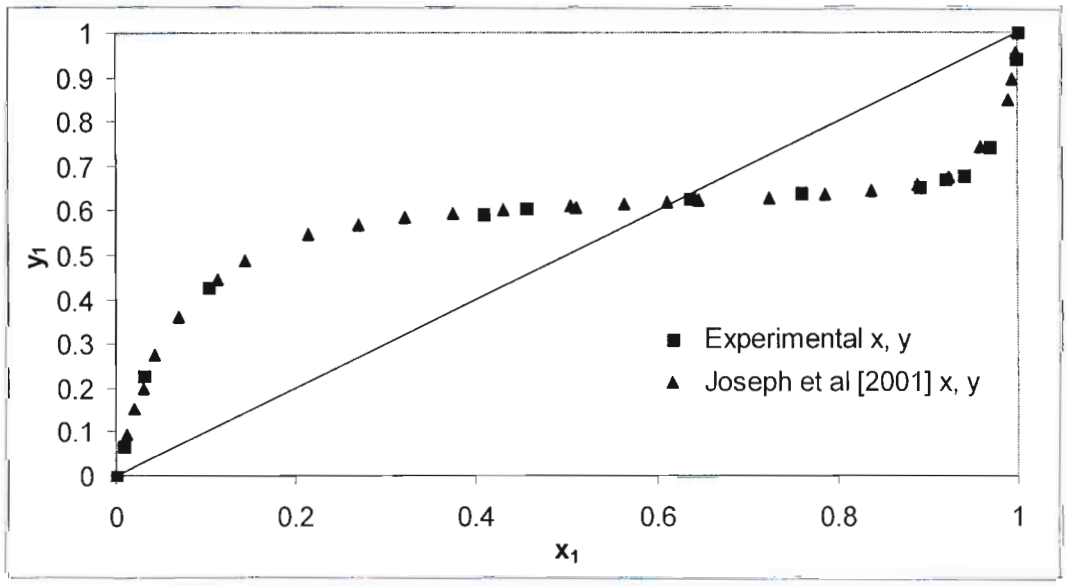

Figure 6.4 Experimental x-y plot for cyclohexane (1) + ethanol (2) system at 40 kPa

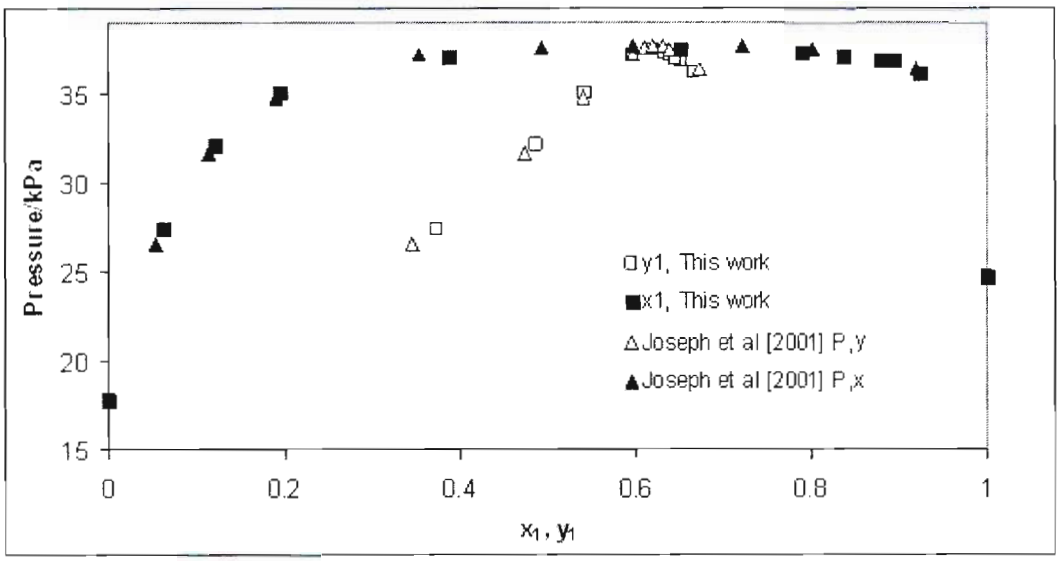

Figure 6.5 P-x-y plot for cyclohexane (1) + ethanol (2) system at 313.15 K

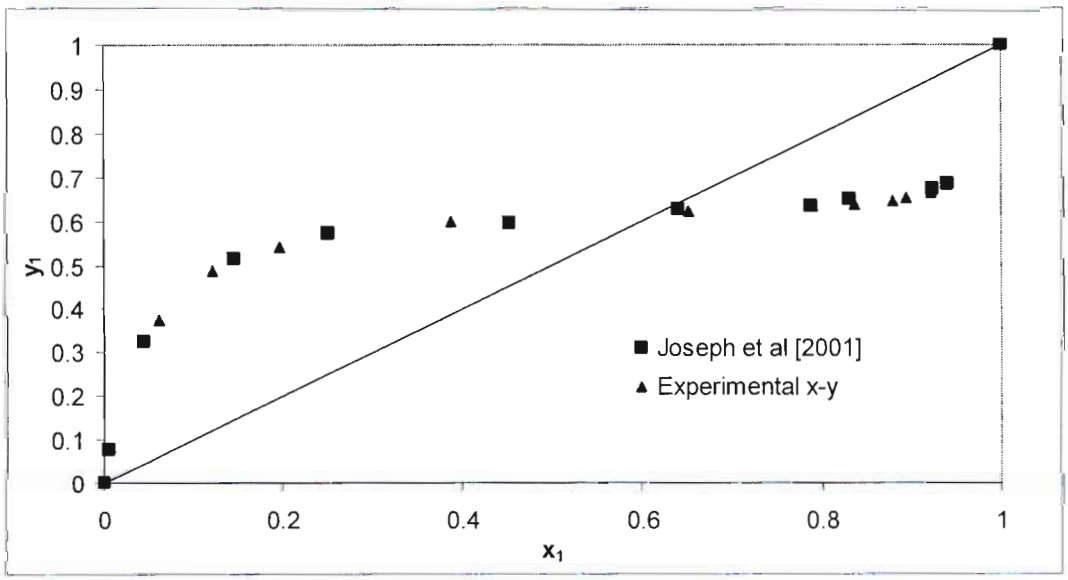

Figure 6.6 Experimental x-y plot for cyclohexane (1) + ethanol (2) system at 313.15 K

6.2.2 Ethanol (1) + n-dodecane (2) system

This section presents previously unmeasured binary VLE data for the system of ethanol (1) + n-dodecane (2) at 333.15 K and 343.15 K. The experimental data is listed in Table 6.3 and is shown in Figures 6.7 to 6.10. These data sets are not available in the open literature. The non-ideal behaviour observed in Figures 6.11to 6.16 are typical of chemical mixtures with high relative volatility.

Table 6.3 VLE measurements for ethanol(1) + n-dodecane(2) system at 343.15 K and 333.15 K

P (kPa)	x_1	y_1
	343.15 K	
73.62	1.000	1.000
72.09	0.980	0.998
71.42	0.968	0.997
70.73	0.955	0.996
70.26	0.913	0.996
69.83	0.880	0.995
68.94	0.847	0.992
67.53	0.724	0.991
67.45	0.602	0.981
66.89	0.552	0.981
73.12	0.992	0.999
66.32	0.326	0.979
60.00	0.125	0.900
0.42	0.000	0.000
	333.15 K	
47.09	1.000	1.000
46.52	0.979	0.999
45.83	0.943	0.995
45.23	0.885	0.996
45.63	0.724	0.982
44.76	0.589	0.985
44.55	0.469	0.981
44.23	0.325	0.972
40.23	0.124	0.850
0.22	0.000	0.000

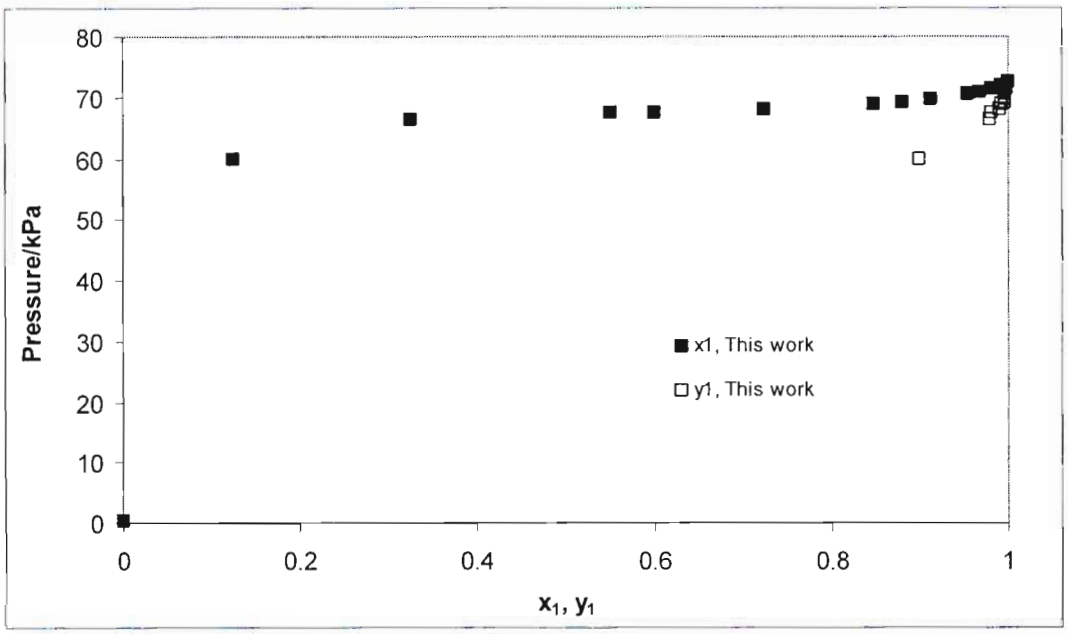

Figure 6.7 P-x-y plot for ethanol (1) + n-dodecane (2) system at 343.15 K

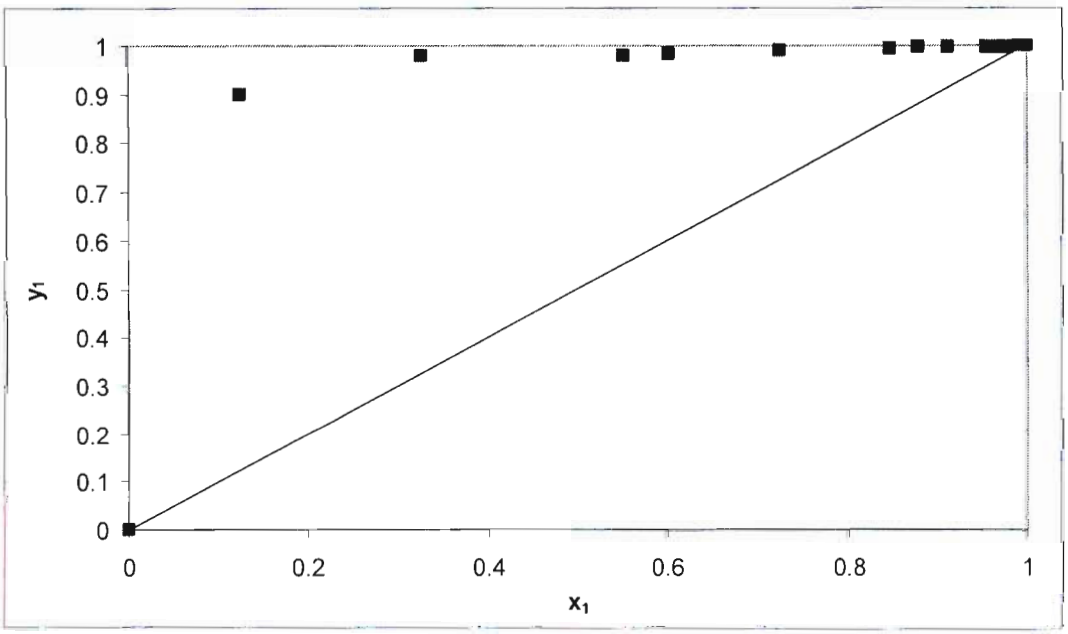

Figure 6.8 x-y plot for ethanol (1) + n-dodecane (2) system at 343.15 K

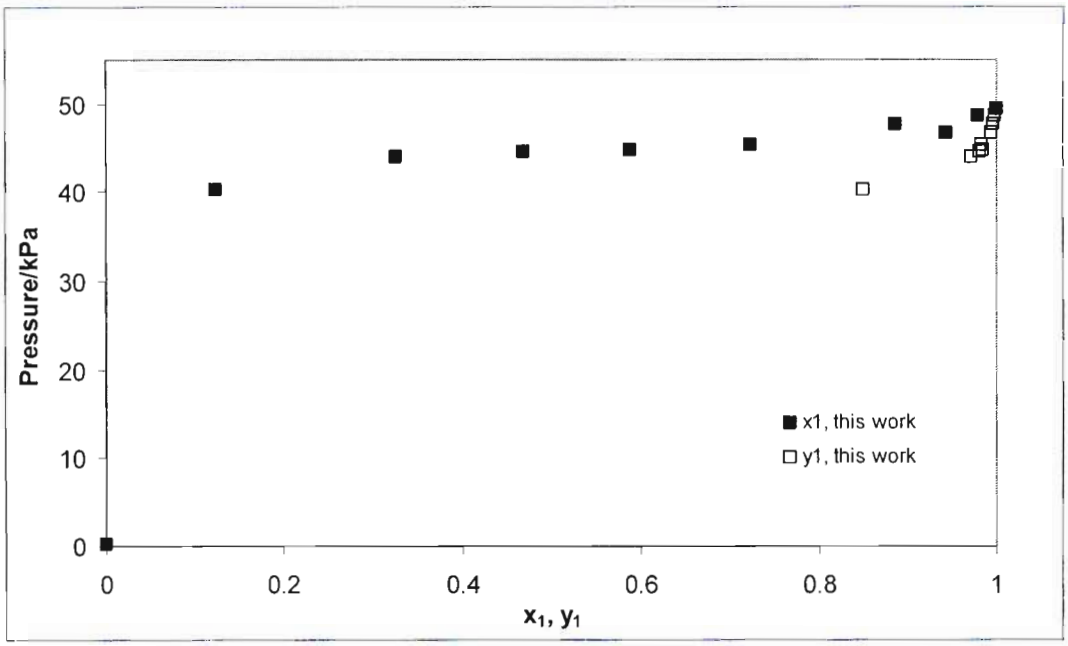

Figure 6.9 P-x-y plot for ethanol (1) + n-dodecane (2) system at 333.15 K

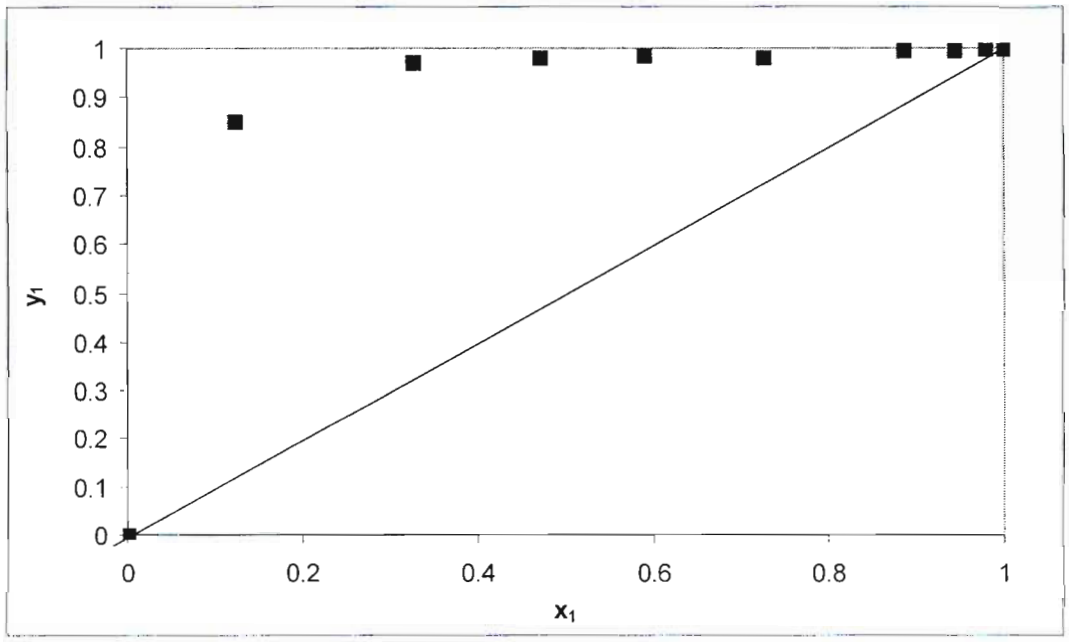

Figure 6.10 x-y plot for ethanol (1) + n-dodecane (2) system at 333.15 K

6.2.3 2-propanol (1) + n-dodecane (2) system

Isothermal VLE data was measured for the 2-propanol (1) + n-dodecane (2) system at 333.15 K, 343.15 K and 353.15 K. The measured data is listed in Table 6.4 and is shown in Figures 6.11 to 6.16. These data sets are not available in the open literature. As with the n-dodecane + ethanol binary VLE systems, the non-ideal behaviour observed in Figures 6.11to 6.16 are typical of chemical mixtures with high relative volatility.

Table 6.4 VLE measurements for 2-propanol (1) + n-dodecane (2) system at 343.15 and 333.15 K

P (kPa)	x1	y1
	353.15 K	
73.12	0.992	0.999
72.09	0.980	0.998
71.42	0.968	0.997
70.73	0.955	0.996
70.26	0.913	0.996
69.83	0.880	0.995
68.94	0.847	0.992
67.53	0.724	0.991
67.45	0.602	0.981
66.89	0.552	0.981
66.32	0.326	0.979
60.00	0.125	0.900
	343.15 K	
60.35	0.999	0.985
60.17	0.998	0.970
59.34	0.998	0.949
58.32	0.998	0.919
57.42	0.997	0.880
54.29	0.962	0.673
53.78	0.957	0.599
51.74	0.949	0.511
51.32	0.943	0.325
45.65	0.892	0.123
	343.15 K	
38.80	0.969	0.998
37.94	0.948	0.997
37.68	0.919	0.996
36.82	0.859	0.979
35.88	0.796	0.969
34.72	0.643	0.968
33.88	0.581	0.953
32.29	0.472	0.932
31.52	0.263	0.920
28.96	0.135	0.850

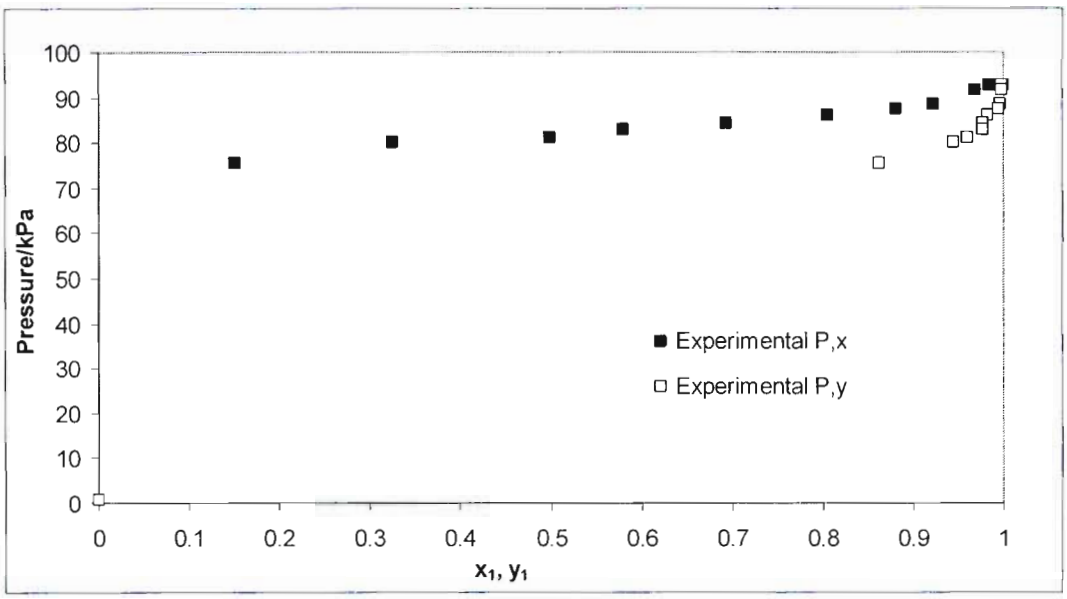

Figure 6.11 P-x-y plot for 2-propanol (1) + n-dodecane (2) system at 353.15 K

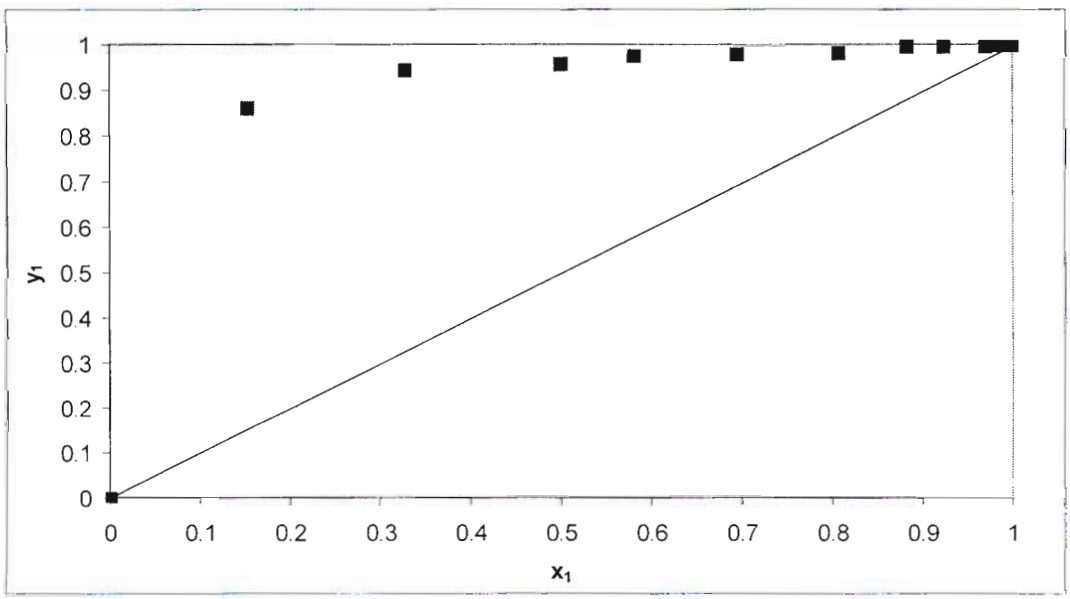

Figure 6.12 x-y plot for 2-propanol (1) + n-dodecane (2) system at 353.15 K

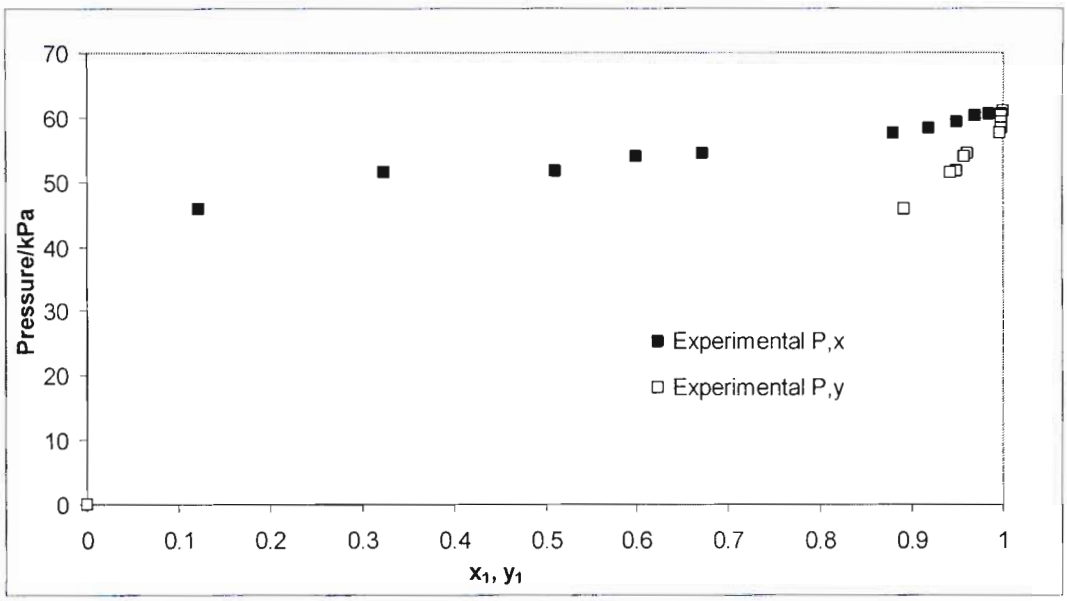

Figure 6.13 P-x-y plot for 2-propanol (1) + n-dodecane (2) system at 343.15 K

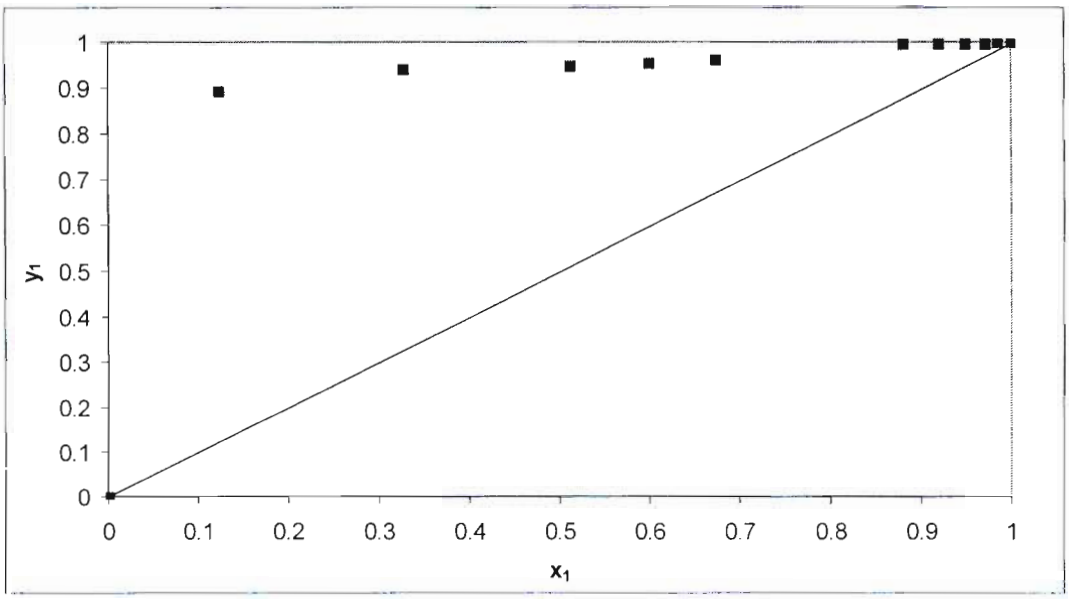

Figure 6.14 x-y plot for 2-propanol (1) + n-dodecane (2) system at 343.15 K

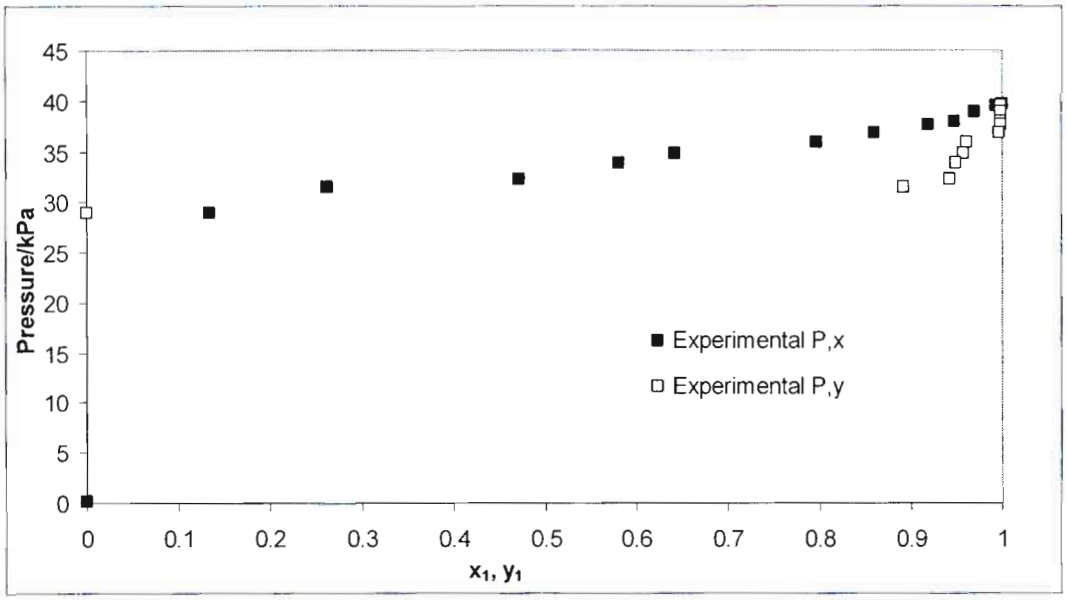

Figure 6.15 P-x-y plot for 2-propanol (1) + n-dodecane (2) system at 333.15 K

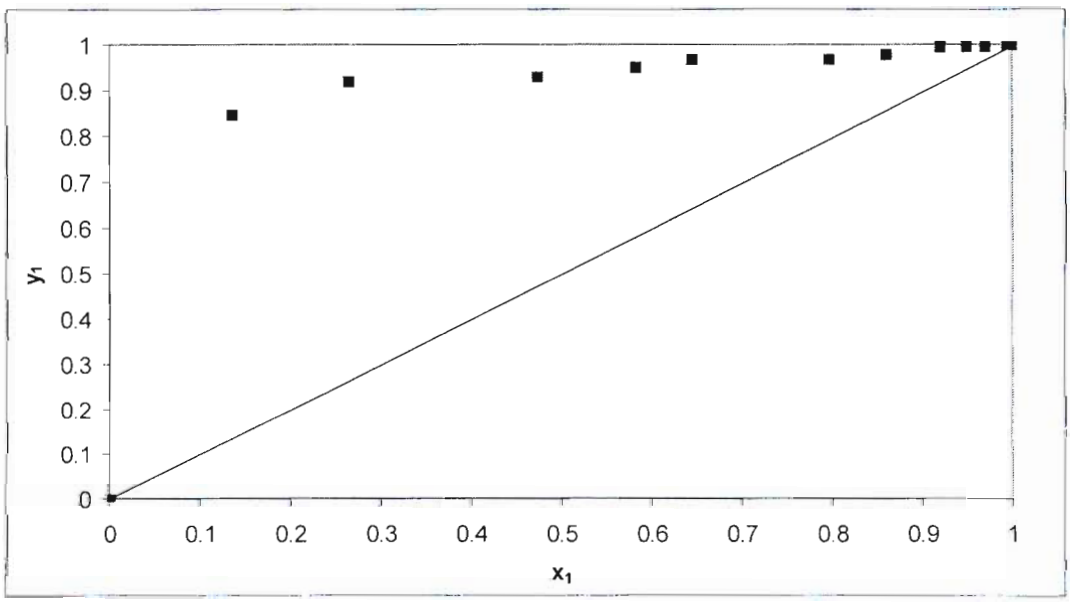

Figure 6.16 x-y plot for 2-propanol (1) + n-dodecane (2) system at 343.15 K

6.3 LLE measurements

6.3.1 Binary LLE measurement

Binary LLE data was measured for the n-heptane + methanol system at atmospheric pressure and was compared to literature data shown in Figure 6.17. This system was previously measured by Nagatani et al. [1987]. The LLE apparatus used by Nagatani et al. [1987] was similar to that used in this study. The literature data is plotted against the measured LLE data shown in Figure 6.17. Binary LLE data is listed in Table 6.5. The measured LLE data show excellent agreement with literature data, as is observed in Figure 6.17.

Table 6.5 Binary LLE data for n-heptane (1) + methanol (2) system at atmospheric pressure

	Top Phase		Bottom Phase	
T/K	x_1	x_2	x_1	x_2
288.65	0.126	0.874	0.874	0.126
309.75	0.209	0.791	0.791	0.124
283.16	0.119	0.881	0.881	0.074
319.05	0.257	0.743	0.743	0.120
303.15	0.166	0.834	0.834	0.115

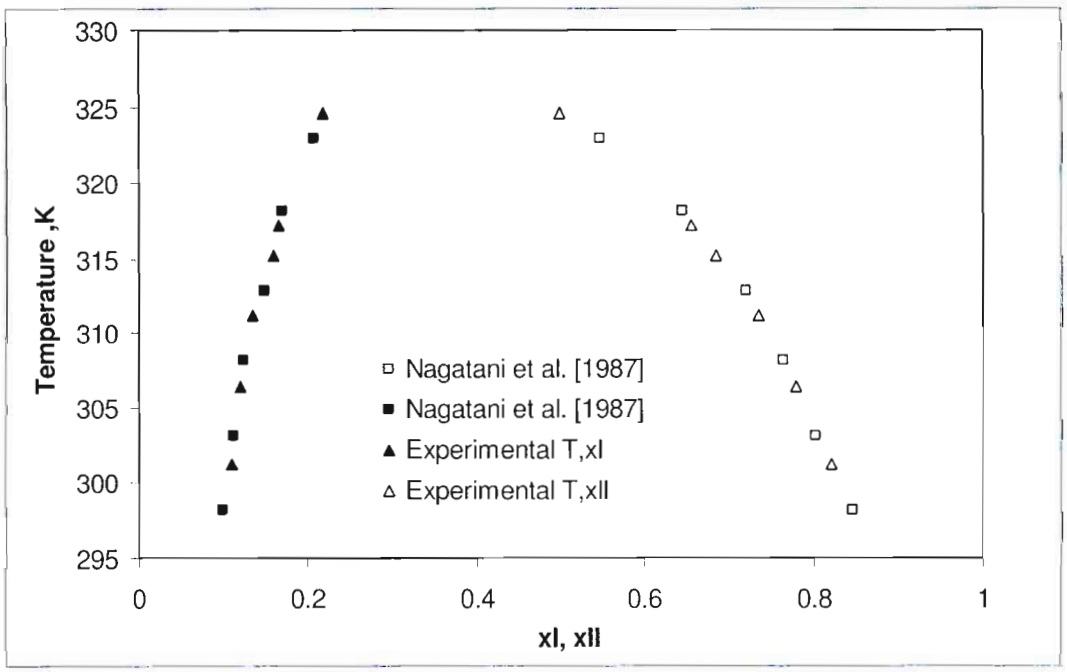

Figure 6.17 P-x plot for n-heptane (1) + methanol (2) system at 101.325 kPa

6.3.2 Ternary LLE data

6.3.2.1 n-Dodecane (1) + water (2) + ethanol (3) system

Ternary isobaric LLE data were measured for this n-dodecane + ethanol + water system at 343.15 K and 353.15 K. Measurements were acquired at atmospheric pressure and are not available in literature. Experimental data is listed in Table 6.5 and Table 6.6 and presented using an equilateral triangle shown in Figure 6.18 and Figure 6.19. This system exhibits a Type I system, [Treybal, 1963].

Table 6.6 Experimental LLE data for n-dodecane (1) + water (2) + ethanol (3) system at 333.15 K

Phase 1			Phase 2		
x_1	x_2	x_3	x_1	x_2	x_3
0.9918	0.0082	0.0000	0.0022	0.9978	0.0000
0.9817	0.0158	0.0025	0.0022	0.9848	0.0130
0.9832	0.0154	0.0014	0.0030	0.9604	0.0366
0.9323	0.0108	0.0569	0.0076	0.8491	0.1433
0.9340	0.0122	0.0538	0.0043	0.7435	0.2522
0.8671	0.0133	0.1196	0.0038	0.6243	0.3719
0.8260	0.0128	0.1612	0.0240	0.3191	0.6569

Table 6.7 Experimental LLE data for n-dodecane (1) + water (2) + ethanol (3) system at 323.15 K

Phase 1			Phase 2		
x_1	x_2	x_3	x_1	x_2	x_3
0.9960	0.0040	0.0000	0.0004	0.9996	0.0000
0.9210	0.0082	0.0708	0.0012	0.9880	0.0108
0.9844	0.0109	0.0047	0.0021	0.9640	0.0339
0.9323	0.0108	0.0569	0.0061	0.8320	0.1619
0.9340	0.0122	0.0538	0.0029	0.7420	0.2551
0.8671	0.0190	0.1139	0.0029	0.6102	0.3869
0.8260	0.0112	0.1628	0.0210	0.3080	0.6710

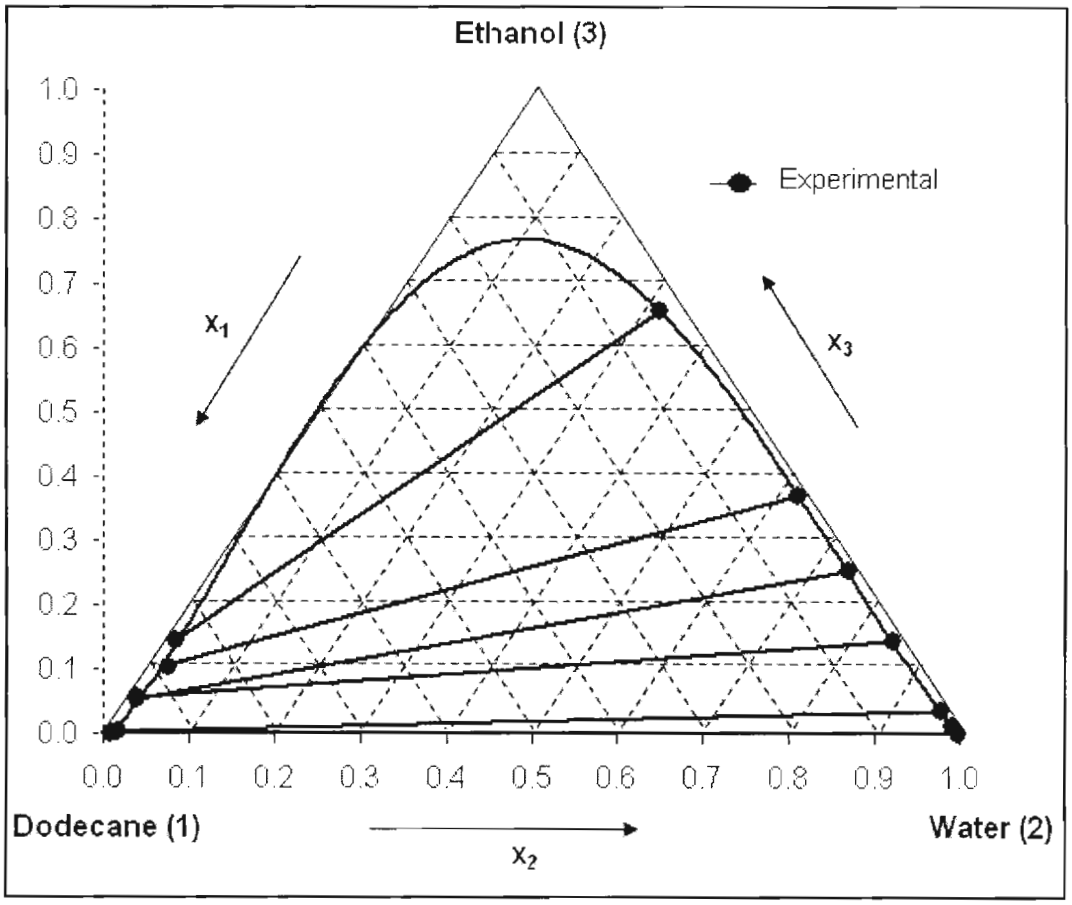

Figure 6.18 Experimental LLE data for n-Dodecane (1) + water (2) + ethanol (3) system at 333.15 K

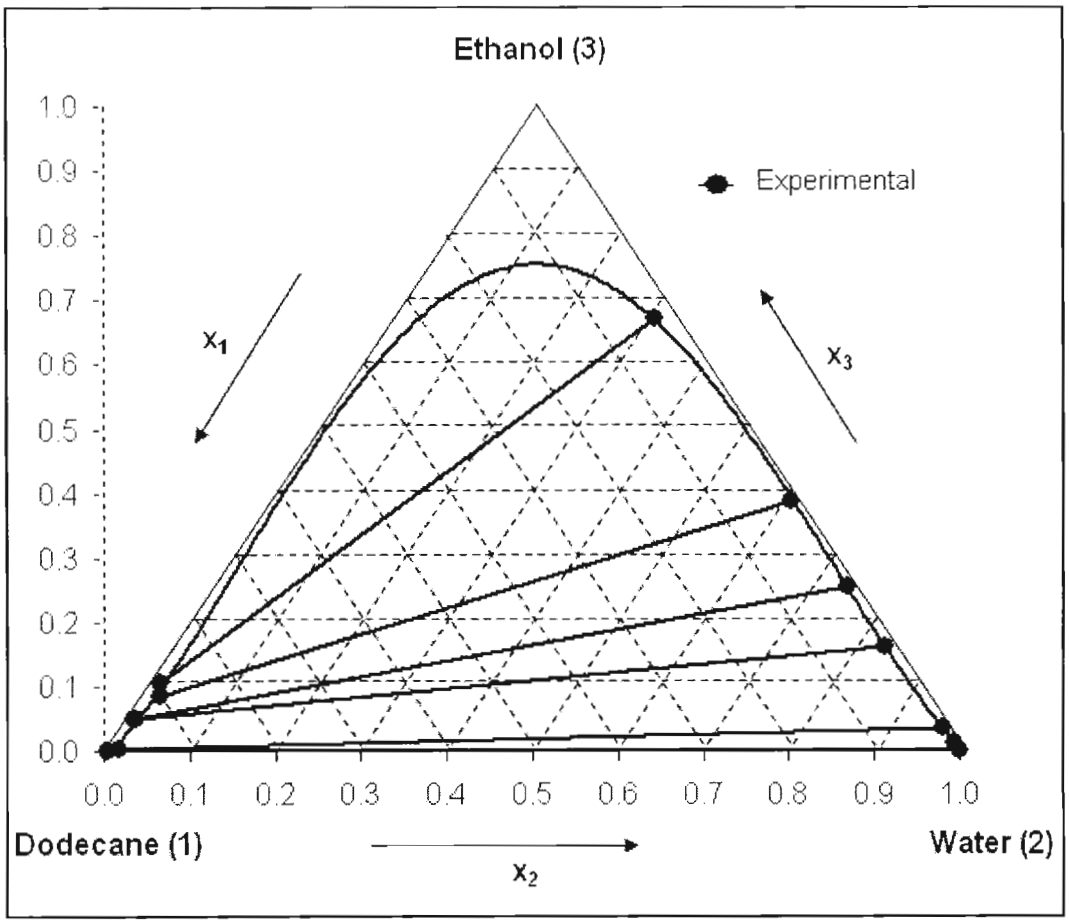

Figure 6.19 Experimental LLE data for n-Dodecane (1) + water (2) + ethanol (3) system at 323.15 K

6.3.2.2 n-Dodecane (1) + water (2) + 2-propanol (3) systems

Ternary isobaric LLE data was measured for the n-dodecane + 2-propanol + water system at 328.15 K and 333.15 K. LLE data measurements were acquired at atmospheric pressure and are not available in literature. Experimental data is listed in Table 6.7 and Table 6.8 and is presented using an equilateral triangle shown in Figure 6.18 and Figure 6.19. This system exhibits a Type I system, [Treybal, 1963].

Table 6.8 Experimental LLE data for n-dodecane (1) + water (2) + 2-propanol (3) system at 328.15 K

Phase 1			Phase 2		
x_1	x_2	x_3	x_1	x_2	x_3
0.9933	6.729E-03	0.0000	0.0009	0.9991	0.0000
0.9932	7.429E-04	0.0060	0.0068	0.9587	0.0345
0.9871	7.251E-04	0.0122	0.0062	0.9210	0.0729
0.9638	2.417E-04	0.0359	0.0076	0.8403	0.1521
0.9707	6.363E-04	0.0286	0.0257	0.7433	0.2310
0.9622	5.259E-04	0.0373	0.0138	0.6950	0.2912
0.9488	2.365E-03	0.0488	0.0563	0.5465	0.3972
0.9422	2.028E-03	0.0558	0.0780	0.4971	0.4250

Table 6.9 Experimental LLE data for n-dodecane (1) + water (2) + 2-propanol (3) system at 333.15 K

Phase 1			Phase 2		
x_1	x_2	x_3	x_1	x_2	x_3
0.9933	6.729E-03	0.0000	5.474E-04	0.9995	0.0000
0.9904	5.623E-04	0.0090	4.478E-03	0.9789	0.0166
0.9777	2.550E-03	0.0198	4.131E-03	0.9240	0.0719
0.9762	1.599E-04	0.0236	1.551E-02	0.8308	0.1537
0.9750	5.362E-04	0.0244	1.211E-02	0.7823	0.2055
0.9295	3.293E-03	0.0672	9.350E-02	0.4935	0.4130
0.9632	1.748E-04	0.0366	4.563E-02	0.6950	0.2594

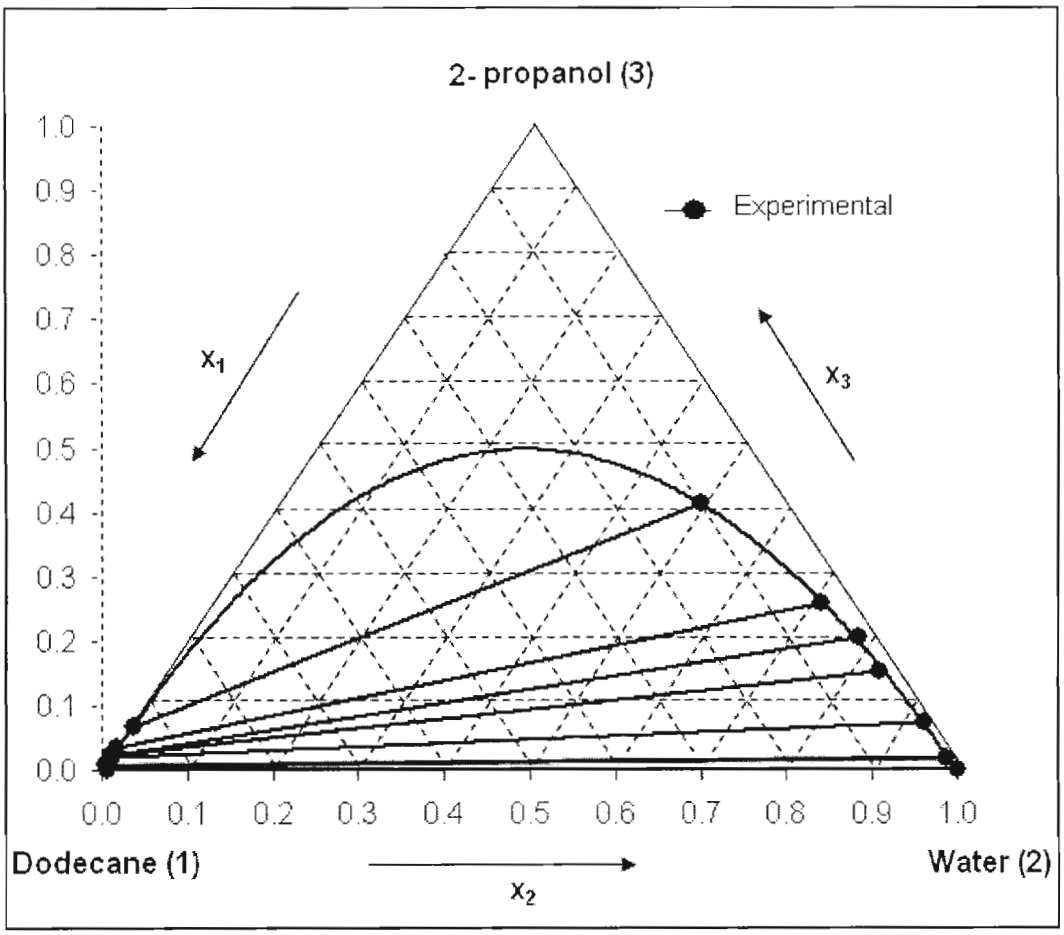

Figure 6.20 Experimental LLE data for n-dodecane (1) + water (2) + 2-propanol (3) system at 333.15 K

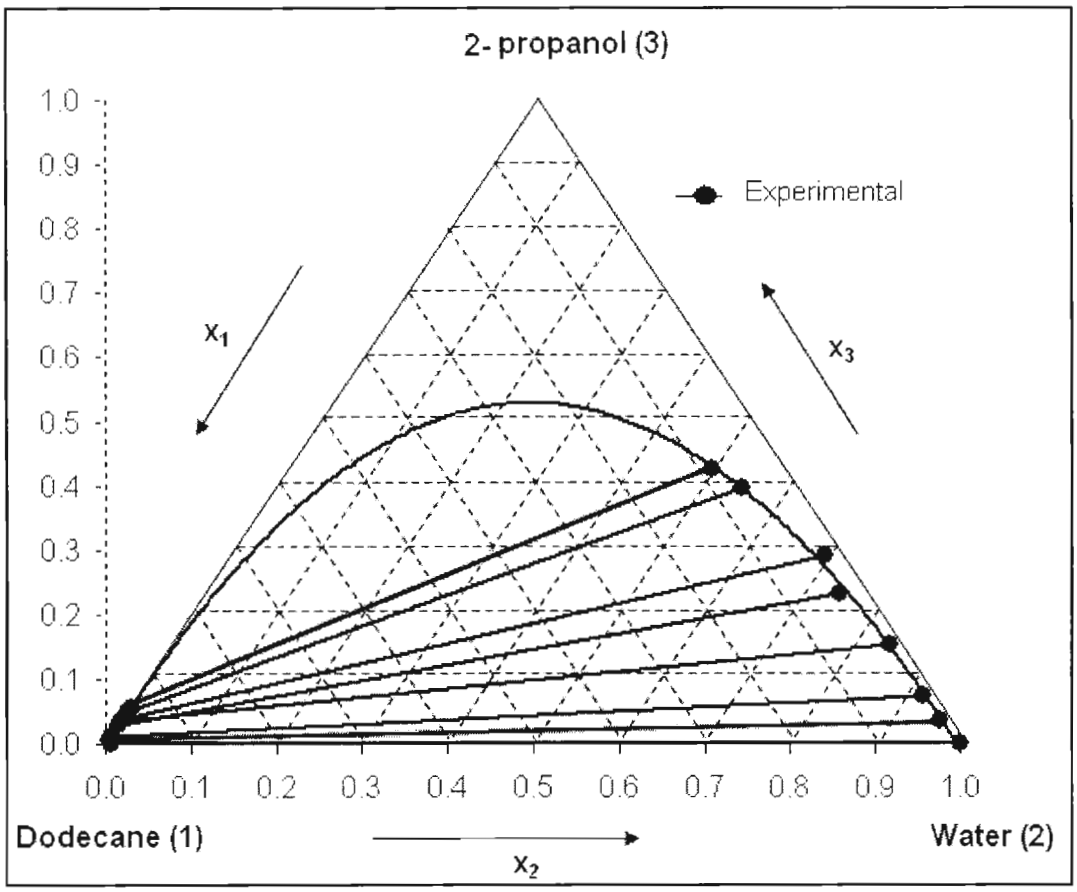

Figure 6.21 Experimental LLE data for n-dodecane (1) + water (2) + 2-propanol (3) system at 328.15 K

CHAPTER 7
DISCUSSION

In this chapter, theoretical concepts reviewed in Chapter 3 are applied to experimental phase equilibrium data (PED). The following sections present the correlation and reduction of binary VLE data measurements at sub-atmospheric pressures and ternary LLE data measurements at atmospheric pressure.

7.1 Chemical purity

PED was measured using highly pure chemicals (>99%). It was therefore imperative to verify the purity of each chemical. The chemical purity was measured using the Hewlett Packard Gas Chromatograph (discussed in chapter 5) and the method followed to evaluate chemical purity is outlined in Raal and Mühlbauer [1998]. The results are shown in Table 7.1. Table 7.2 tabulates the pure component properties for all the chemicals used in this study:

Table 7.1 Chemical purity analysis

Chemical name	Supplier	Claimed purity (mass %)	GC peak Area (area %)
Ethanol	Merck Ltd	99.7	99.70
Cyclohexane	Merck Ltd	99.5	99.65
Methanol	Rochelle Chemicals	99.5	99.65
n-Dodecane	Merck Ltd	99.6	99.68
n-Heptane	Merck Ltd	99.2	99.25

Table 7.2 Pure component properties

Pure Chemical	Molar Mass (kg/kmol)	ω	T_c (K)	P_c (kPa)	Z_c	V (cm^3/mol)
Methanol	32.042	0.564	512.6	80.97	0.224	118
Ethanol	46.069	0.645	513.9	61.48	0.24	167
2-Propanol	60.096	0.668	508.3	47.62	0.248	220
Cyclohexane	84.161	0.210	553.5	40.73	0.273	308
n-Heptane	100.204	0.350	540.2	27.4	0.261	428
n-Dodecane	170.340	0.575	658.3	18.2	0.258	713

7.2 Vapour pressure data

Vapour pressure data was measured for selected chemicals used in this study i.e. ethanol and 2-propanol. The Antoine equation (Equation (7-1)) is a contemporary equation widely used to represent vapour pressure data. The regressed parameters in the Antoine equation for ethanol and 2-propanol are listed in Table 7.2. This vapour pressure data was correlated by Equation (7.1) (given in Reid et al. [1988]):

$$Ln P^{sat} / kPa = A - \frac{B}{(T/K + C)} \tag{7-1}$$

The adjustable parameters in the Antoine equation (Equation (7-1)) were optimized by minimizing Equation (7-2):

$$\Delta P_i = \left| (P_i)_{measured} - (P_i)_{calculated} \right| \tag{7-2}$$

The regressed parameters for the Antoine equation are tabulated alongside the Antoine constants from Reid et al [1988] in Table 7.3.

Table 7.3 Regressed parameters in the Antoine equation

	Ethanol	2-Propanol
A	15.150	19.845
B	2862.424	5574.456
C	-79.812	-10.924
ΔP_i [kPa]	0.176	0.16

Values for the minimized function ΔPi [kPa] indicate that the calculated vapour pressure data for ethanol and 2-propanol fit the experimental data well.

7.3 VLE measurements

7.3.1 Experimental activity coefficients

Experimental activity coefficients were calculated directly from experimental binary VLE data measurements. This was possible due to the availability of the full P-T-x-y data set. Liquid phase activity coefficients were calculated using Equation (7-3). The pressure dependence for activity coefficients at high pressure is significant but at low to moderate pressure, this pressure dependency can be ignored, [Raal and Mühlbauer, 1998]:

$$y_i = \frac{x_i \gamma_i P_i^{sat}}{\Phi_i P} \tag{7-3}$$

The vapour phase correction factors, Φi at sub-atmospheric were evaluated using second virial coefficients. Second virial coefficients were calculated using the Tsonopoulos [1974] and Pitzer and Curl [1957] correlations. Experimental activity coefficients are tabulated in Tables 7.3 to 7.4 and are graphically represented in Section 7.3.2.

Table 7.4 Experimental activity coefficients for ethanol (1) + n-dodecane (2) system

x_1	γ_1	γ_2	x_1	γ_1	γ_2
	323.15K			**333.15K**	
			0.992	1.000	3.735
0.979	1.000	3.735	0.980	1.001	3.623
0.885	1.002	1.646	0.968	1.001	3.511
0.943	1.001	1.674	0.955	1.003	3.388
0.725	1.016	1.560	0.913	1.010	3.055
0.589	1.046	1.477	0.880	1.020	2.819
0.469	1.101	1.395	0.847	1.032	2.615
0.325	1.251	1.285	0.724	1.108	2.017
0.124	2.209	1.111	0.602	1.237	1.623
0.325	1.251	1.285	0.552	1.309	1.503
0.124	2.788	1.111	0.326	1.838	1.153
			0.125	2.788	1.021

Table 7.5 Experimental activity coefficients for 2-propanol (1) + n-dodecane (2) system

x_1	γ_1	γ_2	x_1	γ_1	γ_2	x_1	γ_1	γ_2
	333.15K			**345.15K**			**353.15K**	
0.992	1.000	12.876	1	1.001	12.332	0.992	1.000	2.413
0.969	1.004	10.406	0.984782	1.004	10.751	0.980	1.000	2.364
0.948	1.012	8.741	0.969835	1.012	9.078	0.968	1.001	2.314
0.919	1.026	7.169	0.94913	1.027	7.336	0.955	1.002	2.259
0.859	1.070	5.129	0.918887	1.053	5.827	0.913	1.007	2.107
0.796	1.133	3.889	0.879952	1.309	2.657	0.880	1.013	1.996
0.643	1.361	2.417	0.67279	1.454	2.209	0.847	1.021	1.898
0.581	1.491	2.093	0.599065	1.688	1.835	0.724	1.071	1.595
0.472	1.811	1.686	0.5105	2.582	1.356	0.602	1.153	1.381
0.263	3.109	1.238	0.325	6.048	1.074	0.552	1.197	1.312
0.135	5.479	1.079				0.326	1.499	1.100
						0.125	2.453	1.014

7.3.2 Low pressure binary VLE (LPVLE) data reduction

Binary VLE data reduction entails fitting thermodynamic models to VLE data to determine optimum parameters for these models, [Raal and Mühlbauer, 1998]. Common methods available for LPVLE data regression are the direct and combined method. This section utilizes the combined method to regress binary LPVLE data. This is the preferred method for LPVLE data regression according to Raal and Mühlbauer [1998].

The gamma-phi method employs liquid-phase activity coefficients models to account for non-ideal liquid phase behaviour. The following three activity coefficients models were utilized: the Wilson, NRTL and UNIQUAC models. The vapour phase non-ideality was accounted for by evaluating second virial coefficients (discussed in Chapter 3). Second virial coefficients are the preferred method used to account for the vapour phase non-ideality at low pressures, [Prausnitz et al., 1980]. Second virial coefficients were evaluated using the method of Tsonopoulos [1974] and Pitzer and Curl [1957].

The adjustable parameters in the gamma-phi method were optimized by minimising the least squares regression with the objective function which is the minimum of the squared difference between the experimental and calculated pressures for isothermal binary VLE data (Equation (7-4)) and by using the difference between the experimental and calculated temperature for isobaric VLE data (Equation (7-5)). These object functions are as good as any other according to Van Ness et al. [1976].

$$S = \sum \left(\partial P\right)^2 \tag{7-4}$$

$$S = \sum \left(\partial T\right)^2 \tag{7-5}$$

The experimental VLE data was regressed with MATLAB® (Version 7.0) using the built-in optimization function, *fminsearch*. This function uses the algorithm based on the Nedel-Mead simplex method, [Lagarias et al., 1998].

7.3.2.1 The cyclohexane (1) + ethanol (2) system

Table 7.6 Activity model parameters and deviations between calculated and experimental measurements for cyclohexane (1) + ethanol (2) system at 313.15 K

Activity coefficient model		313.15 K
Wilson		
	λ_{12}-λ_{21} (J/mol)	5085.248
	λ_{12}-λ_{22} (J/mol)	3279.721
	Average δP (kPa)	0.017
	Average δy_1	0.022
NRTL		
	g_{12}-g_{11} (J/mol)	2676.988
	g_{12}-g_{22} (J/mol)	1684.146
	A	0.960
	Average δP (kPa)	0.027
	Average δy_1	0.053
UNIQUAC		
	u_{12}-u_{11} (J/mol)	-1169.240
	u_{12}-u_{22} (J/mol)	5563.103
	Average δP (kPa)	0.073
	Average δy_1	0.241

Table 7.7 Activity model parameters and deviations between calculated and experimental measurements for cyclohexane (1) + ethanol (2) system at 40 kPa

Activity coefficient model		40 kPa
Wilson		
	λ_{12}-λ_{21} (J/mol)	2097.349
	λ_{12}-λ_{22} (J/mol)	7075.634
	Average δT (K)	0.078
	Average δy_1	0.045
NRTL		
	g_{12}-g_{11} (J/mol)	3570.397
	g_{12}-g_{22} (J/mol)	4697.307
	α	0.405
	Average δT (K)	0.077
	Average δy_1	0.036
UNIQUAC		
	u_{12}-u_{11} (J/mol)	-623.111
	u_{12}-u_{22} (J/mol)	8853.001
	Average δT (K)	0.083
	Average δy_1	0.043

The cyclohexane + ethanol system is a highly non-ideal system consisting of a polar alkanol and non-polar compound. This system exhibits large relative volatilities in the dilute regions which can be explained by nature of the intermolecular forces of the individual components. Cyclohexane is a strongly polar alkanol whereas the ethanol exhibits hydrogen-bonding. This system was used to test the experimental procedure and operation of the VLE apparatus. An isotherm at 313.15 K and an isobar at 40 kPa were measured. The cyclohexane + ethanol binary VLE test system is most often utilized to test the experimental procedure and apparatus due to the extensive literature data available. According to the T-x-y data (Figure 7.2), the cyclohexane + ethanol system displays a minimum boiling azeotrope and in Figure 7.3 an azeotrope is observed for the isobaric measurements.

Activity coefficient model parameters for the cyclohexane + ethanol system are tabulated in Table 7.5 and Table 7.6. Isothermal binary VLE data was regressed by minimizing the pressure residual, (Equation (7-4)) and isobaric VLE data was minimized using the temperature residual, (Equation (7-5)). These residuals were used to judge the best fit model. Values for the residual parameters are listed in Table 7.5 and Table 7.6. All activity coefficient models fitted the experimental data well. Overall, the Wilson and NRTL models fitted the experimental data the best which was also concluded by Joseph et al. [2001]. The UNIQUAC model being a correlative model yielded the worst results. Figures 7.1 to 7.4 graphically represent the comparison between the fit of experimental VLE data against the calculated VLE data using best fit model.

Both systems passed the thermodynamic consistency point test (outlined in Chapter 3) shown in Figure 7.4 and Figure 7.5. Δy_1 is the difference between the calculated and experimental vapour phase compositions.

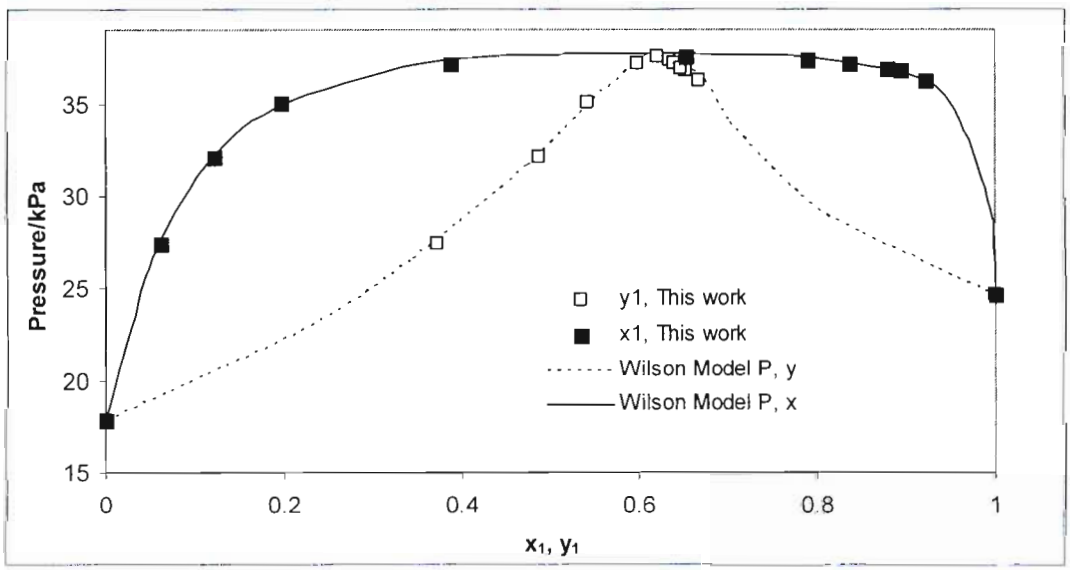

Figure 7.1 P-x-y plot of cyclohexane (1) + ethanol (2) system at 313.15 K

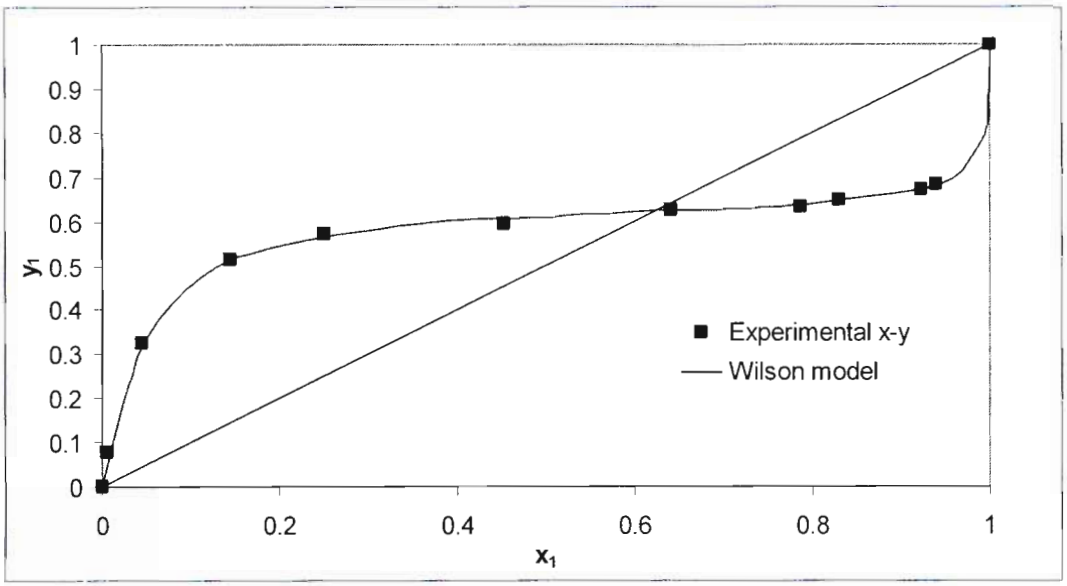

Figure 7.2 x-y plot of cyclohexane (1) + ethanol (2) system at 313.15 K

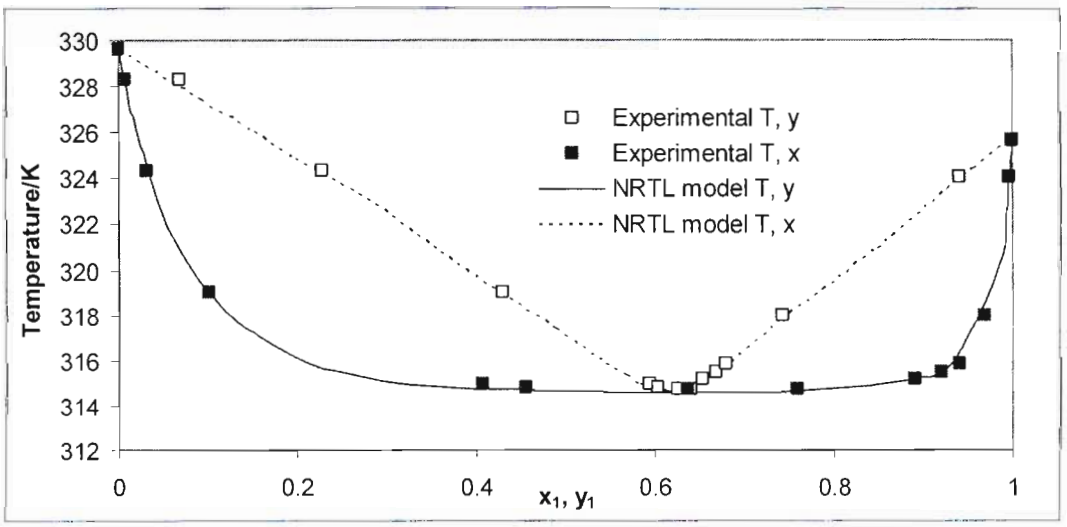

Figure 7.3: T-x-y plot of cyclohexane (1) + ethanol (2) system at 40kPa

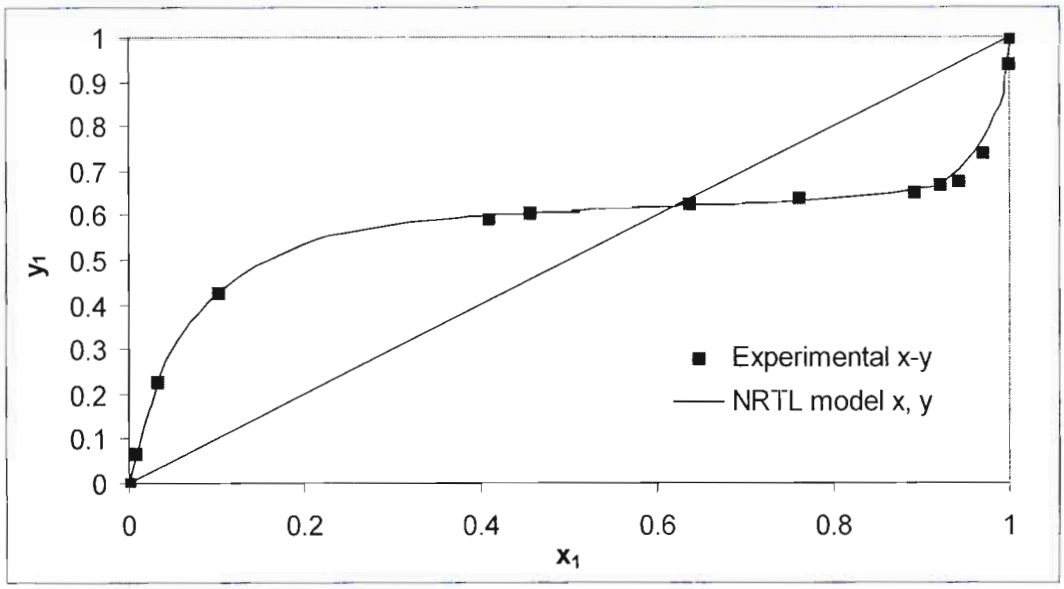

Figure 7.4: x-y plot of cyclohexane (1) + ethanol (2) system at 40kPa

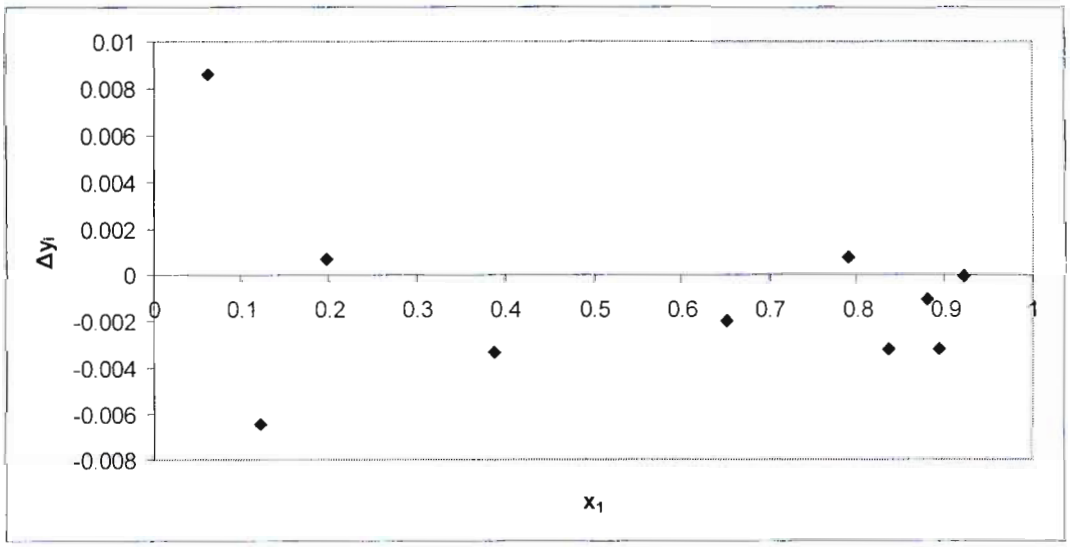

Figure 7.5 Plot used for the Point test for cyclohexane (1) + ethanol (2) system at 40 kPa using y_i data calculated from the NRTL model

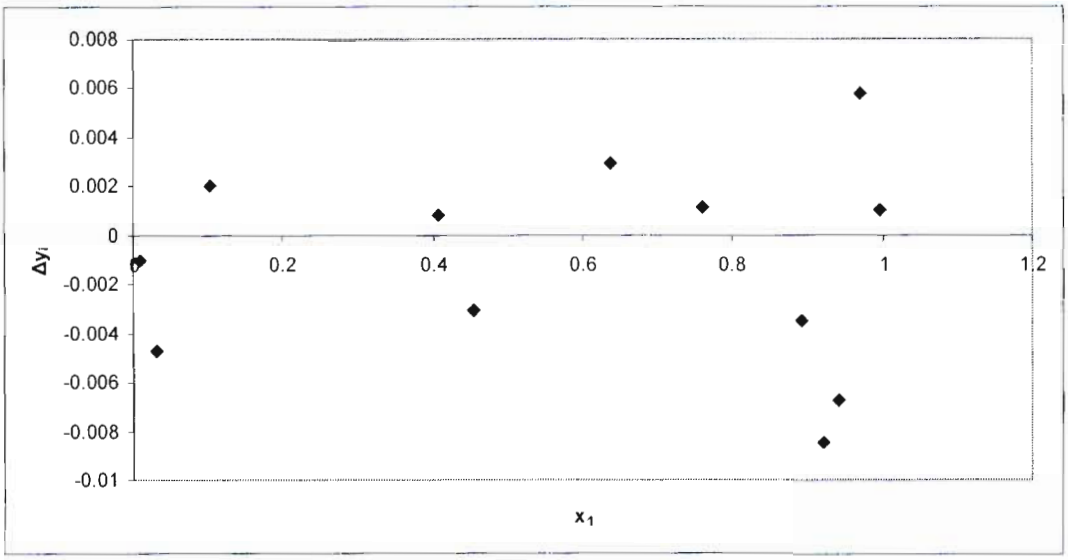

Figure 7.6 Plot used for the Point test for cyclohexane (1) + ethanol (2) system at 313.15 K using y_i compositions calculated from the Wilson model

7.3.2.2 The n-dodecane + 2-propanol and n-dodecane + ethanol systems

The measured binary VLE data for the two binary VLE systems n-dodecane + ethanol and n-dodecane + 2-propanol displayed similar trends and are both discussed below. This would be expected due to the minor difference between the molecular masses of the two alkanols shown in Figure 7.5.

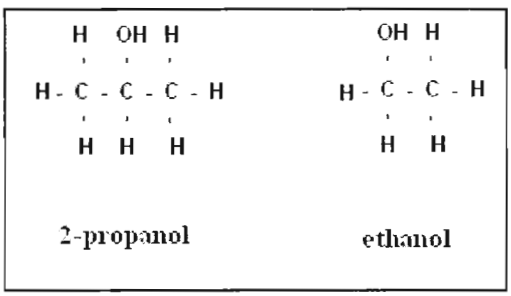

Figure 7.7 Molecular structures of 2-propanol and ethanol

These binary VLE systems have a very high relative volatility and proved difficult to measure using dynamic re-circulating VLE apparatus, [Gillespie, 1976]. This can be largely attributed to

poor equipment design and experimental procedure. This study is aimed to eliminate these two limitations using a modified dynamic re-circulation VLE apparatus.

A review of re-circulating VLE stills was undertaken to quantify previous design flaws inherent to the acquirement of such binary VLE data. Systems of high relative volatility have historically proven tedious and difficult to measure using dynamic VLE stills. Thus binary VLE data of an alkanol + heavy n-alkane acquired using re-circulating VLE stills are limited in open literature. Reddy [2006] presented binary VLE data of n-dodecane + 1-propanol at 373.15 K and 393.15 K using a novel re-circulating VLE apparatus. Lee and Scheller [1967] was the only other reference found in open literature that published binary VLE data of an alkanol + heavy n-alkane using a re-circulating VLE apparatus. Each of these VLE stills had innovative features but was impractical when applied to this study. The re-circulating VLE still of Ndlovu [2005] based on the design of the VLE still of Raal and Mühlbauer [1998] was a robust VLE still capable of acquiring low pressure VLE data from systems of partial miscibility but could not measure systems of high relative volatility (discussed in Chapter 2). The principles underlying the design of the VLE still of Ndlovu [2005] were most applicable to this study. Therefore, the VLE still utilized in this study was a modification made to the VLE still of Ndlovu [2005] (discussed in Chapter 4) to handle systems of high relative volatility.

Operating experimental procedures employed by Ndlovu [2005] were optimized for this study. There were no inherent difficulties associated with the approach to equilibrium in terms of erroneous fluctuations of thermodynamic variables. At equilibrium, the plateau region (discussed in Chapter 5), thermodynamic variables (P, T, x, y) remained constant within predetermined tolerances and a smooth P-x_i-y_i data points were observed as shown in Figure 7.8.

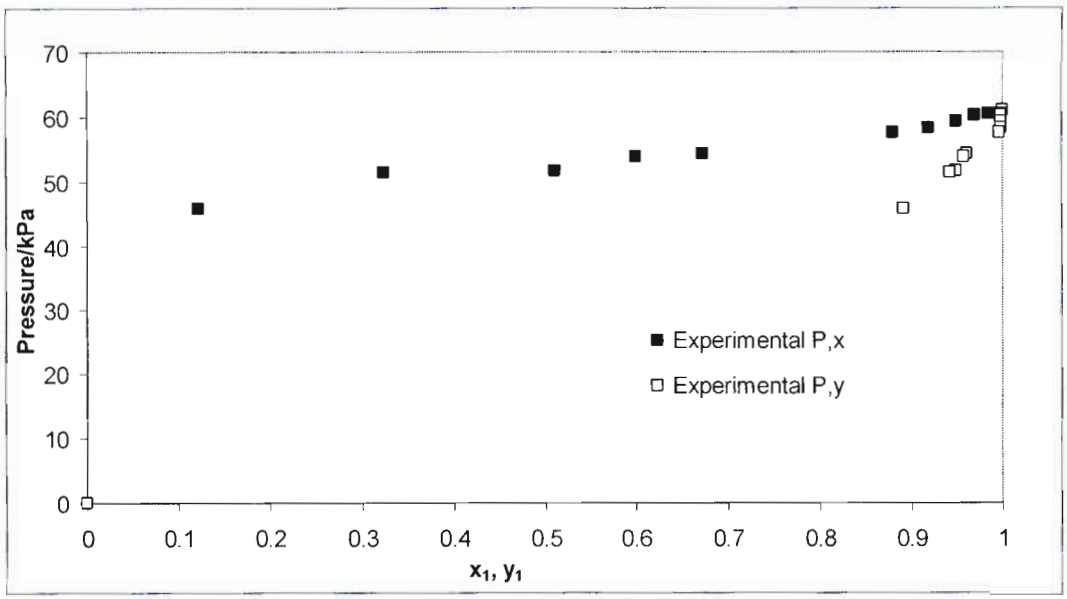

Figure 7.8 P-x-y plot for n-dodecane (2) + 2-propanol (1) system at 343.15K

Experimental isobaric VLE data is represented in Chapter 6 and a typical VLE plot is shown in Figure 7.8. The measured P-x-y data followed specific trends which were large differences between vapour and liquid compositions toward the n-dodecane rich region. However, the experimental activity coefficients calculated using the experimental P-T-x-y data were not coherent with the pure component limits for the γ_i auxiliary departure function used in the normalization of γ_i's in the gamma-phi approach (discussed in Chapter 3) shown in Equation (7-6).

$$\gamma_i \rightarrow 1 \text{ as } x_i \rightarrow 1 \tag{7-6}$$

The experimental activity coefficients were calculated with experimental data using Equation (7-7) and are listed in Tables 7.3 and 7.4. The γ_i values for the n-dodecane component in its pure component limit did not exhibit the above mentioned behaviour and were much too high, [Reddy, 2006]

$$\gamma_i = \frac{y_i \Phi_i P}{x_i P_i^{sat}} \tag{7-7}$$

This can be attributed to the vapour pressure, P_i^{sat} of n-dodecane being much lower than that of the system pressure. The pressure correction term, Φ_i, is close to unity for gases below atmospheric pressure. Therefore, the $\frac{\Phi_i P}{P_i^{sat}}$ term yields a large value and the ratio $\frac{y_i}{x_i}$ has to be significantly small resulting in a huge variation between the two phases composition toward the n-dodecane rich region. Both systems of n-dodecane + alkanol measured displayed this mentioned trend.

This was also noted by Reddy [2006] and Lee and Scheller [1967]. Reddy [2006] measured binary VLE data of the n-dodecane + 1-propaonol system at 373.15 K shown in Figure 7.9. The data presented by Reddy [2006] has majority of measurements towards the alkanol rich phase attesting to the difficulty in acquiring binary VLE data from systems displaying high relative volatility. Reddy [2006] noted errors in the approach to equilibrium toward the n-dodecane rich region.

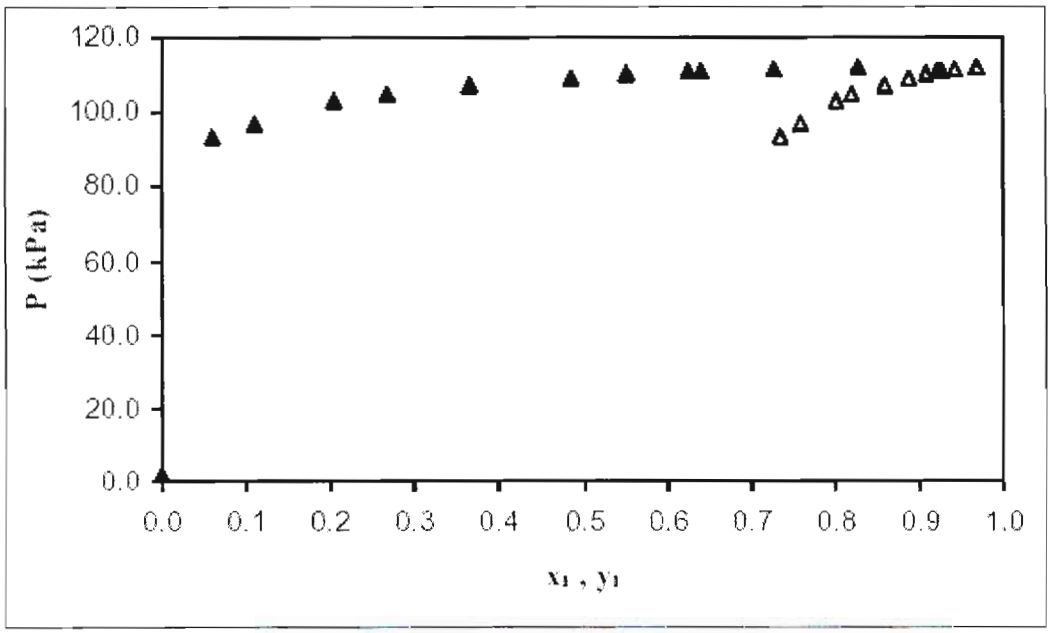

Figure 7.9 1-propanol (1) + n-dodecane (2) system at 373.15K, ▲ – P-x data, Δ – P – y data, [Reddy, 2006]

The only other available binary VLE data in open literature of an alkanol + heavy n-alkane is the binary VLE data presented by Lee and Scheller [1967] for the 1-butanol + decane system at

373.15 K. The VLE data was measured using a re-circulating VLE still and the binary VLE data is shown in Figure 7.10

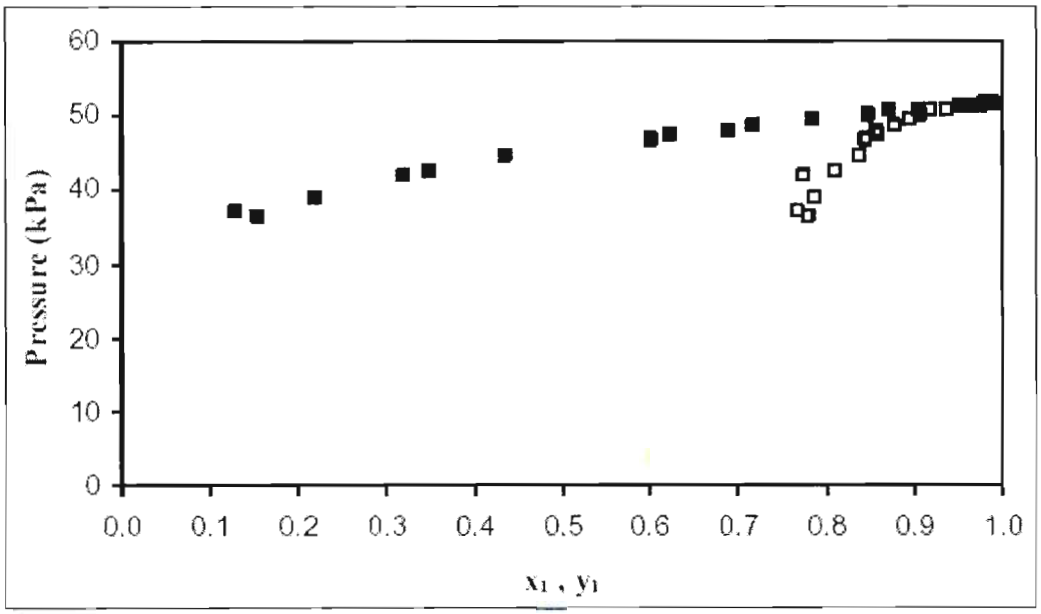

Figure 7.10 1-butanol (1) + decane (2) system at 373.15K, ■ – P-x data, □ – P – y data, [Lee and Scheller ,1967]

The VLE data shown in Figure 7.10 has increased scatter as the liquid phase composition approaches the n-alkane rich phase which is apparent in this study (shown in subsequent sections). This lack of measurement in the alkane rich phase was a problem shared by Reddy [2006] even though the relative volatility between 1-butanol and decane being lower than that between 1-propanol and n-dodecane.

Indeed similar observations were apparent in this study shown in Figure 7.8, where the attempt to measure points in the n-dodecane rich region resulted in an error in the approach to equilibrium. This resulted in large fluctuations of thermodynamic variables such as pressure and composition. This problem can also be attributed to large heat loads required to boil the n-dodecane causing the light alkanol to flash. Flashing of the more volatile component was credited to ineffective mixing inside the VLE still. Therefore, the task of acquiring binary VLE data of systems of high relative volatility would be better suited to different experimental methods such as static methods.

7.3.2.3 The n-dodecane + 2-propanol and n-dodecane + ethanol systems data reduction

After comparing VLE data presented by Lee and Scheller [1967] shown in Figure 7.10 for 1-butanol + decane shows its trend similar to experimental data trends presented in this study. However, the systems presented in this study have a larger relative volatility and it would be correct to assume that the measured vapour phase composition for the n-dodecane + alkanol in this study to be much lower for a respective P-x_i value.

This was evident as Gibbs excess models yielding large deviations between the predicted and measured vapour phase compositions for each system, (typical data reduction shown in Figure 7.11). Thus inaccuracies were present during the vapour phase measurements. Van Ness et al [1973] concluded that the main uncertainty associated with re-circulating VLE stills is the vapour phase measurements and recommends that the vapour phase be computed using experimental T-x_i data. Due to the large deviations in the predicted compositions, calculated vapour compositions are graphically presented against experimental P-T-x data shown in Section 7.3.2.4.

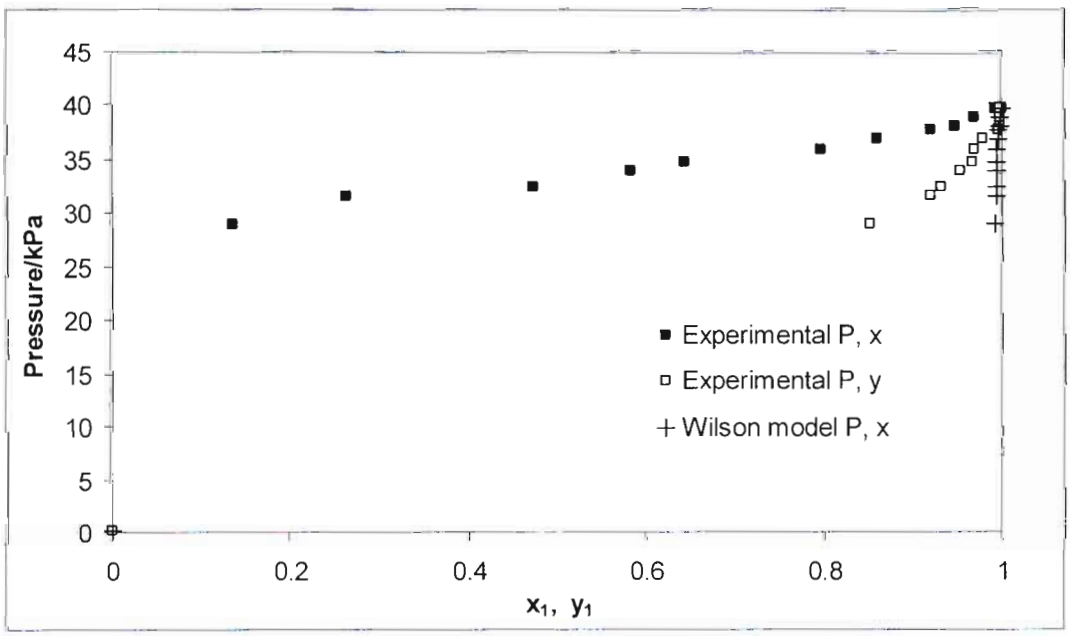

Figure 7.11 P-x-y plot of 2-propanol (1) + n-dodecane (2) system at 333.15K, ▪ - experimental P-x_i data, □-P-$y_{i,}$, + - P-y_i Wilson model

The erroneous VLE data reduction results were also observed by Reddy [2006] shown in Figure 7.12. Reddy [2006] used the gamma-phi method with the Wilson equation to model activity coefficients and second virial coefficients to model fugacity coefficients to regress binary VLE data. Similar conclusions were reached by Ellis [1952] and Gillespie [1946] using re-circulating VLE stills measuring systems of high relative volatility.

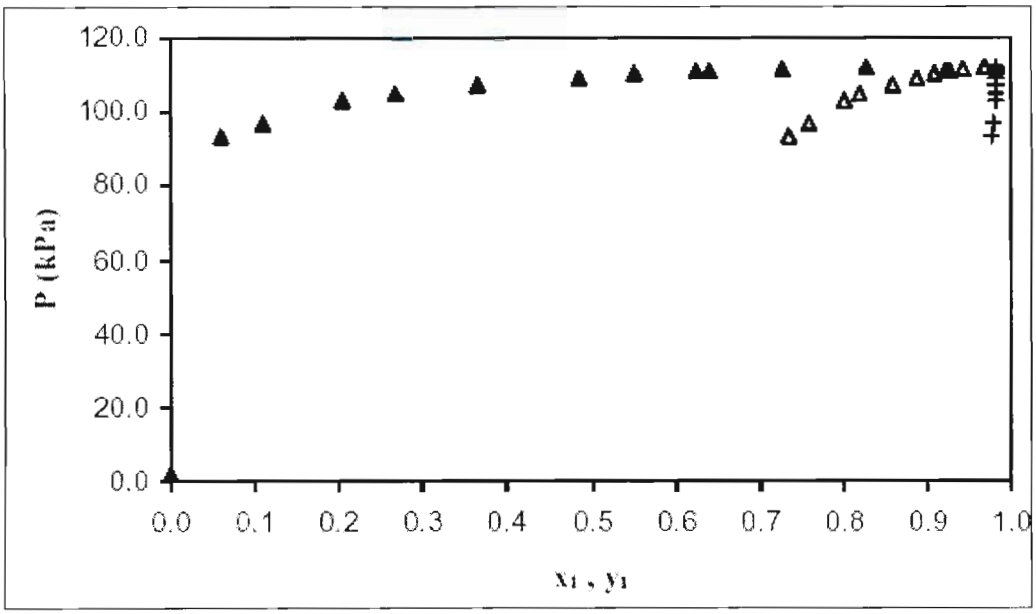

Figure 7.12 P-x-y plot of 1-propanol (1) + n-dodecane (2) system at 373.15K, ▲ - experimental P-x_i data, Δ-P-$y_{i,,}$ + - P-y_i calculated vapour composition, Reddy [2006]

7.3.2.4 2-Propanol (1) + n-dodecane (2) system

Table 7.8 Activity model parameters and deviations between calculated and experimental measurements for 2-propanol (1) + n-dodecane (2) system

Activity coefficient model		333.15K	343.15K	353.15K
Wilson				
	λ_{12}-λ_{21} (J/mol)	9002.349	9650.867	8534.146
	λ_{12}-λ_{22} (J/mol)	1725.576	1848.416	1277.69
	Average δP (kPa)	0.010	0.023	0.054
	Average δy_1	0.003	0.011	0.013
NRTL				
	g_{12}-g_{11} (J/mol)	2146.54	2145.874	4216.318
	g_{12}-g_{22} (J/mol)	1973.212	2131.191	2597.485
	α	0.091	-0.067	-0.479
	Average δP (kPa)	0.019	0.031	0.113
	Average δy_1	0.028	0.020	0.014
UNIQUAC				
	u_{12}-u_{11} (J/mol)	308.855	455.279	453.442
	u_{12}-u_{22} (J/mol)	-283.016	1566.403	-538.123
	Average δP (kPa)	0.024	0.294	0.093
	Average δy_1	0.031	0.102	0.014

The n-dodecane + 2-propanol system displayed a high relative volatility and consequently, proved problematic to regress with the chosen Gibbs excess models. Table 7.8 shows the regressed data results. The best fit data was judged using the pressure residual according to Equation (7-4). Figures 7.12 to 7.18 graphically presents the binary VLE data reduction and Figures 7.19 to 7.21 shows the experimental activity coefficients calculated using P-T-x-y data (Equation (7-7)). It is apparent that the Wilson model is superior to NRTL and UNIQUAC models, tabulated in Table 7.8, although the NRTL model could also be recommended in place of the Wilson model for specific conditions. The UNIQUAC model yielded the worst fit; this can be attributed to the UNIQUAC being a correlative model and was the least computationally efficient due to its algebraic form.

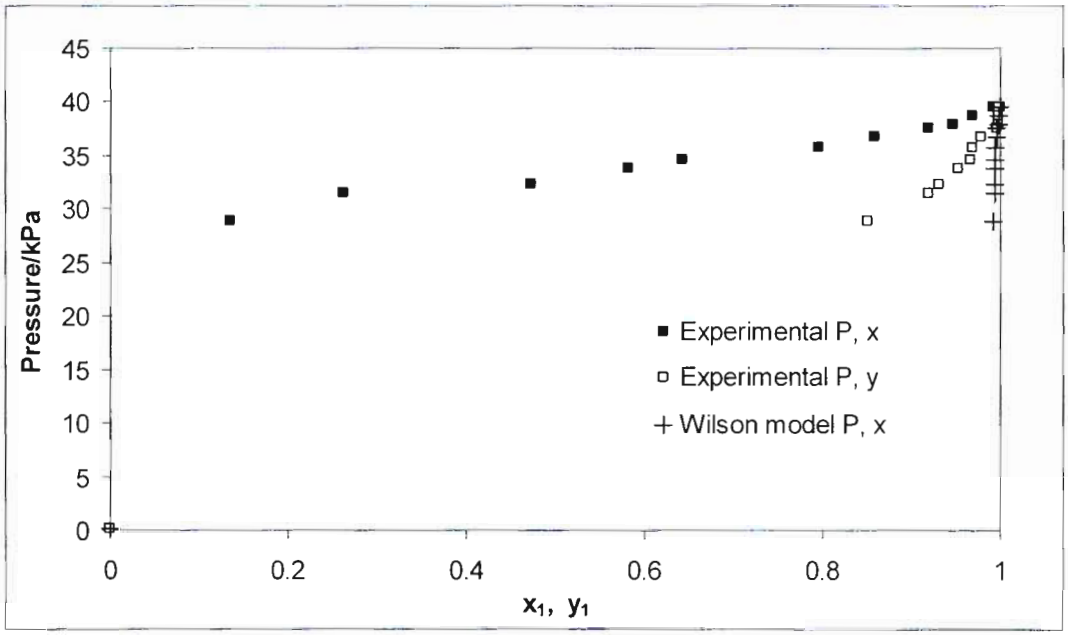

Figure 7.13 P-x-y plot of 2-propanol (1) + n-dodecane (2) system at 333.15K, ▪ - experimental P-x_i data, + - P-y_i Wison model

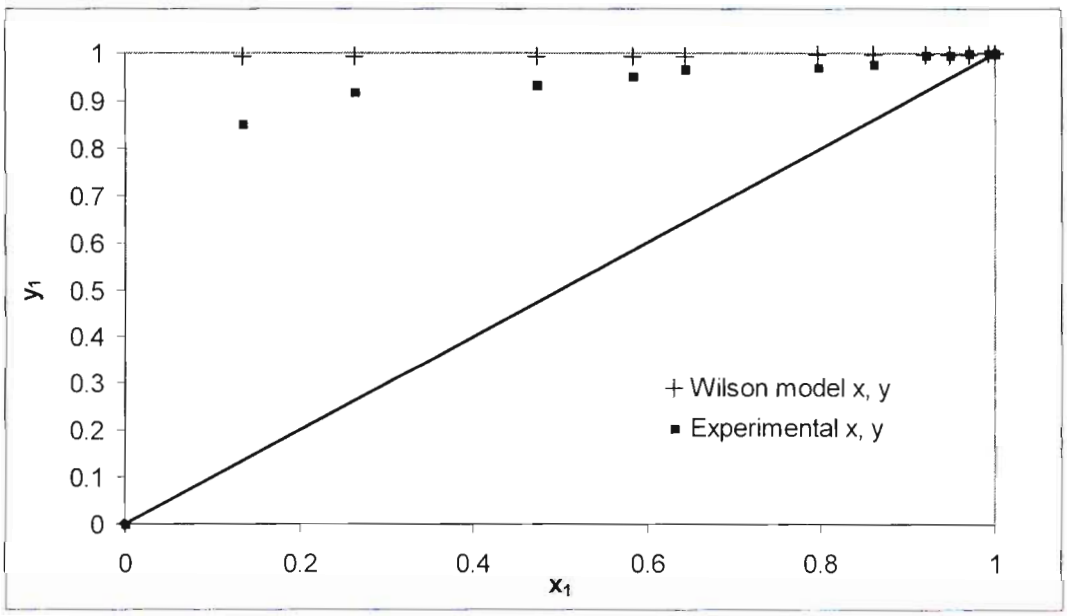

Figure 7.14 x-y plot of 2-propanol (1) + n-dodecane (2) at 333.15K

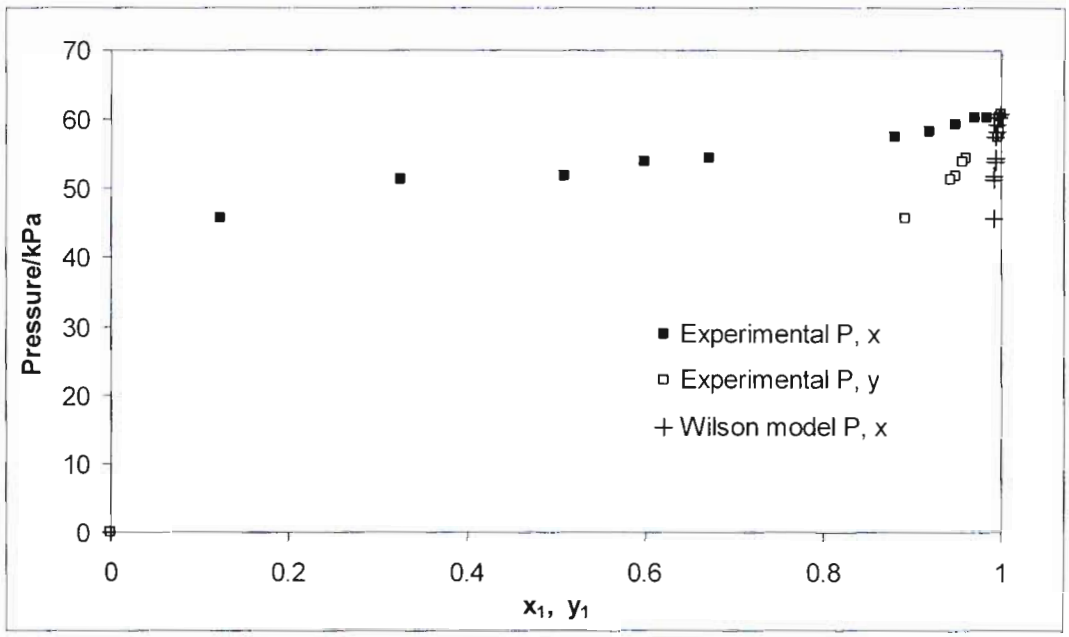

Figure 7.15 P-x-y plot of 2-propanol (1) + n-dodecane (2) system at 343.15K. ▪ - experimental P-x_i data, □-P-$y_{i,}$, + - P-y_i Wilson model

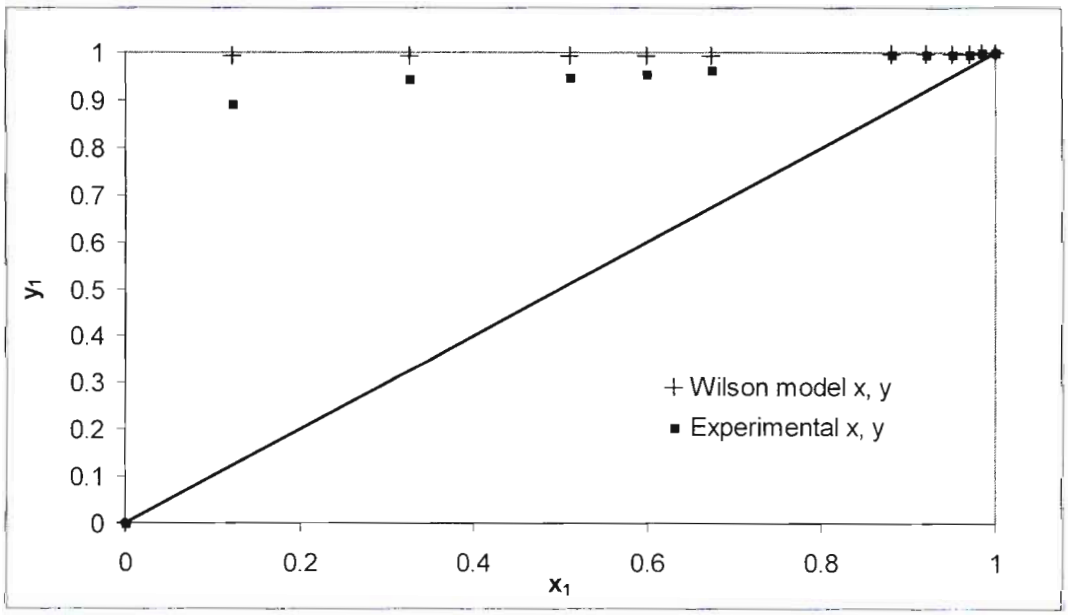

Figure 7.16 x-y plot of 2-propanol (1) + n-dodecane (2) system at 343.15K

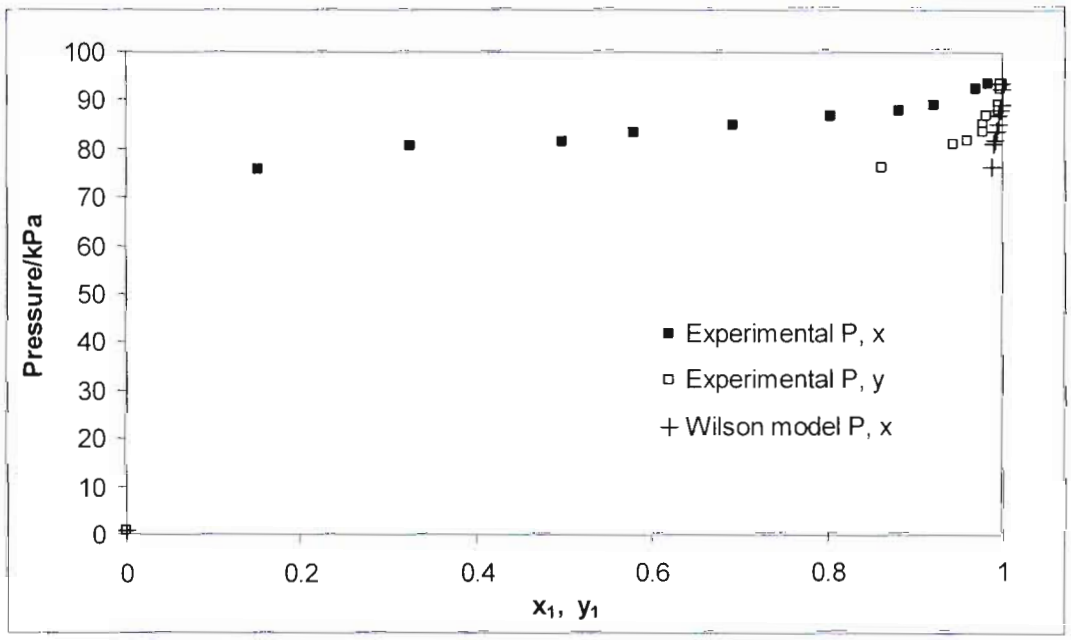

Figure 7.17 P-x-y plot of 2-propanol (1) + n-dodecane (2) system at 353.15K, ▪ - experimental P-x_i data, □-P-$y_{i,}$, + - T-y_i, Wilson model

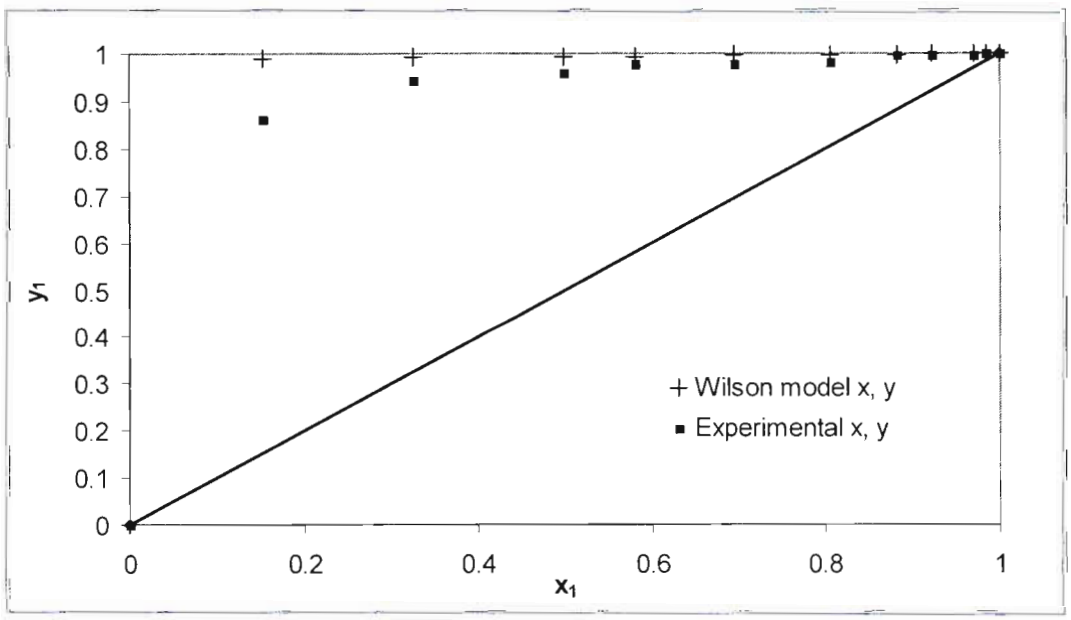

Figure 7.18 x-y plot of 2-propanol (1) + n-dodecane (2) system at 353.15K

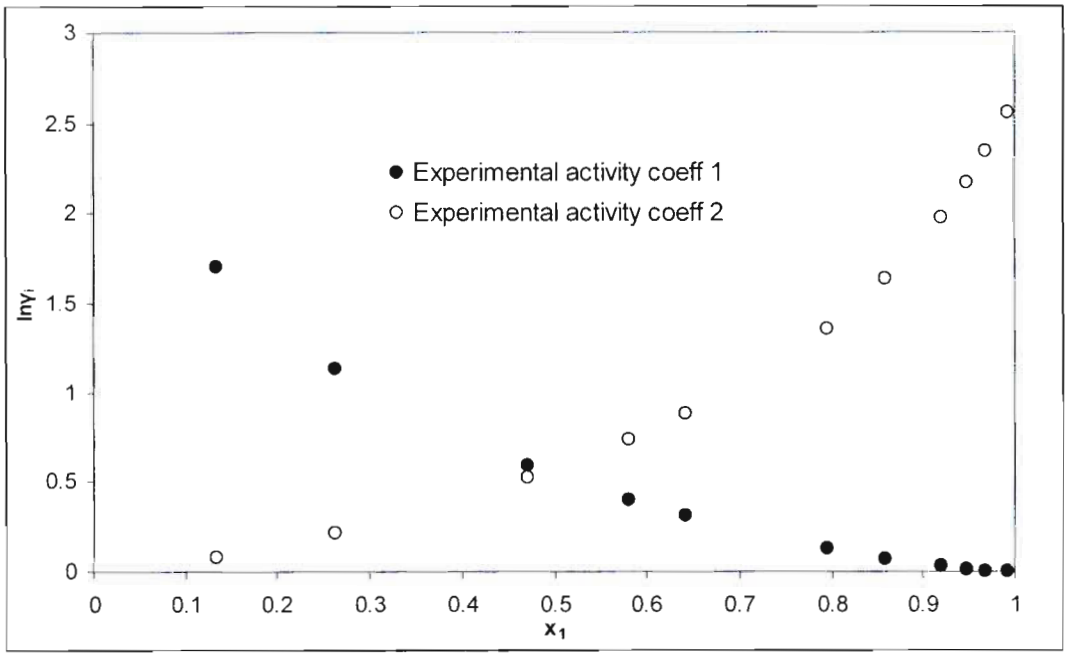

Figure 7.19 Plot of experimental activity coefficients for the 2-propanol (1) + n-dodecane (2) system at 333.15K

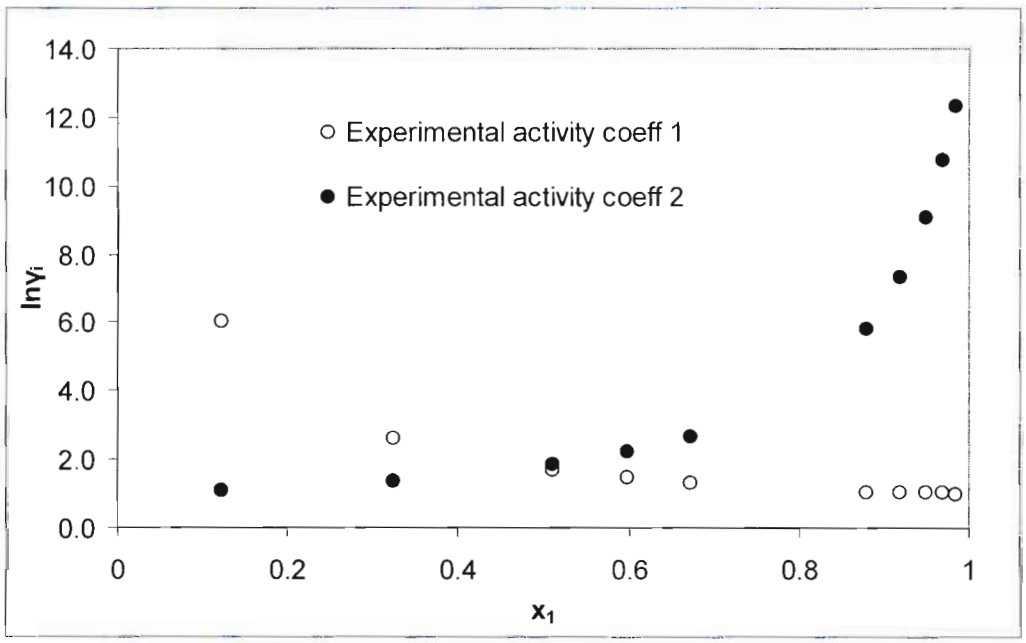

Figure 7.20 Plot of experimental activity coefficients for the 2-propanol (1) + n-dodecane (2) system at 343.15K

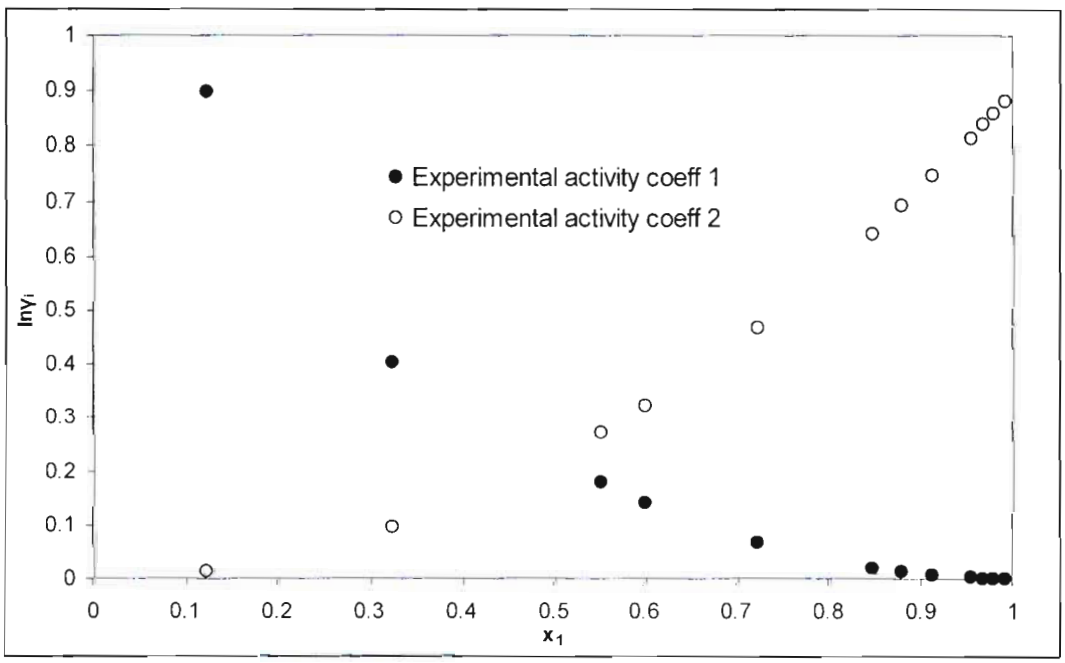

Figure 7.21 Plot of experimental activity coefficients for the 2-propanol (1) + n-dodecane (2) system at 353.15K

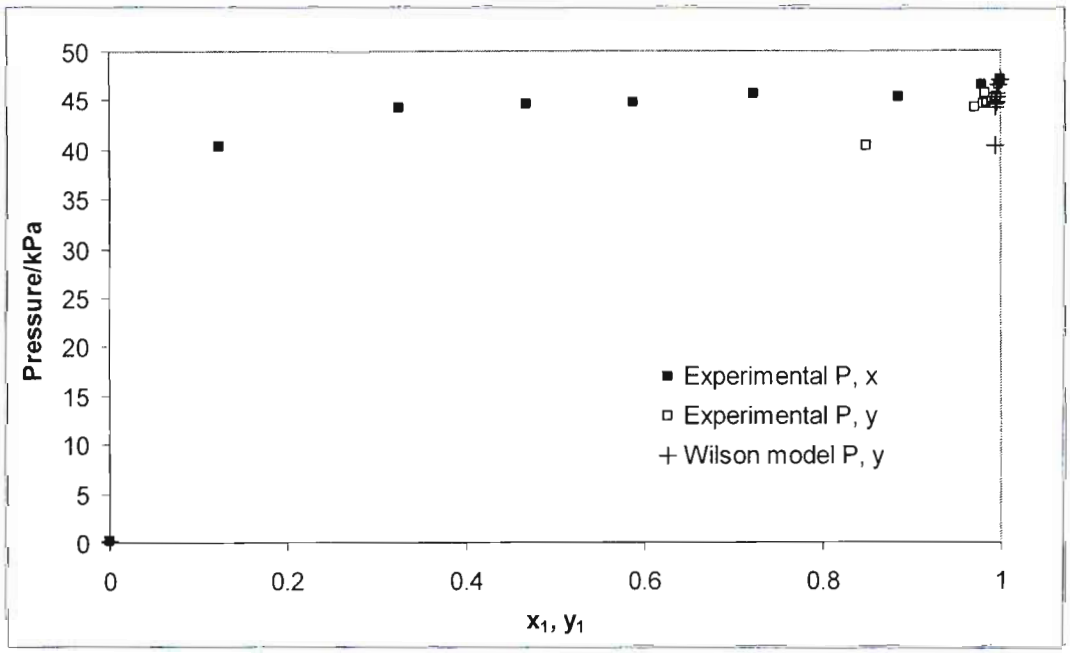

Figure 7.22 P-x-y plot of ethanol (1) + n-dodecane (2) system at 333.15K, ▪ - experimental P-x_i data, □-P-$y_{i,}$, + - P-y_i, Wilson model

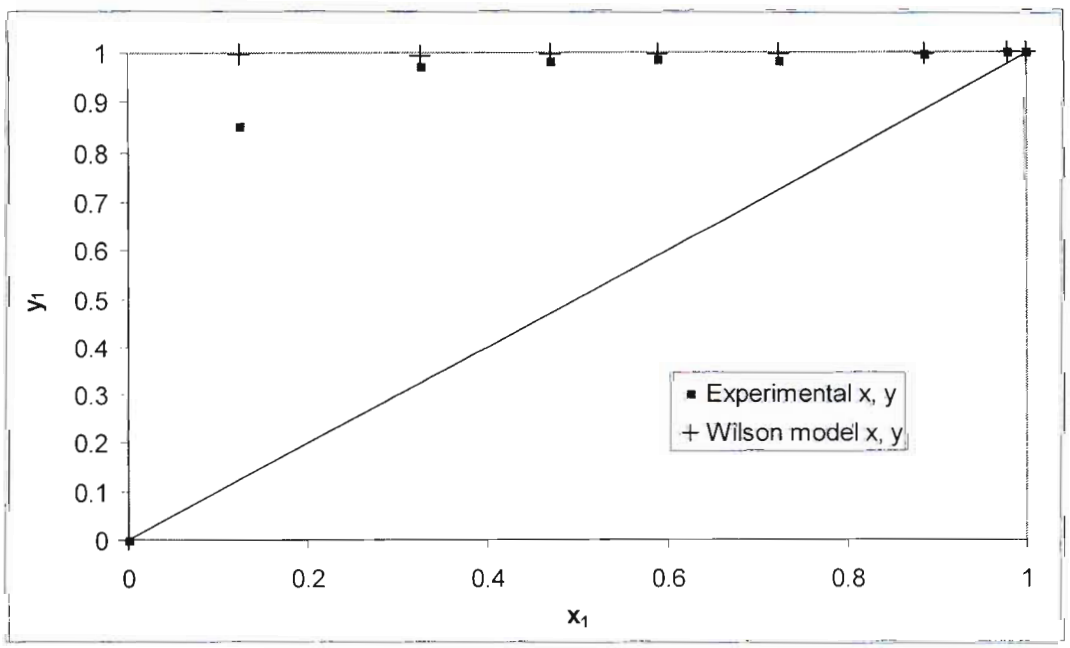

Figure 7.23 x-y plot of n-dodecane (2) / ethanol (1) system at 333.15K

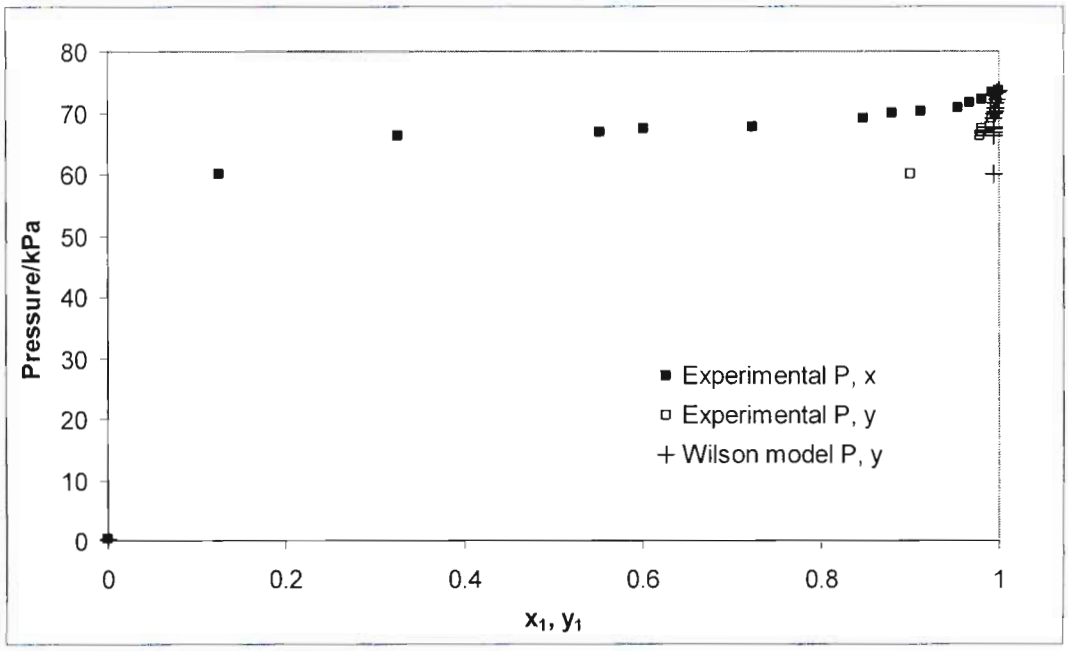

Figure 7.24 P-x-y plot of ethanol (1) + n-dodecane (2) system at 353.15K, ▪ - experimental P-x_i data, □-P-$y_{i,,}$ + - P-y_i Wilson model

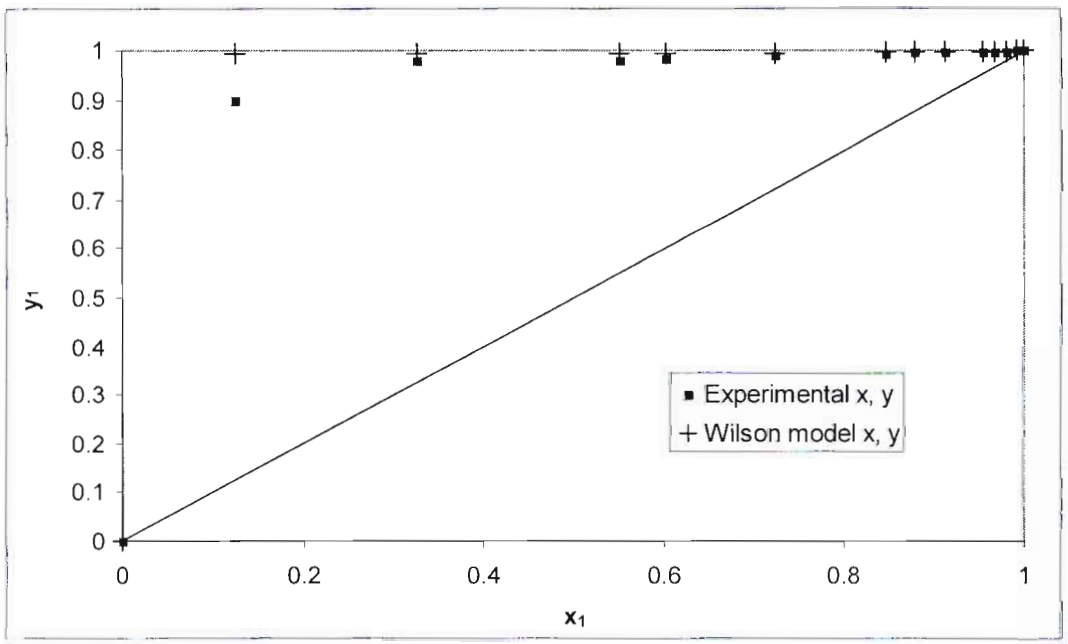

Figure 7.25 x-y plot of ethanol (1) + n-dodecane (2) system at 343.15K

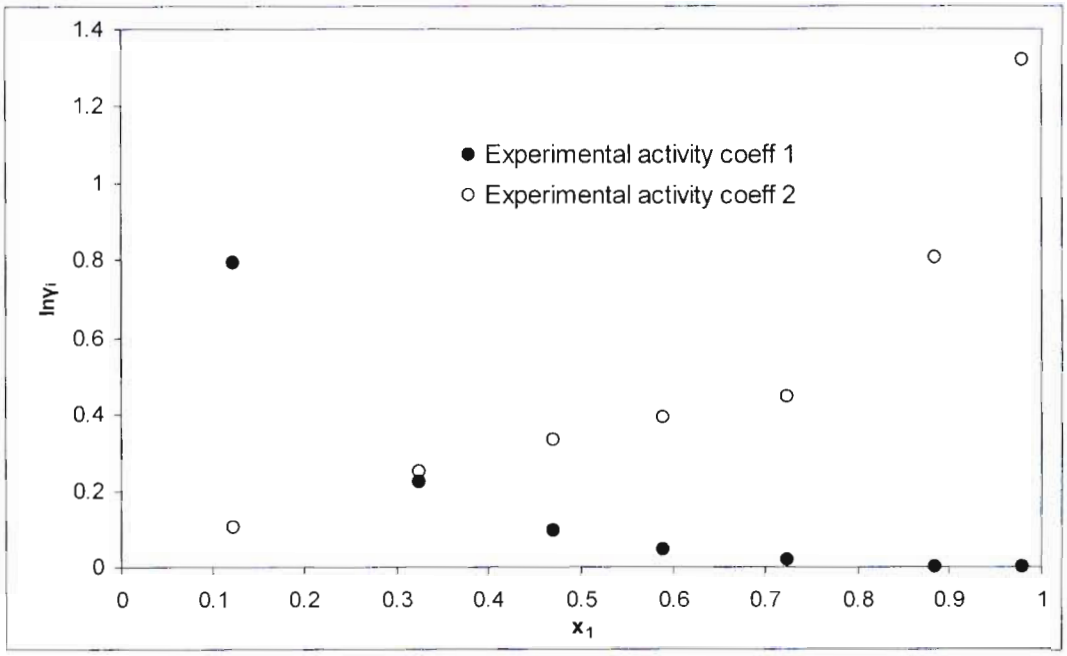

Figure 7.26 Plot of experimental activity coefficients for the ethanol (1) + n-dodecane (2) system at 333.15K

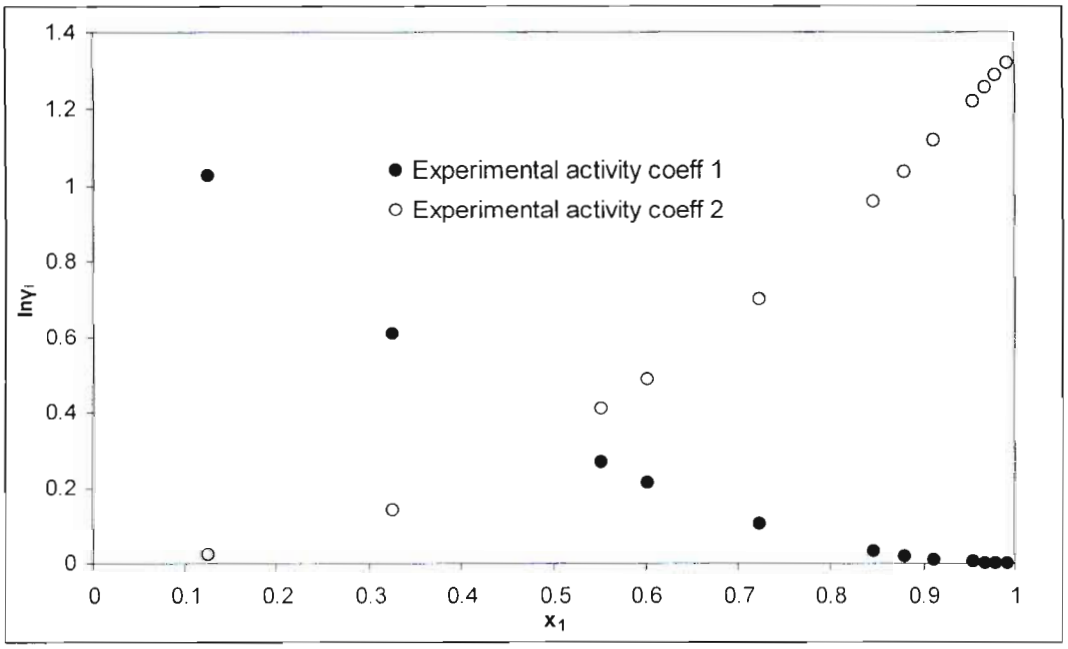

Figure 7.27 Plot of experimental activity coefficients for the ethanol (1) + n-dodecane (2) system at 343.15K

7.4 Experimental LLE experimental data reduction

7.4.1 Binary LLE

Since both LLE and VLE are governed by thermodynamic fundamentals there is only a single relationship for the activity coefficient, [Raal and Mühlbauer, 1998]. Thereby, activity coefficient parameters are found using mutual solubility data shown by Equation (7.8) (discussed in Chapter 3).

$$x_i^{\alpha} \gamma_i^{\alpha} = x_i^{b} \gamma_i^{b} \tag{7-8}$$

The activity coefficient models used were the Margules 3-suffix and the Van Laar model.

7.4.1.1 n-Heptane + methanol system

n-Heptane + methanol system was employed as the binary LLE test system ensuring the LLE apparatus operated correctly and the experimental procedure was accurate. The experimental data matched the data of Nagatani et al [1987] well (shown in Chapter 6).

Two activity coefficient models were used to regress the binary LLE data (discussed in Chapter 3). The temperature dependant model parameters are listed in Table 7.10 for each temperature measurement. The model parameters, A_{21} and A_{12}, were evaluated for each respective model using Equations (3-42), (3-43), (3-48) and (3-49). The regressed parameters were approximated within the temperature range using a quadratic function in the program Microsoft EXCEL®. The quadratic function was optimized based on a least squares deviation, R^2 (R^2=1 being a perfect fit). The regressed parameters in the respective models are displayed in Table 7.10 and a graphical representation of the best fit polynomial is shown in Figures 7.26-7.27.

Table 7.10 Regressed binary LLE data

	Margules 3-Suffix		Van Laar	
T (K)	A_{21}	A_{12}	A_{12}	A_{21}
324.55	1.618	2.473	2.339	1.336
317.22	1.861	2.532	2.471	1.750
315.22	1.927	2.543	2.494	1.861
311.25	2.026	2.625	2.586	1.959
306.35	2.148	2.677	2.651	2.106
301.25	2.301	2.725	2.713	2.281

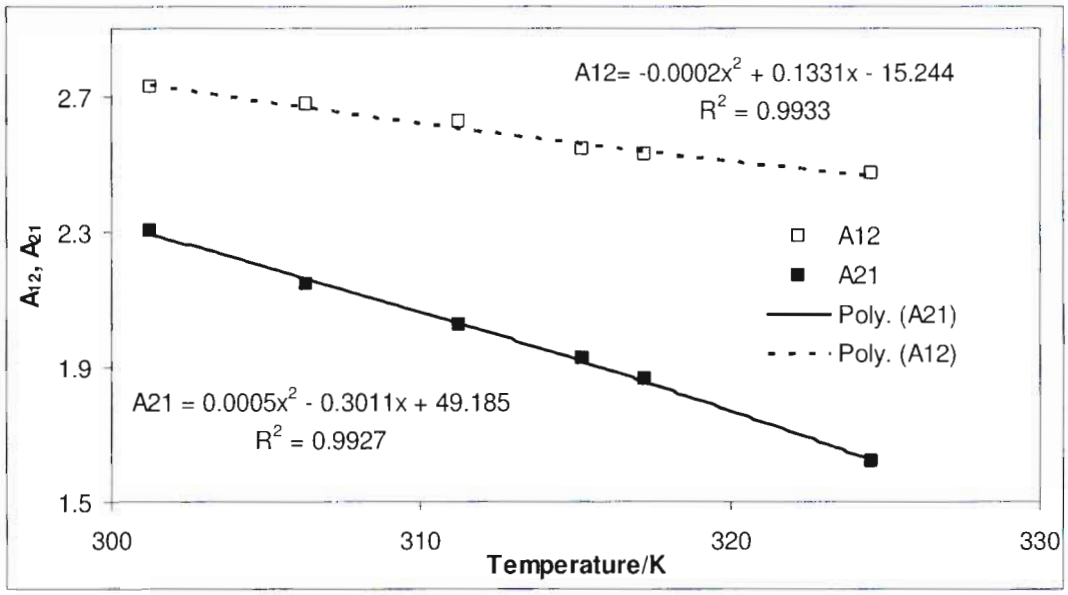

Figure 7.28 Margules 3-suffix parameters of n-heptane (1) + methanol (2) system at 101.325 kPa

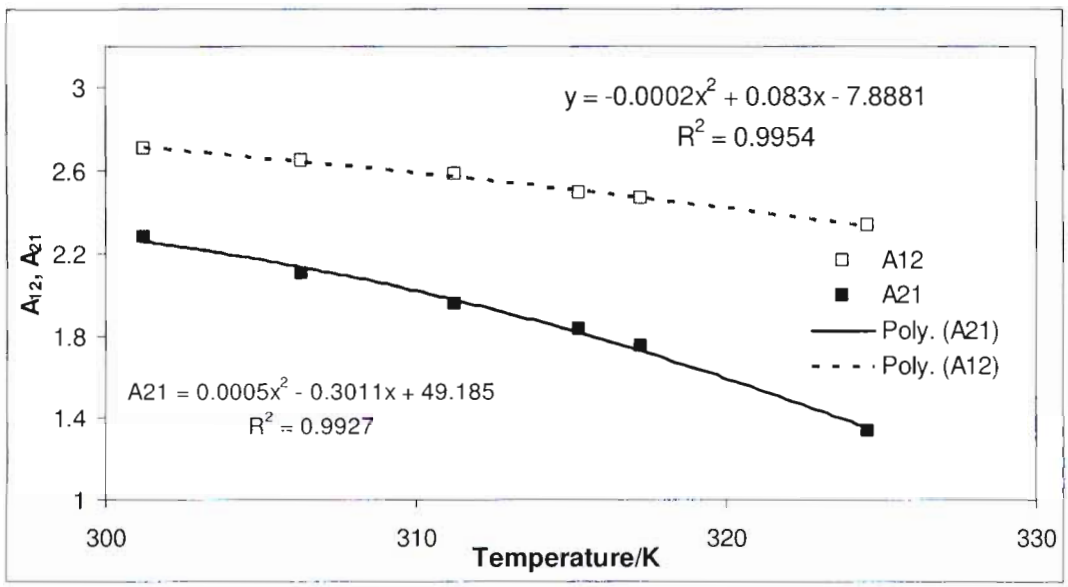

Figure 7.29 Van Laar parameters of n-heptane (1) + methanol (2) system at 101.325 kPa

7.4.2 Ternary LLE data regression

Ternary LLE was correlated by regressing the binodial curve and tie lines independently (discussed in Chapter 3). Both systems investigated produced two liquid phases. The tie lines were regressed using the NRTL and modified-UNIQUAC models which produced the activity coefficients for the respective phases. The NRTL parameter, αij was made equal for all binary pairs and fixed at following values 0.20, 0.25, 0.30, 0.35 and 0.40. The tie lines were regressed using the algorithm of Walas [1985] and optimized with the least squares object algorithm of Novek et al [1987]. The regression was accomplished using MATLAB® (Version 7.0.). The built-in optimization function, *fminsearch* was used which finds the minimum of an unconstrained multi-variable function using the algorithm was based on a Nedler-Mead simplex method, [Lagarias et al., 1998]. The best fit model was judged using the RMSD, Equation (7-9). The MATLAB® (Version 7.0.) code employed to regress ternary LLE data is displayed in Appendix D.

$$RMSD = \left[\frac{\sum_{a}\sum_{b}\sum_{c} x_{abc}(\exp)^2 - x_{abc}(calc)^2}{6k} \right] \tag{7-9}$$

The binodial curves were modeled using the β–density function and Log γ equation. The binodial curves were correlated by using the sum of the square of the difference between the experimental and calculated mole fractions. The regression was accomplished by using the Newton-Rhapson method in the Microsoft EXCEL® program. The parameters were optimized by minimizing the standard deviation term shown in Equation (7-10).

$$\sigma = \left[\left(\sum_{i=1}^{n} x_2 calc - x_2 \exp \right)^2 / (n-3) \right]^{0.5} \tag{7-10}$$

7.4.2.1 n-Dodecane + water + light alkanol systems

The ternary LLE system, n-dodecane + water + light alkanol would theoretically display two separate phases at appropriate overall compositions. This can be explained by looking at the molecular structure of each chemical illustrated in Figure 7.30.

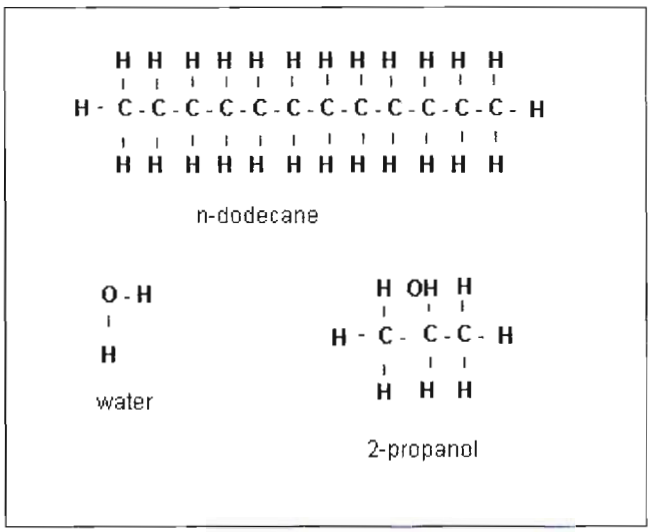

Figure 7.30 Selected molecular structure

n-Dodecane is a hydrophobic non-polar saturated hydrocarbon which forms an immiscible liquid mixture with water being a highly polar compound exhibiting hydrogen-bonding. The light alkanol exhibits hydrogen bonding and hydrophobic qualities due to the hydroxyl bond and carbon-hydrogen bonds respectively. These two properties make the light alkanol miscible in both the water and n-dodecane thereby possibly creating a two partially miscible phases.

A large two phase envelope would be expected between the ternary mixture caused by the high immiscibility between water and n-dodecane. However, a single liquid mixture could be expected at elevated concentrations of the light alkanol described as a type 1 ternary LLE system (Chapter 3), Treybel, [1963].

Indeed, all ternary LLE systems displayed type 1 systems, Treybel, [1963], shown in subsequent sections. The extracted light alkanol can be easily separated from n-dodecane using distillation methods due to the high relative volatility making n-dodecane a useful solvent for the extraction of light alkanols from water.

7.4.2.2 n-Dodecane (1) + water (2) + ethanol (3) system

n-Dodecane is immiscible in water but miscible in ethanol creating a large two phase region which can be classified as a type I system for both temperatures, Treybal [1963]. A homogenous phase is found near the ethanol rich region. The binodial curve displays a smooth trend typical of a type I system. Acquirement of experimental tie line data at elevated ethanol concentrations was limited due to the thin top phase (n-dodecane rich phase) envelope. Sampling of this phase was difficult due to limitations in the LLE still design as was observed for the n-dodecane + 2-propanol + water ternary LLE system.

The tie line regression revealed the NRTL to be the best fit model for both systems at 333.15K (α_{ij}=0.2) and 323.15K (α_{ij}=0.3), listed in Table 7.11. The Log γ function fitted the 333.15K system the best whereas the β-function fitted the 323.15K system. However, both curve fitting models accurately reproduced the binodial curve tabulated in Table 7.12. Figure 7.30 and Figure 7.31 graphically represent the regressed data against experimental LLE data.

Table 7.10 Regressed LLE tie line data for the n-dodecane (1) + water (2) + ethanol (3) system

Correlation models			
NRTL		**Modified UNIQUAC**	
333.15K			
g_{21}-g_{11} (J/mol)	12499.370	u_{21}_u_{11}(J/mol)	6366.158
g_{12}-g_{22} (J/mol)	8293.293	u_{12}_u_{22} (J/mol)	8946.685
g_{13}-g_{33} (J/mol)	1631.002	u_{13}_u_{33} (J/mol)	6023.702
g_{31}-g_{11} (J/mol)	6399.212	u_{31}_u_{11} (J/mol)	6107.298
g_{23}-g_{33} (J/mol)	1677.707	u_{23}_u_{33} (J/mol)	6352.824
g_{32}-g_{22} (J/mol)	1090.729	u_{32}_u_{22} (J/mol)	5767.954
RMSD	0.010	RMSD	0.071
NRTL		**Modified UNIQUAC**	
323.15K			
g_{21}-g_{11} (J/mol)	10949.081	u_{21}_u_{11}(J/mol)	6766.595
g_{12}-g_{22} (J/mol)	10071.252	u_{12}_u_{22} (J/mol)	8293.853
g_{13}-g_{33} (J/mol)	208.002	u_{13}_u_{33} (J/mol)	5365.566
g_{31}-g_{11} (J/mol)	13565.870	u_{31}_u_{11} (J/mol)	6879.458
g_{23}-g_{33} (J/mol)	15464.351	u_{23}_u_{33} (J/mol)	5856.118
g_{32}-g_{22} (J/mol)	-4652.032	u_{32}_u_{22} (J/mol)	5350.005
RMSD	0.014	RMSD	0.074

Table 7.11 Regressed binodial curve data for the n-dodecane (1) + water (2) + ethanol (3) system at 101.325 kPa

Different functions			
Log γ		β Function	
		333.15K	
A_1	4.437	B_1	4.498
A_2	1.323	B_2	1.327
A_3	1.812	B_3	1.196
σ	0.0079	σ	0.0089
		323.15K	
A_1	4.425	B_1	4.966
A_2	1.321	B_2	1.367
A_3	1.845	B_3	1.364
σ	0.00058	σ	0.00056

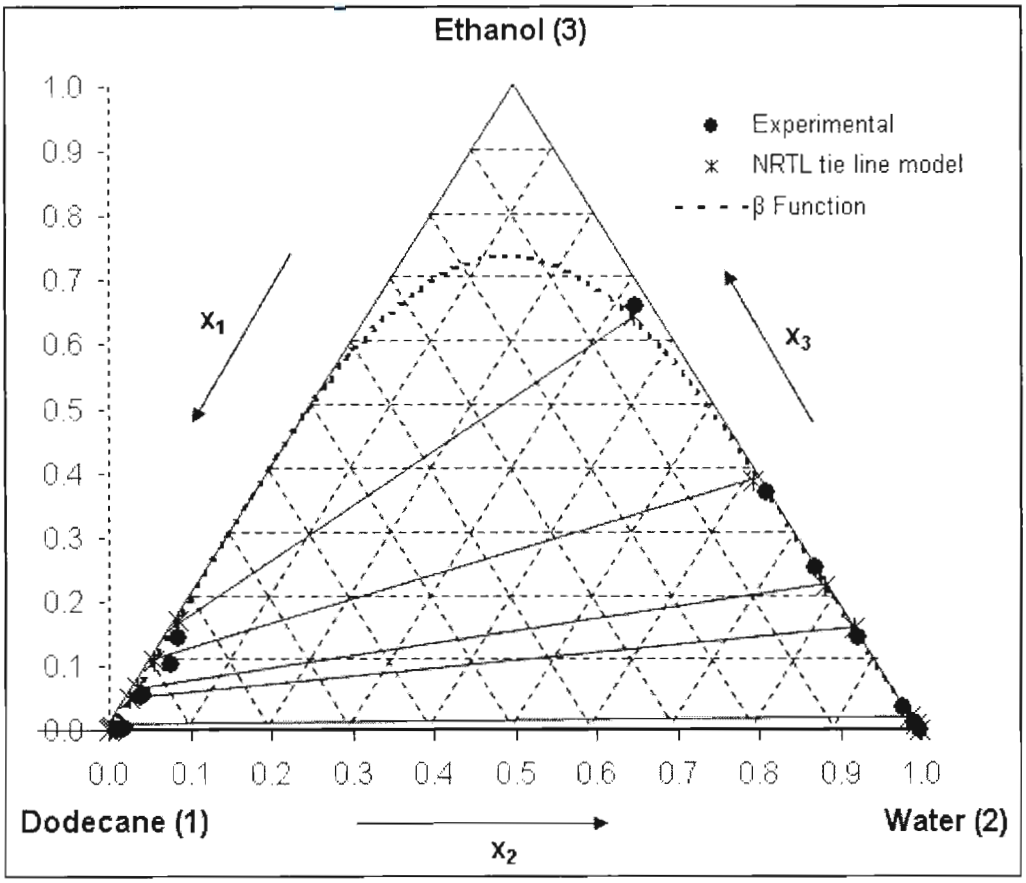

Figure 7.30 n-dodecane (1) + water (2) + ethanol (3) system at 333.15K and 101.325 kPa

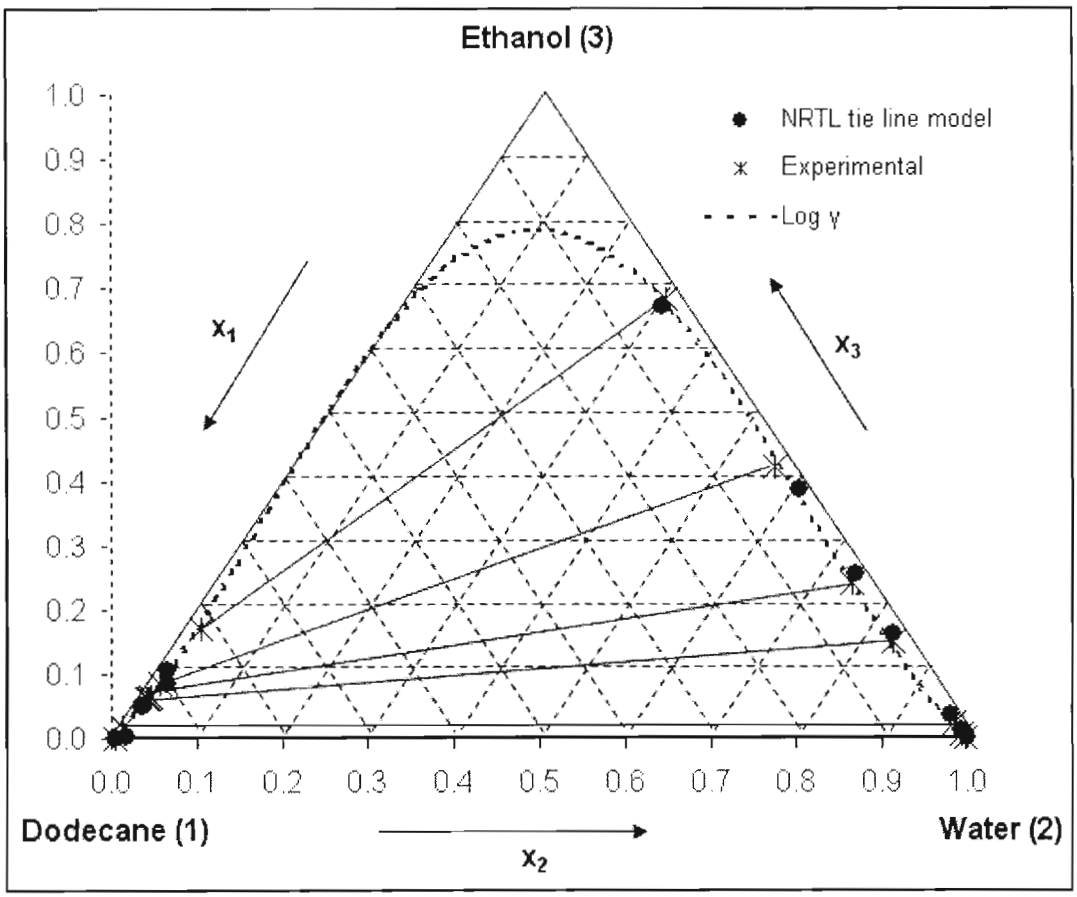

Figure 7.31 n-Dodecane (1) + water (2) + ethanol (3) system at 323.15K and 101.325 kPa

7.4.2.3 n-Dodecane (1) + water (2) + 2-propanol (3)

n-Dodecane is immiscible in water but miscible in 2-propanol creating a large two phase region which can be classified as a type I system for both temperatures according to Treybal [1963]. A homogenous phase is found near the 2-propanol rich region. It must be noted that during measurement, the n-dodecane rich phase (top phase) envelope was very thin for higher concentrations of 2-propanol. Even after altering the overall composition of the water and n-dodecane mixture, did not make a significant difference to the size of the top phase envelope. This resulted in a lack of experimental tie-line data toward the 2-propanol rich region because of difficulty in sampling as was observed in the n-dodecane + ethanol + water ternary LLE system.

The binodial curve displays a smooth trend typical of a type I system shown in Figure 7.32 and 7.33. The tie line regression revealed the NRTL to be the best fit model for the system at 328.15K (α_{ij}=0.3) and the modified UNIQUAC for the 333.15K listed in Table 7.13. The β-function best fitted both binodial curves. However as with the n-dodecane + ethanol + water LLE system, both curve fitting models accurately reproduced the binodial curve tabulated in Table 7.14. Figure 7.32 and Figure 7.33 graphically represent the regressed data against experimental LLE data.

Table 7.13 Regressed LLE tie line data for the n-dodecane (1) + water (2) + 2-propanol (3) system at 101.325 kPa

Correlation models			
NRTL		**Modified UNIQUAC**	
333.15K			
G_{21}-g_{11} (J/mol)	10703.781	u_{21}_u_{11}(J/mol)	6322.695
G_{12}-g_{22} (J/mol)	14119.822	u_{12}_u_{22} (J/mol)	9919.695
G_{13}-g_{33} (J/mol)	4468.484	u_{13}_u_{33} (J/mol)	6102.918
g_{31}-g_{11} (J/mol)	1255.216	u_{31}_u_{11} (J/mol)	5950.993
g_{23}-g_{33} (J/mol)	8856.341	u_{23}_u_{33} (J/mol)	6135.156
g_{32}-g_{22} (J/mol)	-5186.07	u_{32}_u_{22} (J/mol)	5783.481
RMSD	0.054	**RMSD**	0.043
NRTL		**Modified UNIQUAC**	
328.15K			
g_{21}-g_{11} (J/mol)	12769.190	u_{21}_u_{11}(J/mol)	5565.006
g_{12}-g_{22} (J/mol)	14930.321	u_{12}_u_{22} (J/mol)	8009.028
g_{13}-g_{33} (J/mol)	7624.4221	u_{13}_u_{33} (J/mol)	5917.572
g_{31}-g_{11} (J/mol)	-538.877	u_{31}_u_{11} (J/mol)	8004.725
g_{23}-g_{33} (J/mol)	1512.952	u_{23}_u_{33} (J/mol)	5835.887
g_{32}-g_{22} (J/mol)	880.684	u_{32}_u_{22} (J/mol)	5347.231
RMSD	0.059	**RMSD**	0.036

Table 7.14 Regressed binodial curve data for the n-n-dodecane (1) + water (2) + ethanol (3) system at 101.325 kPa

Different correlations			
Log γ		β Function	
		333.15K	
A_1	1.638	B_1	1.784
A_2	0.929	B_2	0.959
A_3	1.210	B_3	0.899
σ	0.00081	σ	0.00073
		328.15K	
A_1	1.960	B_1	2.148
A_2	1.005	B_2	1.037
A_3	1.277	B_3	0.946
σ	0.00093	σ	0.00079

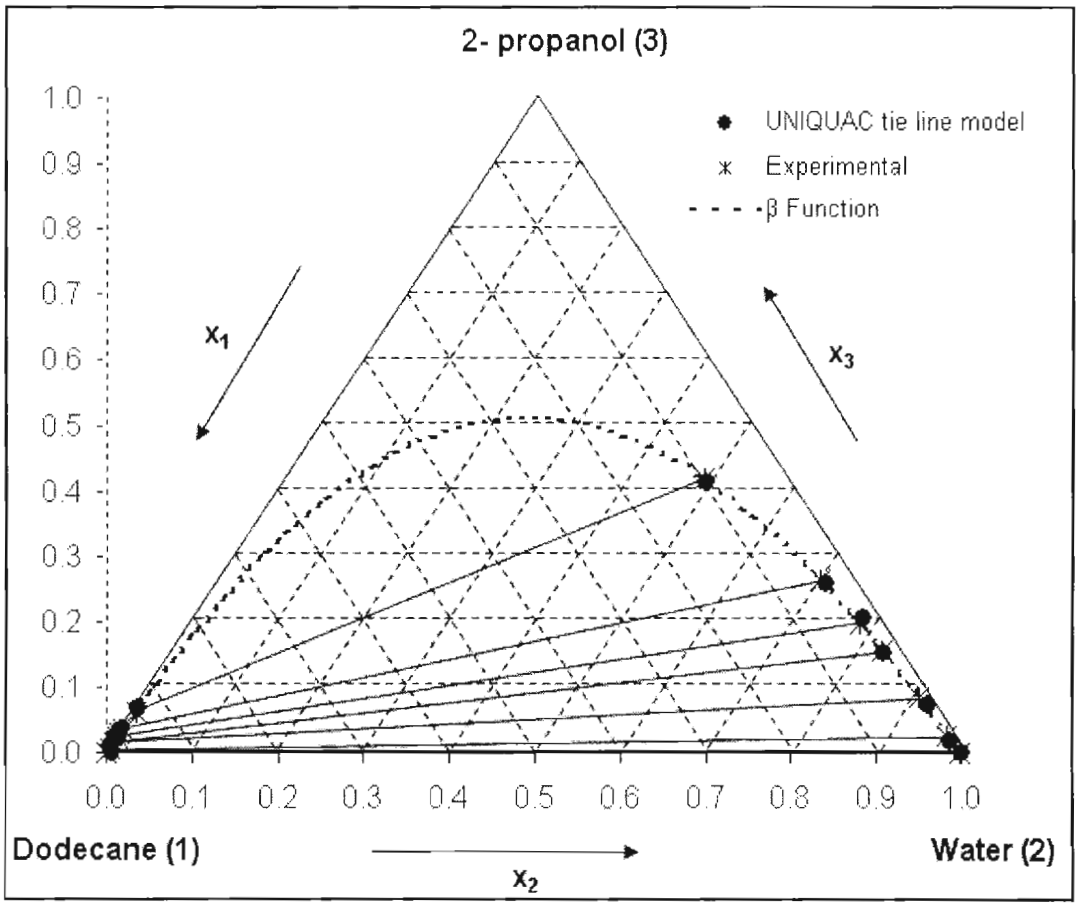

Figure 7.32 n-Dodecane (1) + water (2) + 2-propanol (3) system at 333.15K and 101.325 kPa

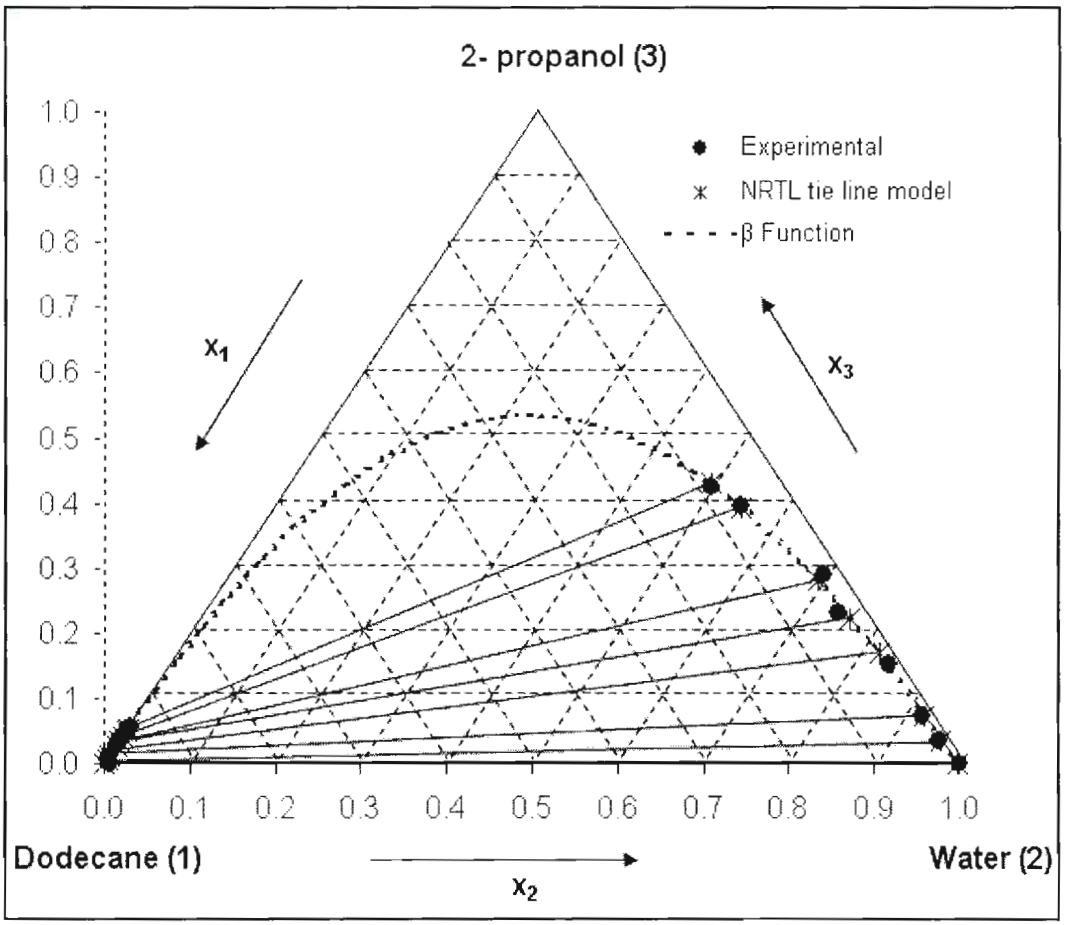

Figure 7.33 n-Dodecane (1) + water (2) + 2-propanol (2) system at 328.15K and 101.325 kPa

CHAPTER 8
CONCLUSION

This study encompassed phase equilibrium data (PED) measurement of selected isothermal binary vapour liquid equilibrium (VLE) systems of n-dodecane + alkanol at sub-atmospheric pressures on a newly re-constructed re-circulating VLE still designed to handle binary chemical systems with high relative volatility. Ternary liquid liquid equilibrium (LLE) data measurement of dodecane + water + an alkanol at atmospheric pressure and particular temperatures were undertaken using the LLE still of Ndlovu [2005]..

An innovative mixing system was introduced into the VLE still of Ndlovu [2005] compromising of a mixing tee, glass spiral placed inside this mixing tee and a novel mixing chamber. The VLE still was designed for operation at sub-atmospheric pressure and temperatures below 473.15 K, and measurement of binary VLE data for organic compounds. Previously unmeasured isothermal binary VLE data for n-dodecane + ethanol and for n-dodecane + 2-propanol was acquired using the VLE still.

The new VLE still design improved the rate of VLE data measurements and increased the range of measurable systems. However, it is evident from the VLE data obtained for systems with n-dodecane + alkanol that the present VLE still design did not adequately evaluate chemical systems of this severity.

Previously unmeasured ternary LLE data was attained using the LLE still of Ndlovu [2005]. Ternary LLE data for n-dodecane + water + ethanol and n-dodecane + water + 2-propanol were measured at atmospheric pressure for selected temperatures. All measured ternary LLE data systems displayed type I ternary LLE data systems, [Treybal, 1963].

CHAPTER 9
RECOMMENDATIONS

It is evident from the binary vapour-liquid equilibrium data obtained for systems with large relative volatilities (n-dodecane + alkanol) that the present design of the VLE equipment is not capable of handling data measurement for binary mixtures of this nature. Therefore, the following recommendations are proposed to further improve the efficiency and operation of the VLE still for such systems:

1. The addition of mechanical mixing to the boiling chamber improving the current mixing. This would entail a re-design of the base of the boiling chamber and the recycle line.
2. The addition of 3 mm wire mesh packing into the return tee increasing the contact area for the return liquids.
3. The re-design of the equilibrium chamber consisting of an annular Cottrell pump. The Cottrell pump would bubble the vapour/liquid mixture into a liquid kept at a constant level inside this chamber encompassing the principal of gas stripping.
4. Larger vapour sample traps whereby mechanical mixing would be introduced.
5. The binary VLE systems should be re-measured using a different experimental method such as the static method since discrepancies with vapour phase samples were encountered.

REFERENCES

A. Dashtizadeh, G. R. P., V. Taghikhani, C. Ghotbi. (2006). "A new two-parameter cubic equation of state for predicting phase behaviour of pure compounds and mixtures." *Fluid Phase Equilibria*, 242, 19-28.

Abrams, D S and Prausnitz, J M, (1975), "Statistical Thermodynamics of Liquid Mixtures: A New Expression for the Excess Gibbs Energy of Partly or Completely Miscible Systems", *American Institute of Chemical Engineers Journal*, Vol. 21, pp. 116-128.

Alders, L, (1959), "Liquid-Liquid Extraction", 2nd edition, Elsevier, Amsterdam.

Agnes Szanyi, P. M., Zsolt Fonyo. (2004). "Novel hybrid separation processes for solvent recovery based on positioning the extractive heterogeneous-azeotropic distillation." *Chemical Engineering and Processing*, 43, 327-338.

Aly, I. A. a. G. (1996). "Effect of computation techniques for equation of state binary interaction parameters on the prediction of binary VLE data." *Computers chem. Engng*, 20(1), 79-91.

Anderson, T F and Prausnitz, J M, (1978), "Application of the UNIQUAC Equation to Calculation of Multicomponent Phase Equilibria. 1: Vapour-Liquid Equilibria; 2: Liquid-Liquid Equilibria", *Industrial and Engineering Chemistry. Process Design and Development*, Vol. 17, pp. 552-567.

Andreas Grenner, M. K., Jurgen Schmelzer. (2005). "An equipment for dynamic measurements of vapour-liquid equilibria and results in binary systems containing cyclohexylamine." *Fluid Phase Equilibria*, 233, 170-175.

Andreas Grenner, M. K., Jurgen Schmelzer. (2005). "An equipment for dynamic measurements of vapour–liquid equilibria and results in binary systems containing cyclohexylamine." *Fluid Phase Equilibria*, 233, 170-175.

B. Schafer, R. L. (1995). "Modeling of thermodynamic properties of associated solutions with

equilibrium constants defined on activities." *Fluid Phase Equilibria*, 112, 101-123.

Baker, E M, Hubbard, R O H, Huguet, J H and Michalowski, S S, (1939), "Equilibria in the Systems Ethanol - Water, Ethanol - Cellosolve, and Cellosolve - Water", *Industrial and Engineering Chemistry*, Vol. 31, pp. 1260-1262.

Barbara Wisniewska-Goclowska, S. K. M. (2001). "A new modification of the UNIQUAC equation including temperature dependent parameters." *Fluid Phase Equilibria*, 180, 103-113.

Black, C, (1958), "Vapour Phase Imperfections in Vapour-Liquid Equilibria", *Industrial and Engineering Chemistry*, Vol. 50, pp. 391-402.

Browarzik, D. (2005). "Phase-equilibrium calculations for non-aqueous and aqueous associating systems using continuous thermodynamics." *Fluid Phase Equilibria*, 230, 143-152.

C. Browarzik, D. B. (2005). "Liquid–liquid equilibrium calculation in binary water + nonionic surfactant CiEj systems with a new mass-action law model based on continuous thermodynamics." *Fluid Phase Equilibria*, 235, 127-138.

Chao-Yang Gau, J. F. B., Mark A. Stadtherr. (2000). "Reliable nonlinear parameter estimation in VLE modeling." *Fluid Phase Equilibria*, 168, 1-18.

D.C. Kannan, J. L. D., R.P. Danner. (2005). "A free-volume term based on the van der Waals partition function for the UNIFAC model." *Fluid Phase Equilibria*, 228-229, 321-328.

Dandekar, A. Y., Chen, G.-J., Guo, T.-M., Khataniar, S., and Patil, S. (2005). "Prediction of VLE and VLLE of systems containing hydrocarbon reservoir fluids and aqueous methanol solutions with a cubic EOS." *Journal of Canadian Petroleum Technology*, 44(3), 46-53.

Dymond, J H and Smith, E B, (1980), "The Virial Coefficients of Gases and Gaseous Mixtures", Clarendon Press, Oxford.

Ellis, S R M and Garbett, R D, (1960), "A New Equilibrium Still for the Study of Partially Miscible Systems", *Industrial and Engineering Chemistry*, Vol. 52, pp. 385-388.

Eubank, P. T. (2006). "Equations and procedures for VLLE calculations." *Fluid Phase Equilibria*, 241, 81-85.

Fredunslund, A, Gmehling, J and Rasmussen, P, (1977), "Vapour-Liquid Equilibrium using UNIFAC", Elsevier, Amsterdam.

G. Raabe, J. J., J. Koehler. (2001). "Experimental studies of phase equilibria in mixtures relevant for the description of natural gases." *Fluid Phase Equilibria*, 185, 199-208.

Gillespie, D T C, (1946), "Vapour-Liquid Equilibrium Still for Miscible Liquids", *Industrial and Engineering Chemistry, Analytical*, Vol. 18, pp. 575-577.

Gui-Bing Hong, M.-J. L., Ho-mu Lin. (2002). "Multiphase coexistence for mixtures containing water, 2-propanol, and ethyl acetate." *Fluid Phase Equilibria*, 203, 227-245.

Hála, E, Pick, J, Fried, V and Villim, O, (1967), "Vapour-Liquid Equilibrium", 2nd edition, Pergamon Press, Oxford.

Hayden, J D and O'Connell, J P, (1975), "Generalized Method for Predicting Second Virial Coefficients", *Industrial and Engineering Chemistry. Process Design and Development*, Vol. 14, pp. 209-216.

Heertjies, P M, (1960), "Determination of Vapour-Liquid Equilibrium of Binary Mixtures", *Chemical and Process Engineering*, Vol. 41, pp.385-386.

Hernández-Garduza, O, García-Sánchez, F and Neau, E, (2001), "Generalization of Composition-Dependent Mixing Rules for Multicomponent Systems: Prediction of Vapour-Liquid and Liquid-Liquid Equilibria", *Chemical Engineering Journal*, Vol. 84, pp. 283-294.

Hitoshi Kosuge, K. I. (2005). "Estimation of isobaric vapor–liquid–liquid equilibria for partially miscible mixture of ternary system." *Fluid Phase Equilibria*, 233, 47-55.

Hlavatý, K, (1972), "Correlation of the Binodal Curve in a Ternary Liquid Mixture with One

Pair of Immiscible Liquids", *Collection of Czechoslovak Chemical Communications*, Vol. 37, pp. 4005-4007.

Humphrey, J L, Rocha, J A and Fair, J R, (1984), "Essentials of Extraction", *Chemical Engineering (New York)*, Vol. 91, pp. 76-95.

Homer, A. I. K. a. J. (1996). "Evaluation of a model for the prediction of phase equilibria from general molecular parameters II Binary liquid-liquid equilibria at low pressures." *Chemical Engineering Science*, 51(1), 141-148.

I.U. Westhaus, R. S. (2004). "From raw physical data to reliable thermodynamic model parameters through DECHEMA Data Preparation Package." *Fluid Phase Equilibria*, 222-223, 49-54.

Joseph, M A, Raal, J D and Ramjugernath, D, (2001), "Phase Equilibrium Properties of Binary Systems with Diacetyl from a Computer Controlled Vapour-Liquid Equilibrium Still", *Fluid Phase Equilibria*, Vol. 182, pp. 157-176.

Juan Carlos Asensi, J. M., Maria del Mar Olaya, Francisco Ruiz, Vincente Gomis. (2002). "Isobaric vapour--liquid equilibria data for the binary system 1-propanol+1-pentanol and isobaric vapour–liquid–liquid equilibria data for the ternary system water+1-propanol+1-pentanol at 101.3 kPa." *Fluid Phase Equilibria*, 200, 287-293.

Jurgen Bausa, W. M. (2000). "Quick and reliable phase stability test in VLLE flash calculations by homotopy continuation." *Computers and Chemical Engineering*, 24, 2447-2456.

Katja Egner, J. G., Andreas Pfennig. (1999). "GEQUAC, an excess Gibbs energy model describing associating and nonassociating liquid mixtures by a new model concept for functional groups." *Fluid Phase Equilibria*, 158-160, 381-389.

Koichi Iwakabe, H. K. (2001). "Isobaric vapor–liquid–liquid equilibria with a newly developed still." *Fluid Phase Equilibria*, 192, 171-186.

Kojima, K. (1997). "Compilation of group contribution preduction of VLE and excess enthalpy." *Fluid Phase Equilibria*, 136, 63-77.

L. Fedele, S. B., R. Camporese, R. Stryjek. (2004). "VLLE measurements and correlation for the pentafluoroethane (R125) + n-butane (R600) system." *Fluid Phase Equilibria*, 222-223, 283-289.

Lee, S C, (1931), "Partial Pressure Isotherms", *Journal of Physical Chemistry*, Vol. 35, pp. 3558-3582.

Letcher, T M, Heyward, C and Wooten, S, (1986), "Phase Separation in Petrol - Alcohol Blends", *South African Journal of Chemistry*, Vol. 39, pp. 19-22.

Letcher, T M, Siswana, P M, van der Watt, P and Radloff, S, (1989), "Phase Equilibria for (an Alcohol + p-Xylene + Water) at 298.2 K", *Journal of Chemical Thermodynamics*, Vol. 21, pp. 1053-1060.

Liu, H, Hu, Y and Peng, C, (2002), "Liquid-Liquid Equilibria of Copolymer Mixtures Bases on an Equation of State", *Fluid Phase Equilibria*, Vol. 201, pp. 19-35.

M. Mohsen-Dia, H. M., G.A. Mansoori. (2003). "A cubic hard-core equation of state." *Fluid Phase Equilibria*, 206, 27-39.

M. Solorzano-Zavala, F. B.-A., E.R. Bazua. (1996). "Comparative study of mixing rules for cubic equaitons of state in the prediction o multicomponent vapor-liquid equilibria." *Fluid Phase Equilibria*, 122, 99-116.

Malanowski, S, (1982), "Experimental Methods for Vapour-Liquid Equilibria. Part I. Circulation Methods", *Fluid Phase Equilibria*, Vol. 8, pp. 197-219.

Marquardt, D W, (1963), "An Algorithm for Least-Squares Estimation of Non-Linear Parameters", *Journal. Society of Industrial and Applied Mathematics*, Vol. 11, pp. 431-441.

Ming-Jer Lee, L.-H. T., Gui-Bing Hong, Ho-Mu Lin. (2004). "Multiphase equilibria for binary and ternary mixtures containing propionic acid, n-butanol, butyl propionate, and water." *Fluid Phase Equilibria*, 216, 219-228.

Min-Lon Yu, Y.-P. C. (1997). "VLE calculations by applying a modified perturbed hard sphere EOS." *Fluid Phase Equilibria*, 129, 21-35.

N.A. Smirnova, A. I. V., G.I. Kuranov. (1998). "New applications of equations of state in molecular models of complex fluid mixtures." *Fluid Phase Equilibria*, 150-151, 161-171.

Naveed Aslam, A. K. S. (2006). "Sensitivity of azeotropic states to activity coefficient model parameters and system variables." *Fluid Phase Equilibria*, 240, 1-14.

Narasigadu, C, (2006), "Phase equilibrium investigation of the water and acetonitrile solvent with heavy hydrocarbons", Master of Science in Engineering (Chemical Engineering) Thesis, University of KwaZulu-Natal, South Africa.

Ndlovu, M, (2005), "Development of a Dynamic Still for Measuring Low Pressure Vapour-Liquid-Liquid Equilibria (Systems of Partial Liquid Miscibility)", Master of Science in Engineering (Chemical Engineering) Thesis, University of KwaZulu-Natal, South Africa.

Novak, J P, Matous, J and Pick, J, (1987), "Liquid-Liquid Equilibria", Elsevier, Amsterdam.

Null, H R, (1980), "Phase Equilibrium in Process Design", Robert E Krieger, New York.

O'Connell, J P and Prausnitz, J M, (1967), "Emperical Correlation of Second Virial Coefficients for Vapour-Liquid Equilibrium Calculations", *Industrial and Engineering Chemistry. Process Design and Development*, Vol. 6, pp. 245-250.

Ohta, T, Todoriki, H and Yamada, T, (2004), "Representation of Liquid-Liquid Equilibria at Low and High Pressures using EOS-GE Mixing Rules", *Fluid Phase Equilibria*, Vol. 225, pp. 23-27.

Othmer, D F, (1928), "Composition of Vapours from Boiling Binary Solutions. Improved Equilibrium Still", *Industrial and Engineering Chemistry*, Vol. 20, pp. 743-766.

Perry, R H and Green, D W, (1998), "Perry's Chemical Engineers' Handbook", 7th edition, McGraw-Hill, New York.

Pitzer, K S and Curl, R F, (1957), "Emperical Equation for the Second Virial Coefficient", *Journal of the American Chemical Society*, Vol. 79, pp. 2369-2370.

Pitzer, K S, Lippmann, D Z, Curl, R F, Huggins, C M and Petersen, D E, (1955), "The Volumetric and Thermodynamic Properties of Fluids. II. Compressibility Factor, Vapour Pressure and Entropy of Vapourization", *Journal of the American Chemical Society*, Vol. 77, pp. 3433-3440.

Prausnitz, J M, Anderson, T F, Grens, E A, Eckert, C A, Hseih, R and O'Connell, J P, (1980), "Computer Calculations for Multicomponent Vapour-Liquid and Liquid-Liquid Equilibria", Prentice-Hall, Englewood Cliffs, NJ.

Prausnitz, J M, Lichtenthaler, R N and de Azevedo, E G, (1999), "Molecular Thermodynamics of Fluid-Phase Equilibria", 3rd edition, Prentice-Hall, Upper Saddle River, New Jersey.

R. Susilo, J. D. L., P. Englezos. (2005). "Liquid–liquid equilibrium data of water with neohexane, methylcyclohexane, tert-butyl methyl ether, n-heptane and vapor–liquid–liquid equilibrium with methane." *Fluid Phase Equilibria*, 231, 20-26.

Raal, J D and Brouckaert, C J, (1992), "Vapour-Liquid and Liquid-Liquid Equilibria in the System Methyl Butenol-Water", *Fluid Phase Equilibria*, Vol. 74, pp. 253-270.

Raal, J D and Mühlbauer, A L, (1998), "Phase Equilibria: Measurement and Computation", Taylor and Francis, Bristol, PA.

Raal, J D, Gadodia, V, Ramjugernath D and Jalari, R, (2006), "New Developments in Differential Ebulliometry: Experimental and Theoretical", *Journal of Molecular Liquids*, Vol. 125, pp. 45-57.

Rackett, H G, (1970), "Equation of State for Saturated Liquids", *Journal of Chemical and Engineering Data*, Vol. 15, pp. 514-517.

Rangaiah, G. H. a. G. P. (1997). "A method for calculation of vapor-liquid and liquid-liquid equilibria." *Computer chem. Engng*, 21(8), 905-913.

Reddy, P, (2006), "Development of a Novel Apparatus for Vapour-Liquid Equilibrium measurements at moderate pressures", of Doctor of Philosophy in the School of Chemical Engineering at the University of KwaZulu-Natal, Durban.

Reid, R.C., Prausnitz, J.M, Poling, B.E., (1988), "Properties of Liquids and Gases", 4th Edition, McGraw Hill Book Co.,New York, NY

Renon, H and Prausnitz, J M, (1968), "Local Compositions in Thermodynamic Excess Functions for Liquid Mixtures", *American Institute of Chemical Engineers Journal*, Vol. 14, pp. 135-144.

Scathard, G, Raymond, C L and Gilmann, H H, (1938), "Vapour-Liquid Equilibrium. I. Apparatus for the Study of Systems with Volatile Components", *Journal of the American Chemical Society*, Vol. 60, pp. 1275-1287.

Sewnarain, R, Raal J D and Ramjugernath, D, (2002), "Isobaric Vapour-Liquid Equilibria for the Systems Propionic Acid + Butyric Acid, Isobutyric Acid + Butyric Acid, Butyric Acid + Isovaleric Acid and Butyric Acid + Hexanoic Acid at 14 kPa", *Journal of Chemical and Engineering Data*, Vol. 47, pp. 603-607.

Skoog, D A, West, D M and Holler, F J, (1991), "Fundamentals of Analytical Chemistry", 6th edition, Saunders College Publishing, Florida.

Smith, J M, Van Ness, H C and Abbott, M M, (2001), "Introduction to Chemical Engineering Thermodynamics", 6th edition, McGraw-Hill International Editions, New York.

Smith, T E and Bonner, R F, (1949), "Vapour-Liquid Equilibrium Still for Partially Miscible Liquids", *Industrial Engineering Chemistry*, Vol. 41, pp. 2867-2871.

Smyth, C P, (1955), "Dipole Moment and Molecular Structure", McGraw-Hill, New York.

Soave, G, (1972), "Equilibrium Constants from a Modified Redlich-Kwong Equation of State", *Chemical Engineering Science*, Vol. 27, pp. 1197-1203.

Sørensen, J M, Magnussen, T, Rasmussen, P and Fredenslund, A, (1979), "Liquid-Liquid Equilibrium Data: Their Retrieval, Correlation and Prediction, Part I: Retrieval", *Fluid Phase Equilibria*, Vol. 2, pp. 297-309.

Stockhardt, J S and Hull, C M, (1931), "Vapour-Liquid Equilibria and Boiling-Point Composition Relations for Systems n-Butanol-Water and Isobutanol-Water", *Industrial Engineering Chemistry*, Vol. 23, pp. 1438-1440.

Thornton, J D, (1952), "An Improved Type of Vapour-Liquid Equilibrium Still", *Journal of Applied Chemistry*, Vol. 1, pp. 237-239.

Treybal, R E, (1963), "Liquid Extraction", 2nd edition, McGraw-Hill, USA.

Tsonopoulos, C, (1974), "An Emperical Correlation of Second Virial Coefficients", *American Institute of Chemical Engineers Journal*, Vol. 20, pp. 263-272.

V. Gomis, A. F., R. Pedraza, M.D. Saquete. (2005). "Isobaric vapor–liquid and vapor–liquid–liquid equilibrium data for the system water + ethanol + cyclohexane." *Fluid Phase Equilibria*, 235, 7-10.

Van der Waals, J D, (1873), "Over de Continuitet van den Gas - en Vloeistoftoestand", Doctoral Dissertation, Leiden, as given by Anderko (1990).

Van Laar, J J, (1910), "The Vapour Pressure of Binary Mixture", *Zeitschrift feur Physik Chemie*, Vol. 72, pp. 723-751, as given by Walas (1985).

Van Ness, H C, (1959), "Exact Forms of the Unrestricted Gibbs-Duhem Equation", *Chemical Engineering Science*, Vol. 10, pp. 225-228.

Van Ness, H C, (1995), "Thermodynamics in the Treatment of Vapour/Liquid Equilibrium (VLE) Data", *Pure and Applied Chemistry*, Vol. 67, pp. 859-872.

Van Ness, H C, Byer, S M and Gibbs, R E, (1973), "Vapour-Liquid Equilibrium: Part I. An Appraisal of Data Reduction Methods", *American Institute of Chemical Engineers Journal*, Vol. 19, pp. 238-244.

Van Ness, H C, Pedersen, F and Ramussen, P, (1978), "Part V. Data Reduction by Maximum Likelihood", *American Institute of Chemical Engineers Journal*, Vol. 24, pp. 1055-1063.

Van Ness, HC and Abbott, M M, (1982), "Classical Thermodynamics of Nonelectrolyte Solutions: With Applications to Phase Equilibria", McGraw-Hill, New York.

Vetere, A. (2000). "A simple modification of the NRTL equation." *Fluid Phase Equilibria*, 173, 57-64.

Vetere, A. (2004). "The NRTL equation as a predictive tool for vapor–liquid equilibria." *Fluid Phase Equilibria*, 218, 33-39.

Vicente Gomis, F. R., Juan Carlos Asensi. (2000). "The application of ultrasound in the determination of isobaric vapour–liquid–liquid equilibrium data." *Fluid Phase Equilibria*, 172, 245-259.

Walas, S M, (1985), "Phase Equilibrium in Chemical Engineering", Butterworth, Boston.

Wilson, G M, (1964), "Vapour-Liquid Equilibrium. XI: A New Expression for the Excess Free Energy of Mixing", *Journal of the American Chemical Society*, Vol. 86, pp. 127-130.

Yerazunis, S, Plowright, J D and Smola, F M, (1964), "Vapour-Liquid Equilibrium Determination by a New Apparatus", *American Institute of Chemical Engineers Journal*, Vol. 10, pp. 660-665.

Ying Hu, H. L., Wenchuan Wang. (1999). "Molecular thermodynamics for chain-like molecule systems." *Fluid Phase Equilibria*, 158-160, 59-68.

Yo-Li Chou, Y.-P. C. (1996). "A modified mixing model for vapor-liquid equilibrium calculations." *Fluid Phase Equilibria*, 115, 95-112.

Zhenghong Gao, S. W., Qingchi Sun, Fengcai Zhang. (2003). "Isobaric phase equilibria of the system 1-butanol + water containing penicillin G potassium salt at low pressures." *Fluid Phase Equilibria*, 214, 137-149.

Appendix A

Gas Chromatography Calibration graphs

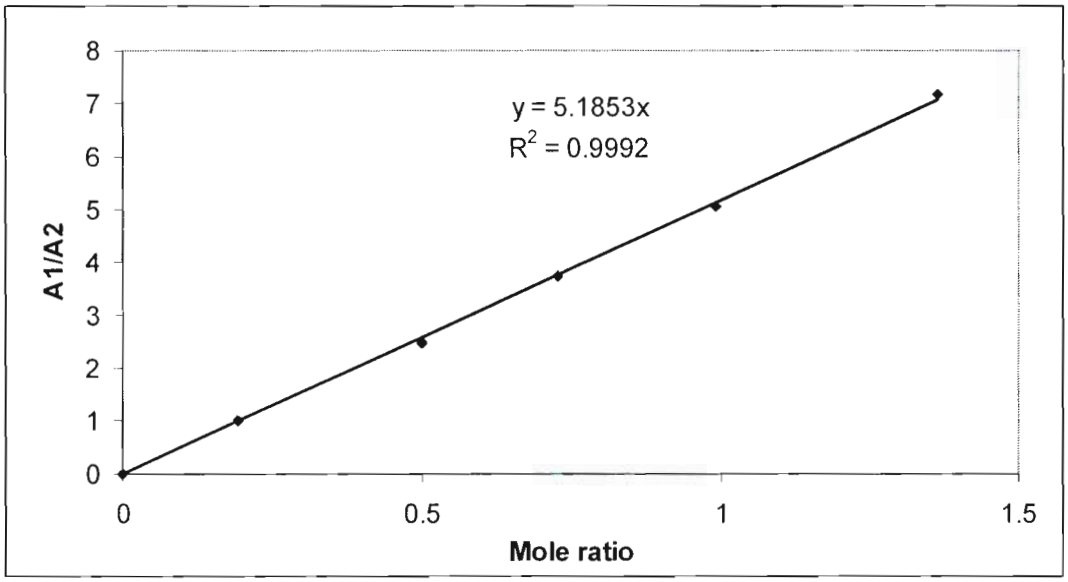

Figure A1. GC Dodecane(1) + ethanol(2) + water(3) calibration

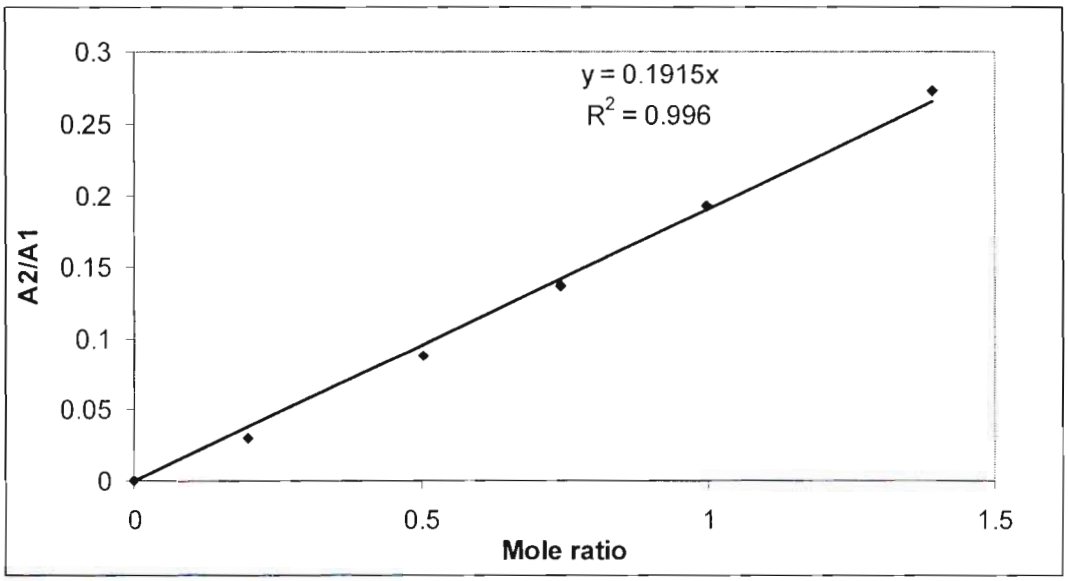

Figure A2. GC Dodecane(1) + ethanol(2) + water(3) calibration

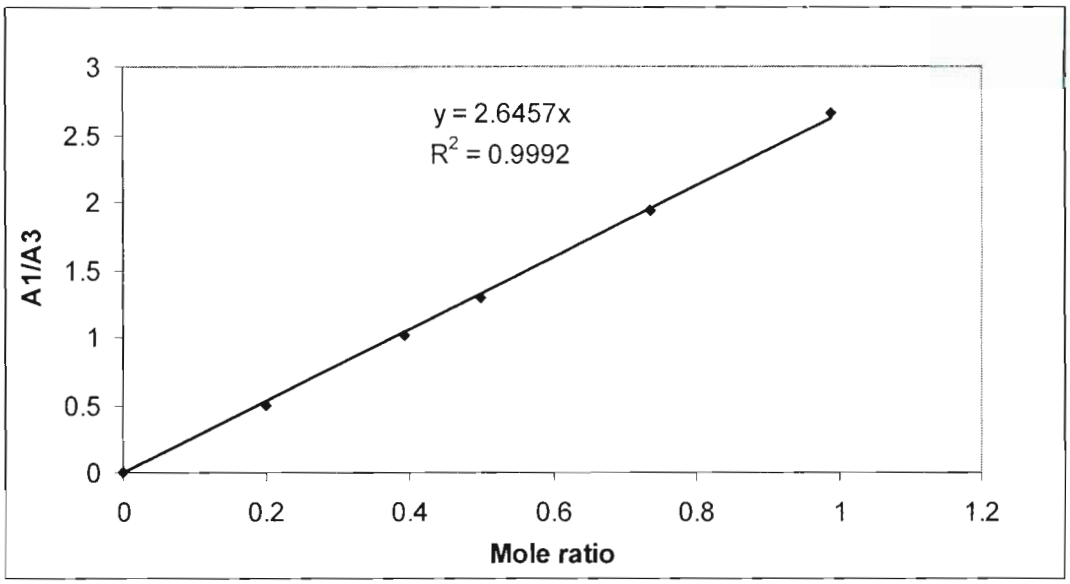

Figure A3. GC Dodecane(1) + ethanol(2) + water(3) calibration

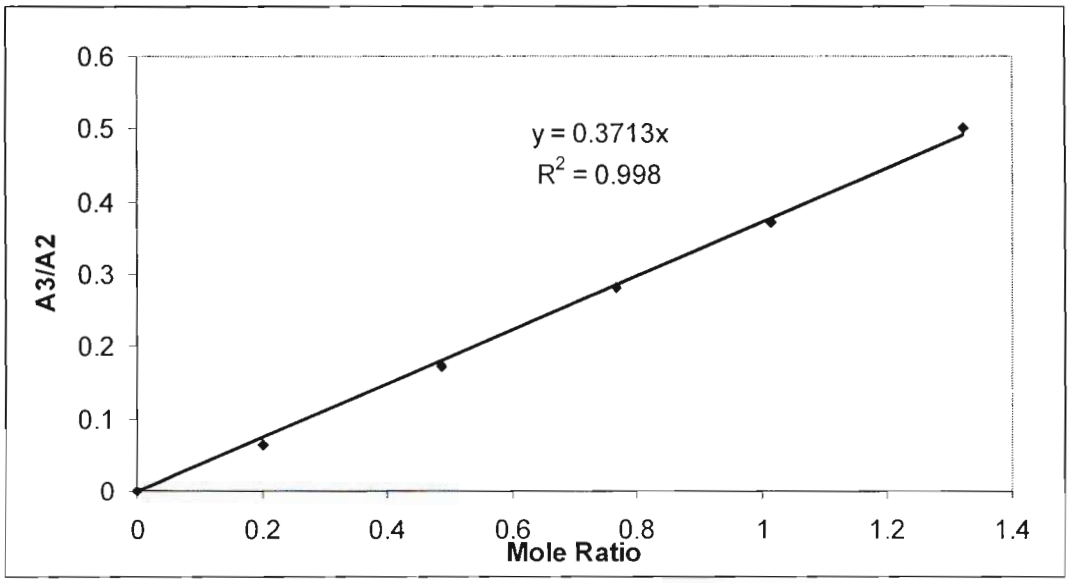

Figure A3. G4 Dodecane(1) + ethanol(2) + water(3) calibration

Appendix B
Temperature calibrations

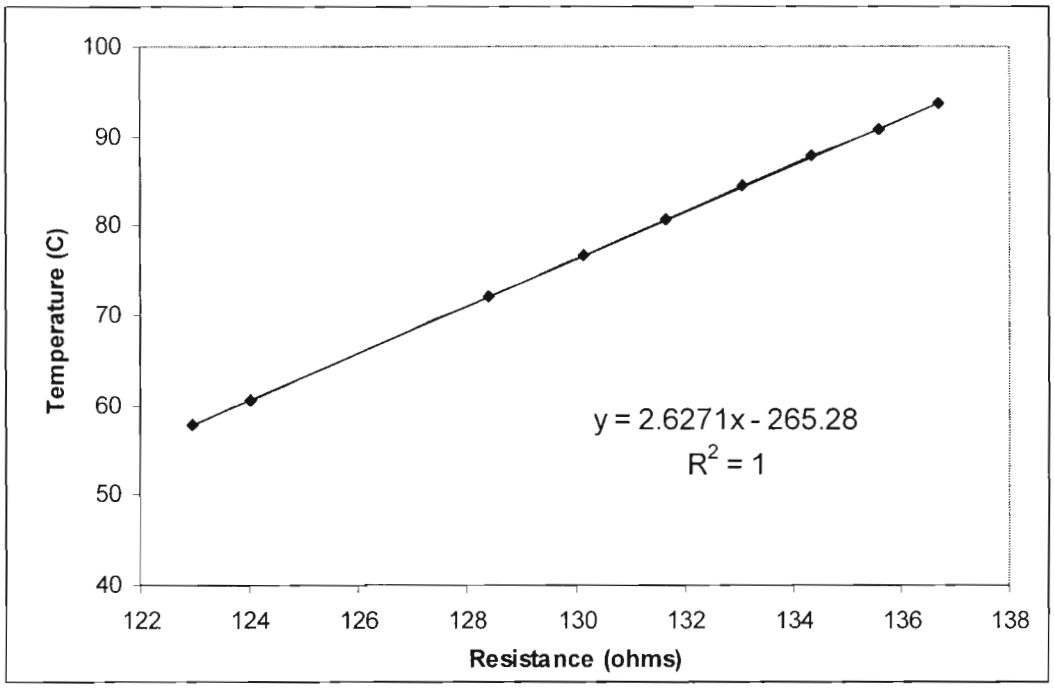

Figure B1. Temperature probe calibration

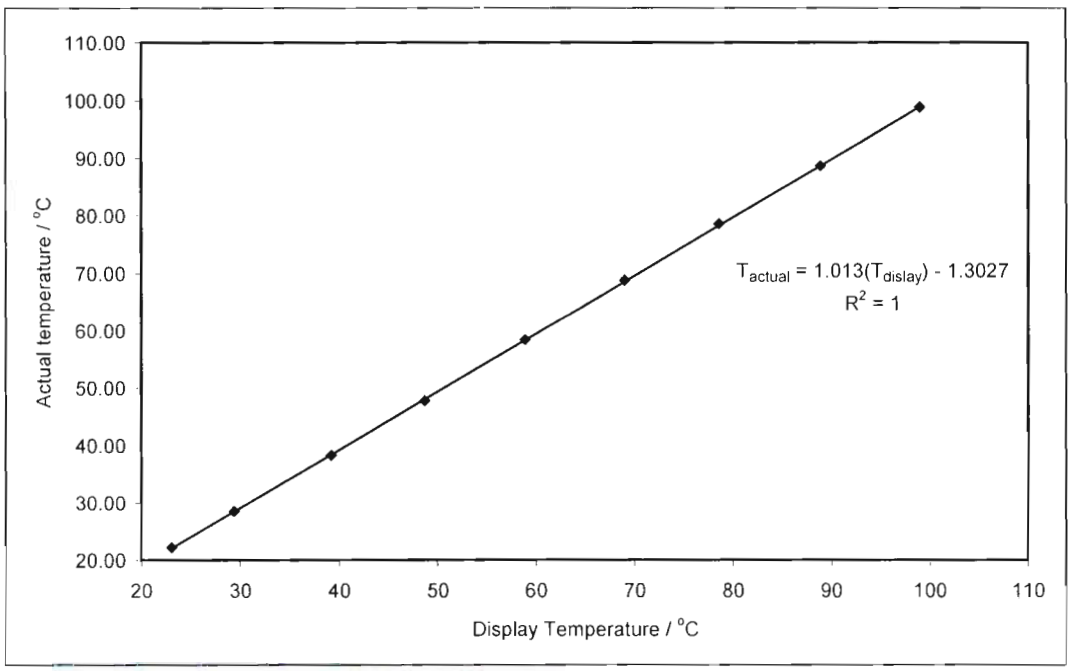

Figure B2. LLE Cell temperature probe calibration

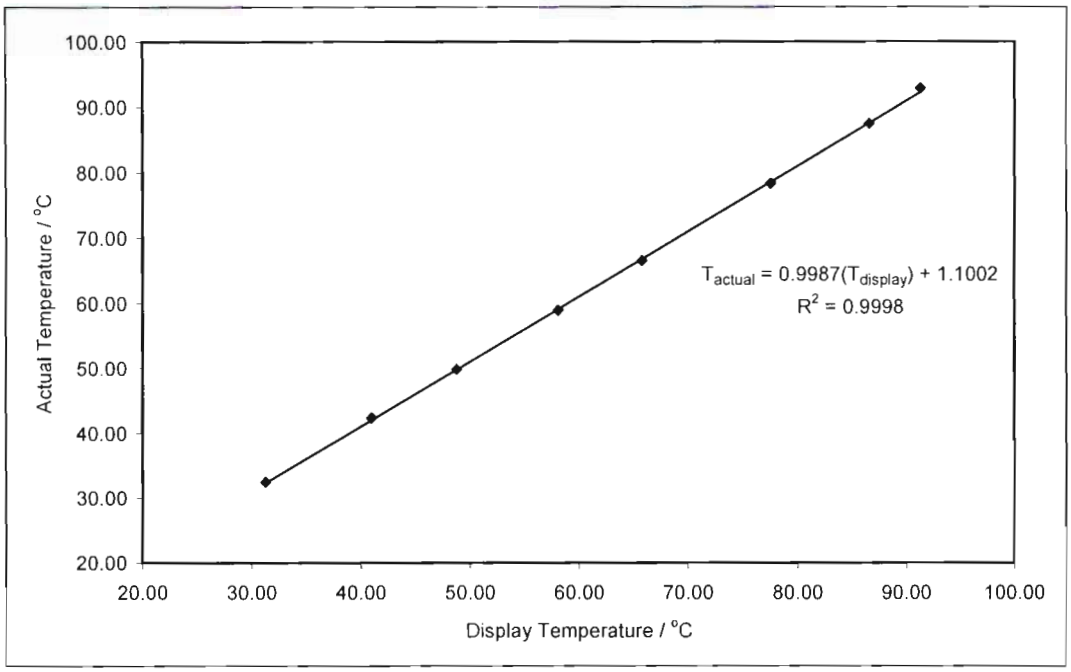

Figure B3. LLE water bath temperature sensor calibration

Appendix C
Binary VLE modeled data

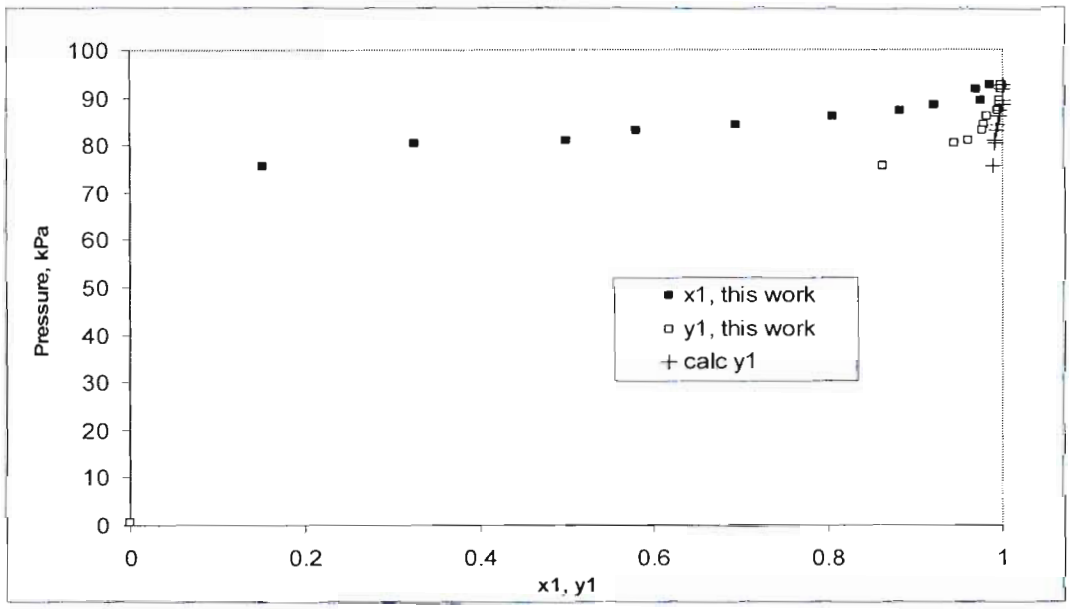

Figure C1. P-x-y plot of experimental and calculated VLE data of dodecane + 2-propanol at 353.15 K

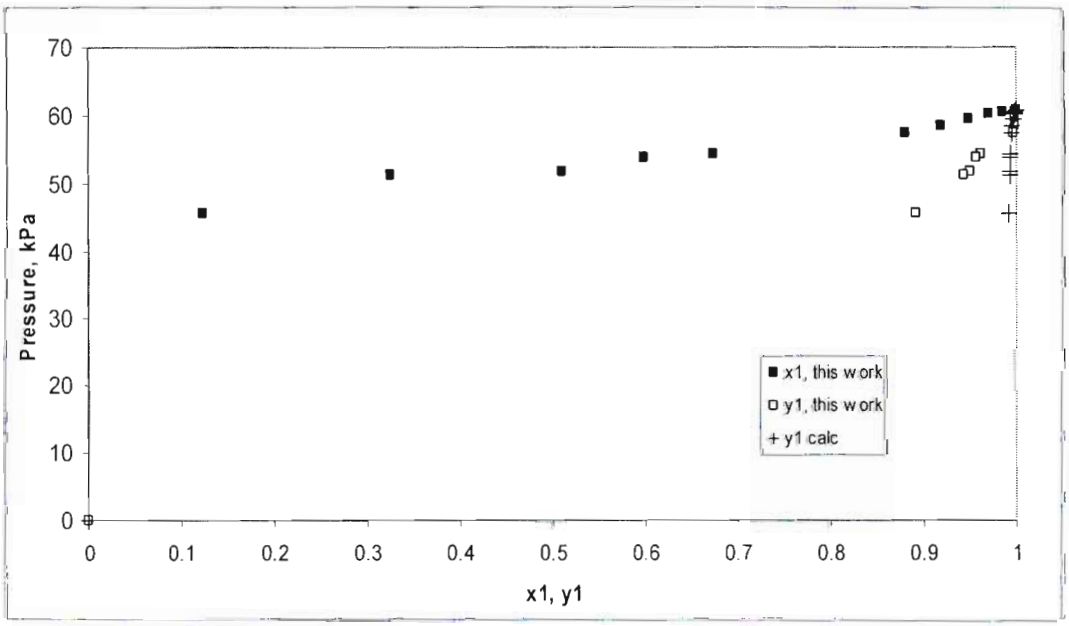

Figure C2. P-x-y plot of experimental and calculated VLE data of dodecane + 2-propanol at 343.15 K

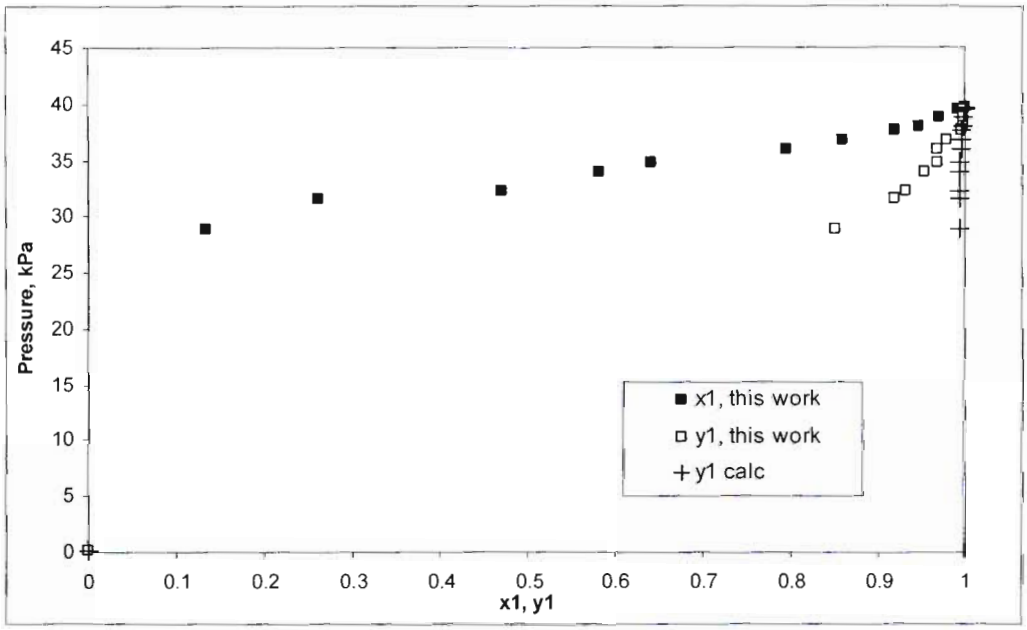

Figure C3. P-x-y plot of experimental and calculated VLE data of dodecane + 2-propanol at 333.15 K

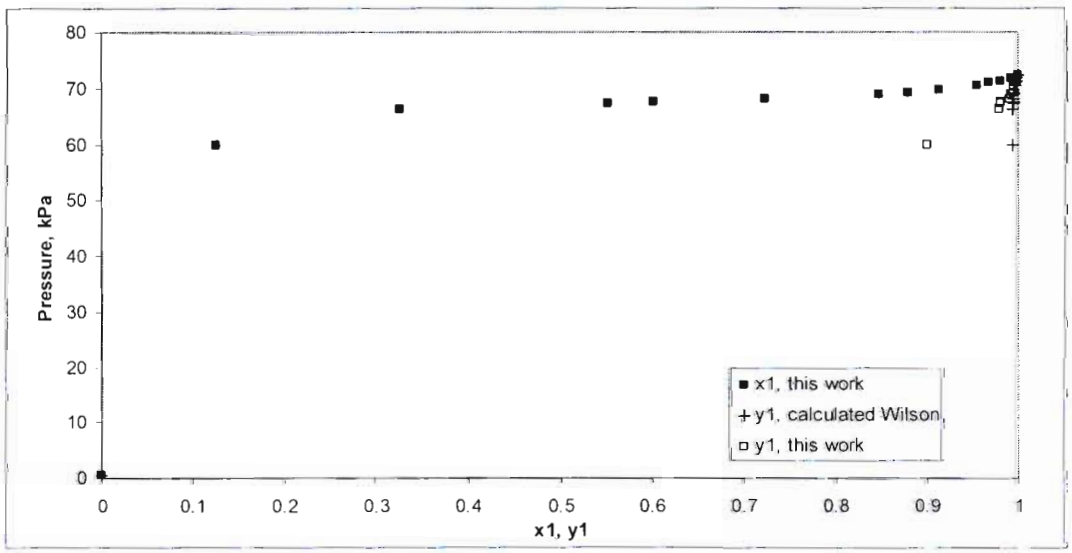

Figure C4. P-x-y plot of experimental and calculated VLE data of dodecane + ethanol at 343.15 K

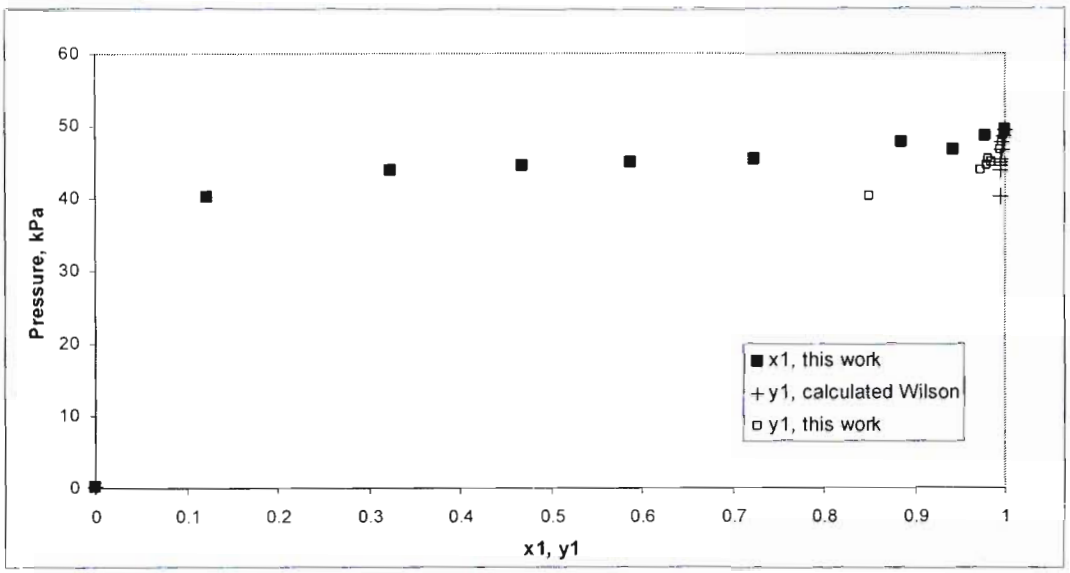

Figure C5. P-x-y plot of experimental and calculated VLE data of dodecane + 2-propanol at 333.15K

Appendix D
MATLAB® code for ternary LLE data regression

D1. File storing measured ternary LLE data

```
% This file inputs the measured Ternary tie line data for the system
% Dodecane (1) - Water (2) - 2-Propanol (3) at 55 degree C
% For regression using the NRTL Equation

%Organic Phase

x1exp = [0.9933 0.9932 0.9871 0.9638 0.9707 0.9622  0.9488 0.9422];
x2exp = [0.0067  0.0007 0.0007 0.0002 0.0006  0.0005 0.0024 0.0020];
x3exp = 1 - x2exp - x1exp;


% Aqueous Phase

x1_exp = [0.000920 0.00675 0.00616 0.00758 0.0257 0.0138 0.0563 0.0779
];
x2_exp = [0.999 0.958 0.920 0.840 0.743 0.695 0.546 0.497];
x3_exp = 1 - x2_exp - x1_exp;

T = 55 + 273.15;% K
R = 8.314;% J/mol K
```

D2. Program to evaluate the NRTL parameters

```
function  [r] = active(p,q)
global  R T alpha1_2 alpha1_3 alpha2_3

% Mole fraction variables
x = p;
param = q;
A12 = param(1); A21 = param(2); A13 = param(3);
A31 = param(4); A23 = param(5); A32 = param(6);
A11 = 0;A22 = 0; A33 = 0;
G11 = 1; G22 = 1; G33 = 1;

x1 = x(1);
x2 = x(2);
x3 = x(3);

%Calculate Gij
G12 = exp(-alpha1_2 * A12);
G21 = exp(-alpha1_2 * A21);
G13 = exp(-alpha1_3 * A13);
G31 = exp(-alpha1_3 * A31);
G23 = exp(-alpha2_3 * A23);
G32 = exp(-alpha2_3 * A32);
```

```
% Terms in the activity coefficient expression for gamma1
% from Malas pg 201-203

a1 = ((A11 * G11 * x1) + (A21 * G21 * x2) + (A31 * G31 * x3)) / ((G11 *
x1) + (G21 * x2) + (G31 * x3));
b1 = (x1 * G11) / (x1 + (G12 * x2) + (G13 * x3));
c1 = A11;
d1 = ((x2 * A21 * G21) + (x3 * A31 * G31)) / (x1 + (x2 * G21) + (x3 *
G31));
e1 = (x2 * G12) / ((G12 * x1) + x2 + (G32 * x3));
f1 = A12;
g1 = ((x1 * A12 * G12) + (x3 * A32 * G32)) / ((x1 * G12) + x2 + (x3 *
G32));
h1 = (x3 * G13) / ((G13 * x1) + (G23 * x2) + x3);
i1 = A13;
j1 = ((x1 * A13 * G13) + (x2 * A23 * G23)) / ((G13 * x1) + (G23 * x2) +
x3);

a2 = ((A12 * G12 * x1) + (A22 * G22 * x2) + (A32 * G32 * x3)) / ((G12 *
x1) + (G22 * x2) + (G32 * x3));
b2 = (x1 * G21) / (x1 + (G12 * x2) + (G13 * x3));
c2 = A21;
d2 = ((x2 * A21 * G21) + (x3 * A31 * G31)) / (x1 + (x2 * G21) + (x3 *
G31));
e2 = (x2 * G22) / ((G12 * x1) + x2 + (G32 * x3));
f2 = A22;
g2 = ((x1 * A12 * G12) + (x3 * A32 * G32)) / ((x1 * G12) + x2 + (x3 *
G32));
h2 = (x3 * G23) / ((G13 * x1) + (G23 * x2) + x3);
i2 = A23;
j2 = ((x1 * A13 * G13) + (x2 * A23 * G23)) / ((G13 * x1) + (G23 * x2) +
x3);

a3 = ((A13 * G13 * x1) + (A23 * G23 * x2) + (A33 * G33 * x3)) / ((G13 *
x1) + (G23 * x2) + (G33 * x3));
b3 = (x1 * G31) / (x1 + (G12 * x2) + (G13 * x3));
c3 = A31;
d3 = ((x2 * A21 * G21) + (x3 * A31 * G31)) / (x1 + (x2 * G21) + (x3 *
G31));
e3 = (x2 * G32) / ((G12 * x1) + x2 + (G32 * x3));
f3 = A32;
g3 = ((x1 * A12 * G12) + (x3 * A32 * G32)) / ((x1 * G12) + x2 + (x3 *
G32));
h3 = (x3 * G33) / ((G13 * x1) + (G23 * x2) + x3);
i3 = A33;
j3 = ((x1 * A13 * G13) + (x2 * A23 * G23)) / ((G13 * x1) + (G23 * x2) +
x3);


act1 = exp(a1 + (b1 * (c1 - d1)) + (e1 * (f1 - g1)) + (h1 * (i1 -
j1)));
act2 = exp(a2 + (b2 * (c2 - d2)) + (e2 * (f2 - g2)) + (h2 * (i2 -
j2)));
```

```
act3 = exp(a3 + (b3 * (c3 - d3)) + (e3 * (f3 - g3)) + (h3 * (i3 -
j3)));

r = [act1 act2 act3];
```

D3. Program to regress ternary LLE tie line data to obtain parameters in NRTL equation

```
function r = Checker2(param)

global T R alpha1_2 alpha1_3 alpha2_3...
    x1exp x2exp x3exp x1_exp x2_exp x3_exp x1call x2call x1_call
x2_call betav...
    ztline1 ztline2 ztline3 ztline4 ztline5 ztline6 ztline7 ztline8
ztline9

error = 0.0001;

      for i = 1:length(x1exp)
        beta = 0.7; % initial guess
        x1cal = x1exp(i);
        x2cal = x2exp(i);
        x3cal = x3exp(i);
        xcal = [x1cal x2cal x3cal];
        if i == 1
            beta = 0.25; % initial guess
            z1 = ztline1(1);
            z2 = ztline1(2);
            z3 = ztline1(3);
            zi = [z1 z2 z3];
            normzi = sum(zi);
            zi = zi ./ sum(zi);

        elseif i == 2
            beta = 0.20; % initial guess
            z1 = ztline2(1);
            z2 = ztline2(2);
            z3 = ztline2(3);
            zi = [z1 z2 z3];
            normzi = sum(zi);
            zi = zi ./ sum(zi);

        elseif i == 3
            beta = 0.19; % initial guess
            z1 = ztline3(1);
            z2 = ztline3(2);
            z3 = ztline3(3);
            zi = [z1 z2 z3];
            normzi = sum(zi);
            zi = zi ./ sum(zi);

        elseif i == 4
            beta = 0.18; % initial guess
            z1 = ztline4(1);
            z2 = ztline4(2);
```

```
    z3 = ztline4(3);
    zi = [z1 z2 z3];
    normzi = sum(zi);
    zi = zi ./ sum(zi);

elseif i == 5
    %beta = 0.21; % initial guess
    z1 = ztline5(1);
    z2 = ztline5(2);
    z3 = ztline5(3);
    zi = [z1 z2 z3];
    normzi = sum(zi);
    zi = zi ./ sum(zi);

elseif i == 6
    %beta = 0.22; % initial guess
    z1 = ztline6(1);
    z2 = ztline6(2);
    z3 = ztline6(3);
    zi = [z1 z2 z3];
    normzi = sum(zi);
    zi = zi ./ sum(zi);

elseif i == 7
    %beta = 0.32; % initial guess
    z1 = ztline7(1);
    z2 = ztline7(2);
    z3 = ztline7(3);
    zi = [z1 z2 z3];
    normzi = sum(zi);
    zi = zi ./ sum(zi);

elseif i == 8
    %beta = 0.33; % initial guess
    z1 = ztline8(1);
    z2 = ztline8(2);
    z3 = ztline8(3);
    zi = [z1 z2 z3];
    normzi = sum(zi);
    zi = zi ./ sum(zi);

else i == 9
    %beta = 0.41; % initial guess
    z1 = ztline9(1);
    z2 = ztline9(2);
    z3 = ztline9(3);
    zi = [z1 z2 z3];
    normzi = sum(zi);
    zi = zi ./ sum(zi);

end

counter = 0;

while counter <= 0
```

```
            x_cal = (zi - (beta .* xcal)) ./ (1-beta);% Aqueous phase
compositions
            gammai = active(xcal,param);
            gamma_i = active(x_cal,param);
            Ki = gammai ./ gamma_i;

            % Use Newton's method to find a solution for beta

            for k = 0:100 % Allow only for 100 iterations
                fbeta = sum(zi ./ (beta + (1-beta)* Ki)) - 1;
                dfbeta = sum(-zi .*(1 - Ki) ./ ((beta + (1 - beta) *
                          Ki) .^2));
                betta(k+1) = beta - 0.5*fbeta /dfbeta;
                if (abs(betta(k+1) - beta) <= error)
                     xcaln = zi ./ (beta + (Ki .* (1 - beta)));
                     normsumxc = sum(xcaln);
                     xcaln = xcaln ./ normsumxc;
                    break
                end% end if
                beta = betta(k+1);
                k = k+1;
            end% end for


            if  (abs(xcaln - xcal)) <= error
                 counter = counter + 1;
                 x_caln = (zi - (beta .* xcaln)) ./ (1-beta);
                 break
             end

            xcal = xcaln;

        end


        x1call(i) = xcal(1);
        x2call(i) = xcal(2);
        x1_call(i) = x_caln(1);
        x2_call(i) = x_caln(2);
        betav(i) = beta;    % this is here only to check on Beta value

    end% end for
    x1call;
    x2call;
    x1_call;
    x2_call;


    err1 = x1exp - x1call ; err2 = x2exp - x2call ;
    err3 = x1_exp - x1_call; err4 = x2_exp - x2_call;

    r = sum(err1.^2 + err2.^2 + err3.^2 + err4.^2);

    plot(x1exp,2exp,'bo',x1call,x2call,'r*')
    drawnow
```

D4. Main program for ternary LLE data regression for NRTL model

```
% Program to regress ternary LLE tie line data to obtain parameters
% in the NRTL equation
% Algorithm from Walas (1985),p 371

close all
clear all
clc          % Initialise workspace

global param T R A1_2 A2_1 A1_3 A3_1 A2_3 A3_2 alpha1_2 alpha1_3
alpha2_3...
    x1exp x2exp x3exp x1_exp x2_exp x3_exp x1call x2call x1_call
x2_call betav...
    ztline1 ztline2 ztline3 ztline4 ztline5 ztline6 ztline7 ztline8
ztline9

cc55; %Call a script to enter the experimental tie line data

param = [1.9 1.9 1.9 1.9 1.9 1.9]; % Initial guess of NRTL parameters
alpha1_2 = 0.2; % set constant alpha for all binaries
alpha1_3 = 0.2;
alpha2_3 = 0.2;

ztline1 =  [    0.6956    0.3044    0.0000];
ztline2 =  [    0.6973    0.2879    0.0148];
ztline3 =  [    0.6928    0.2765    0.0307];
ztline4 =  [    0.6769    0.2521    0.0709];
ztline5 =  [    0.6872    0.2233    0.0895];
ztline6 =  [    0.6777    0.2089    0.1135];
ztline7 =  [    0.6811    0.1655    0.1535];
ztline8 =  [    0.6829    0.1505    0.1666];

param = fminsearch('Checker2',param,...      %starting from an initial
estimate of parameters find an optimum value
              optimset('TolX',1e-
8,'MaxFunEvals',7000,'MaxIter',1000,'Display','Iter'))'  ;%
optimization loop

        % Display parameters
        A1_2 = param(1); A2_1 = param(2); A1_3 = param(3);
        A3_1 = param(4); A2_3 = param(5); A3_2 = param(6);

    g21_g11 =  A2_1 * R * T; g12_g22 =  A1_2 * R * T; g13_g33 =  A1_3
               * R * T;
    g31_g11 =  A3_1 * R * T; g23_g33 =  A2_3 * R * T; g32_g22 =  A3_2
               * R * T;

    disp('The  fitted coefficients are:')
    disp('    ')
     disp(['  A12 = ', num2str(A1_2) ])
     disp(['  A21 = ', num2str(A2_1) ])
     disp(['  A13 = ', num2str(A1_3) ])
     disp(['  A31 = ', num2str(A3_1) ])
     disp(['  A23 = ', num2str(A2_3) ])
```

```
disp([' A32 = ', num2str(A3_2) ])

disp('or')
disp('  ')
disp(['g21_g11 in J/mol:  ', num2str(g21_g11)])
disp(['g12_g22 in J/mol:  ', num2str(g12_g22)])
disp(['g13_g33 in J/mol:  ', num2str(g13_g33)])
disp(['g31_g11 in J/mol:  ', num2str(g31_g11)])
disp(['g23_g33 in J/mol:  ', num2str(g23_g33)])
disp(['g32_g22 in J/mol:  ', num2str(g32_g22)])
disp('  ')

% computing the root mean squared deviation

err1 = x1exp - x1call ; err2 = x2exp - x2call ;
err3 = x1_exp - x1_call; err4 = x2_exp - x2_call;
x3call = 1 - x1call - x2call;
x3_call = 1 - x1_call - x2_call;
err5 = x3exp - x3call; err6 = x3_exp - x3_call;

rmsd = (sum(err1.^2 + err2.^2 + err3.^2 + err4.^2 + err5.^2 +
err6.^2)/(6 * length(x1exp)))^0.5;
disp(['The root mean squared deviation is: ', num2str(rmsd)])

disp('  ')
disp(['The beta values are:', num2str(betav)])

disp('  ')
disp(['The calculated x1 values of phase I are: ',
num2str(x1call)])
disp(['The calculated x2 values of phase I are: ',
num2str(x2call)])
disp(['The calculated x3 values of phase I are: ',
num2str(x3call)])
disp('  ')
disp(['The calculated x1 values of phase II are: ',
num2str(x1_call)])
disp(['The calculated x2 values of phase II are: ',
num2str(x2_call)])
disp(['The calculated x3 values of phase II are: ',
num2str(x3_call)])
```